Dissertation zur Erlangung des Doktorgrades
Der Fakultät für Chemie und Pharmazie
Der Ludwig-Maximilians-Universität München

The role of FKBP5 in transcriptional regulation and in shaping cellular pathways of psychopharmaca action

Lorenz Korbinian Kollmannsberger

aus München, Deutschland

2015

Erklärung

Diese Dissertation wurde im Sinne von §7 der Promotionsordnung vom 28. November 2011 von Herrn Prof. Dr. Haralabos Zorbas betreut.

Eidesstattliche Versicherung

Diese Dissertation wurde eigenständig und ohne unerlaubte Hilfe erarbeitet.

München, den 15.12.2015

_____

Lorenz Korbinian Kollmannsberger

Dissertation eingereicht am: 17.12.2015

Erstgutachter: Prof. Dr. rer. nat. Haralabos Zorbas

Zweitgutachter: PD Dr. Theo Rein

Tag der mündlichen Prüfung: 10.03.2016

Summary

FK506 binding protein 5 (FKBP5) has been linked to stress related diseases and treatment response in depression (Binder et al., 2004). The corresponding protein FKBP51 was first identified as co-chaperone of HSP90 in a complex with steroid hormone receptors, where it diminishes hormone affinity and nuclear translocation efficiency of the receptors (Pratt and Toft, 1997; Wochnik et al., 2005). With FKBP5 transcription being induced by glucocorticoid signalling, an ultra-short feedback loop is provided for regulation and termination of GR activity. Dysregulation of this ultra-short feedback loop interferes with the stress hormone regulation and likely contributes to the association of FKBP5 with stress-related psychiatric disorders. Recently, important actions of FKBP51 beyond glucocorticoid signalling have been characterised in shaping the posttranslational regulation of certain molecular pathways in response to treatment with particular psychopharmaca (Gassen et al., 2014, 2015).

As a contribution to elucidating the role of FKBP5 in stress related diseases, a two-sided approach was taken in this study by analysing the role of FKBP5 in regulation of transcription and in calibrating the responsiveness of these pathways to psychopharmacological treatment.

To elucidate the transcriptional effects of FKBP5 in an unbiased approach, the expression profile of mice with deleted FKBP5 and their litter mates with functional FKBP5 were compared. A marked difference in glyoxalase-1 (GLO1) transcription was observed with higher GLO1 transcription in mice with deleted FKBP5, which was reflected by about two-fold more GLO1 protein in these mice. The efforts in deciphering the role of FKBP5 in elevation of GLO1 expression led to the identification of a duplication of the GLO1 gene inherent to mice with deleted FKBP5; this likely explains the enhanced GLO1 expression in these mice. This observation exemplifies the flanking gene problem and is a note of caution for interpreting data from conventionally generated knock-out mice. Overall, deletion of FKBP5 did not markedly change gene expression.

In the second part of this thesis, the molecular effects of psychopharmacologic drugs were profiled for their dependency on FKBP51 function to modulate intracellular pathways relevant for treatment outcome in a cellular FKBP5 knockout model. For this purpose, psychopharmaca from the classes of SSRIs, SSNRIs, TCAs, atypical

antidepressants, mood stabilisers, and NMDA receptor antagonists were analysed. In addition to GSK3β and AKT, which were reported to interact with and be targeted by FKBP51 recently (Gassen et al., 2015; Pei et al., 2009), ERK was identified as a novel kinase interacting with and being targeted by FKBP51 in this work. With GSK3β, AKT, and ERK, three major kinases were observed to be regulated by psychopharmaca. The effects were not homogeneous across all psychopharmaca and only loosely followed drug classes. Moreover, regulation of these kinases as well as their downstream targets was non-uniformly influenced by FKBP51. With FKBP51 being a stress induced gene, this transcriptional mechanism efficiently links the stress response to the regulation of the targets analysed in this work. Moreover, markers of autophagy, a cellular degradation process which has been linked to neurotransmission, were detected to be regulated by valproic acid (VPA), a mood stabiliser with HDAC inhibitory activity. VPA, as well as a second HDAC inhibitor butyric acid (BUT) enhanced the transcription of late and delayed autophagy markers controlled by FOXO3 signalling.

Considering the versatile action of FKBP51 on targets analysed in this work, the list of proteins modulated by FKBP5 seems by far not complete. The diversity of effects evoked by different psychopharmaca hints to superimposed molecular effects underlying treatment outcome. Better understanding of pathway responsiveness could yield molecular markers for personalised medication that could be utilised to improve treatment outcome in stress related psychiatric diseases.

Contents

1 Introduction

1.1 Physiology of stress disorders

Depressive disorders have been ranked a leading cause of burden (Ferrari et al., 2013). Major depression is a serious and mostly recurrent disorder, strongly impairing quality of life (Ustün et al., 2004). Lifetime prevalence for people from high income countries is about 15 % (Kessler and Bromet, 2013). Major depression represents also an independent risk factor for other diseases like dementia, diabetes, cardiovascular disease and osteoporosis (Knol et al., 2006; Nicholson et al., 2006).

1.1.1 Physiology of the stress reaction

The term stress disorder already implies the fundamental influence of stress in the pathophysiology of a certain group of psychiatric disorders. Stress may arise from all kinds of environmental challenges of physical or psychological nature. In the classical stress concept, every organism needs to adopt to changes of the environment in order to ensure the perpetuation of homeostasis (Chrousos and Gold, 1992). Hence, sensing the stressor and directing the organism to a coping behaviour is an essential strategy of survival. In the concept of allostasis, these dynamic processes not only opt at restoring homeostasis but also include anticipatory mechanisms that prime the organism for future challenges (McEwen, 2000). Effective stress coping includes both the rapid activation of stress response as well as the efficient termination of the stress response afterwards. Overshooting and prolonged stress response, however, can lead to allostatic load and stress related disorders, such as anxiety, depression, schizophrenia or post-traumatic stress disorder (de Kloet et al., 2005).

In mammals, the sensory information derived from a stressor is processed by limbic brain structures including the hippocampus, amygdala and the prefrontal cortex. The stress response itself is then mediated by a fine-tuned hormonal system, which is composed of hormone producing tissues in the hypothalamus, pituitary and adrenal gland and

therefore referred to as hypothalamic-pituitary-adrenal (HPA) axis. Upon perception of a stressor, the paraventricular nucleus of the hypothalamus is activated by the limbic system to synthesise and secrete corticotropin-releasing hormone (CRH) and vasopressin within minutes. One function of CRH is to activate the HPA axis-independent noradrenergic and sympathetic central nervous systems by innervation of the locus coeruleus (Valentino et al., 1983). On the pituitary level of HPA axis signalling, CRH is transported to the anterior lobe of the pituitary via the hypophyseal portal system, where it stimulates the secretion of adrenocorticotropic hormone (ACTH) into the circulatory system (Vale et al., 1981). Acting on the adrenal gland, ACTH exerts the synthesis and secretion of glucocorticoids from the adrenal cortex. This class of steroid hormones, which is mainly represented by cortisol in human and corticosterone in rodents, binds to intracellular steroid hormone receptors, especially the glucocorticoid receptor (GR) and the mineralcorticoid receptor (MR). Activating their receptors, GCs not only trigger adaptional processes in a variety of immunological and metabolic functions by changing gene transcription, but also act on the hypothalamus and the pituitary inhibiting the secretion of CRH and ACTH. This inhibitory mechanism provides a feedback loop for reducing the activity of the HPA axis and the termination of the stress response.

1.1.2 The role of HPA axis dysregulation in stress disorders

Malfunction in HPA-axis has been found in depressive patients, which has led to the definition of the stress hormone dysregulation hypothesis of depression (Holsboer, 2000). This hypothesis originates from clinical observations in depressive patients that show increased secretory pulses and elevated levels of the HPA-axis hormones CRH, ACTH and cortisol. These observations were complemented by monitoring the responsiveness of the HPA-axis with tests of neuroendocrine function, such as the dexamethasone suppression test, the CRH stimulation test and their combination. Diminished suppressibility of corticosteroids by administration of the synthetic glucocorticoid as well as decreased ACTH response after CRH injection are characteristic HPA-axis features in patients with various affective disorders. Moreover, normalisation of HPA axis activity appears to be crucial for therapeutic success in depressive patients (Holsboer et al., 1987).

1.2 FKBP51 in the physiology of stress disorders

Prolonged and excessive activation of the HPA-axis has been implicated in the pathogenesis of mood and anxiety disorders. Therefore, a healthy stress response requires its proper termination, which physiologically is realised via the GR dependent feedback loop acting on the hypothalamus and the pituitary. Of particular importance is hence the fine-tuned molecular system that regulates the activity of the GR (Holsboer, 2000; Pariante and Miller, 2001).

1.2.1 FKBP51 as a regulator of HPA axis activity

The GR is a transcription factor that regulates gene transcription when it is activated by its corticosteroidal ligands. Ligand bound GR shuttles from the cytosol into the nucleus and binds to specific DNA motifs. A switch in the composition of the chaperone complex that binds to the GR tightly controls this translocation and stimulation process (Grad and Picard, 2007). Chaperone complexes ensure the proper folding, maturation and conformation of their target proteins. The GR is associated with a complex of heatshock protein 70 (HSP70), heatshock protein 90 (HSP90) and a number of co-chaperones. In fact, the co-chaperone FK506 binding protein 51 (FKBP51; in this thesis this abbreviation is used for all species) has been found to play a major role in the regulation of the GR complex (Pratt and Toft, 1997).

FKBP51 is a 51 kDa protein encoded by the FKBP5 gene. Together with cyclophilins, FK506 binding proteins (FKBPs) represent the immunophilin protein family named for their ability to bind immunosuppressive drugs. All immunophilins share the common feature of a domain with peptidyl prolyl isomerases activity that is able to catalyse the cis-trans conversion of peptidyl prolyl bonds (FK domain). In addition, FKBP51 is composed of a second FK (FK2) domain that differs slightly from the first FK (FK1) domain and lacks peptidyl prolyl isomerases and FK506 binding ability. C-terminally, FKBP51 provides a tetratricopeptide repeat (TPR) domain, a structural motif that binds to the EEVD motif at the extreme C-terminus of HSP90 (Sinars et al., 2003).

A hint for the importance of FKBP51 in GR signalling was found by the discovery of a differentially regulated HPA axis in New World Monkeys. Compared to other monkeys and primates, intensely increased plasma cortisol levels have been found in these animals. Surprisingly, increased plasma cortisol levels are not accompanied by signs of hyper-cortisolism. The assumption of inhibited affinity of the GR to cortisol in New World Monkeys was substantiated by the detection of FKBP5 overexpression in these

animals together with the elucidation of the role of FKBP51 in regulation of the GR complex (Scammell et al., 2001).

FKBP51 as well as its close homolog FKBP52 bind to the GR HSP90 complex via their TPR domains. After hormone binding, FKBP51 is replaced by FKBP52, which facilitates nuclear translocation and gene transcription by recruiting dynein to the complex (Davies et al., 2005). Overexpression of FKBP5 has been shown to reduce hormone binding affinity and nuclear translocation of the GR by shifting the equilibrium of FKBP51 and FKBP52 associated hormone receptor complexes (Wochnik et al., 2005).

Interestingly, the FKBP5 promoter comprises several intronic glucocorticoid response elements (GREs), which induce transcription upon GR activation (Hubler and Scammell, 2004; U et al., 2004). By this bidirectional regulation, the GR is not only desensitised by the FKBP51 protein but also facilitates the transcription of FKBP5 thereby providing an ultra-short feedback loop in regulation of GR activity (Vermeer et al., 2003). Upon cortisol binding to the GR, FKBP51 is exchanged to FKBP52, which mediates dynein interaction, nuclear translocation, DNA binding and transcriptional activity of the GR. Besides the transcriptional activation of other targets, active GR induces FKBP5 transcription and FKBP51 protein in turn conveys lower GR hormone sensitivity, which terminates the glucocorticoid activity.

1.2.2 FKBP51 in the risk of stress related psychiatric disorders

Based on this molecular evidence, FKBP5 was included as candidate in a genetic association study in major depression. This study provided first evidence for differential FKBP5 expression caused by variations in the FKBP5 gene (Binder et al., 2004). Single nucleotide polymorphisms (SNPs) in the FKBP5 gene were associated with high inducibility of FKBP5 transcription upon GR activity, the recurrence of depressive episodes and reduced HPA-axis hyperactivity during the depressive episode (Binder et al., 2004). Subsequently a lower sensitivity of the GR towards cortisol was found in individuals carrying the SNP associated with the high-induction FKBP5 allele (Binder et al., 2008). Furthermore, this baseline difference in GR sensitivity also affects hormone levels of a stress challenged HPA-axis. A genetic study in stressed healthy individuals showed an association of the highly inducible FKBP5 alleles with a delayed negative feedback represented as a significantly slower recovery from stress-related increases in cortisol levels (Ising et al., 2008).

Differences in allelic expression of FKBP5 might be explained by alterations of interaction of steroid receptors with the intronic GREs in the FKBP5 gene (Hubler and Scammell, 2004; U et al., 2004). Indeed, the SNP rs1360780 that is associated with increased FKPB5 expression is located less than 200 bp from the highly conserved GRE in intron 2 of the FKBP5 gene (Hubler and Scammell, 2004).

These genetic association studies together with the molecular findings provide a mechanism how differences in the FKBP5 genes in the population could prime the individual risk for stress related psychiatric disorders in human. In its two partied function as a cortisol responsive gene on the one hand and a GR sensitivity regulating protein on the other hand, FKBP5 can integrate environmental influences onto genome activity and thus prime the risk for the development of stress related psychiatric disorders. Evidence for the hypothesis that FKBP5 alleles associated with slower return to baseline levels of stress induced cortisol levels increase the risk for stress related psychiatric disorders comes from studies both in mood and anxiety disorders.

The strongest genetic evidence for the role of FKBP5 in stress related psychiatric disorders comes from post-traumatic stress disorder (PTSD), an anxiety disorder resulting from the exposure to a traumatic event. The SNPs rs3800373 and rs1360780 in FKBP5 are associated with the individual risk for increased peri-traumatic dissociation after medical trauma, a prediction factor for PTSD (Koenen et al., 2005; Ozer et al., 2003). Moreover, a potential gene – environment interaction was found for PTSD patients with childhood trauma experience. The four SNPs rs9296158, rs3800373, rs1360780, and rs9470080 interacted with the severity of child abuse as a predictor of adult PTSD symptoms. Interestingly, there were no direct effects of the SNPs on PTSD symptoms and no significant genetic interactions with the level of non–child abuse trauma to predict adult PTSD symptoms (Binder et al., 2008). Childhood trauma in individuals with the high induction FKBP5 allele, however, appears to increase the risk for developing adult PTSD, potentially due to increased GR resistance.

In PTSD patients, however, these same alleles were found to be associated with higher GR sensitivity, which itself is associated with PTSD symptoms (Binder et al., 2008; Yehuda et al., 2004). This hints to a context-dependent effect of the high induction alleles on GR sensitivity. Further support for this hypothesis comes from patients with PTSD that showed reduced FKBP5 mRNA expression, consistent with enhanced GR responsiveness (Yehuda et al., 2009). This environment dependent reversal of FKBP5 function might be explained by epigenetic changes in the FKBP5 gene upon trauma exposure and thus provide a possible molecular framework of how gene – environment interaction shapes the risk for psychiatric disorders.

Besides post translational modification of histones, DNA methylation is one of the major epigenetic marks that alter chromatin structure and thus the accessibility of the DNA to transcriptional regulators. Especially changes in DNA methylation have been reported as long-lasting epigenetic consequences of early trauma (Murgatroyd et al., 2009). In addition, chronic activation of the GR has been shown to induce local changes in DNA methylation, inter alia, at relevant GREs in the FKBP5 locus (Lee et al., 2010). Finally, the observation that combined effects of early life stress and a functional polymorphism in the FKBP5 gene alter the risk for PTSD, provided an example for gene – environment interaction (Klengel et al., 2013). In FKBP risk allele carriers, excessive cortisol release following early life stress exposure led to stronger and stable demethylation around a specific GRE of FKBP5. This resulted in lasting disruption of the ultra-short feedback loop that balances FKBP5 and GR activity, which was accompanied by an increased risk for PTSD in later life.

Associations between FKBP5 polymorphisms and mood disorders, however, are still inconsistent. An over-representation of the high induction alleles in unipolar depression, which was found in both a epidemiologic and a family study, could not be confirmed in several other studies (Binder et al., 2004; Gawlik et al., 2006; Lekman et al., 2008; Papiol et al., 2007; Willour et al., 2009). Disease specific characteristics like weak phenotype definitions and environmental induced disease heterogeneity may contribute to the lack of strong main genetic effects in genome wide association studies. Durable epigenetic changes induced by long term environmental effects, as described for PTSD above, might provide a mechanism that could explain missing heritability in mood disorders as well (Slatkin, 2009).

1.3 Pharmacological treatment of stress disorders

Up to now, worldwide only a minority of people suffering from major depressive disorder receives treatment, and among those treatment outcome remains poor (Kessler, 2012). Conventional medication is based on a hypothesis of pathophysiology developed in the 1960s. As discrepancies arose within this hypothesis on the one hand and treatment response rates remained poor on the other hand, novel pharmacological treatment approaches, however, came into focus (aan het Rot et al., 2009). Taken into account the genetic and environmental induced diversity of stress related psychiatric diseases, a personalised medication strategy would probably largely increase treatment success (Binder and Holsboer, 2006). In order to achieve this, progress has to be made in the characterisation of individual patients on the one hand, and the understanding of mechanism of action of current psychopharmaca as well as the identification of novel drug targets on the other hand.

1.3.1 Treatment approaches based on the monoamine hypothesis

The monoamine deficiency hypothesis, one of the earliest hypotheses of depression pathophysiology, stipulates a deficiency of noradrenergic, serotonergic and/or dopaminergic neurotransmitter in the synaptic cleft as causal factor for the pathophysiology of depression (Carlsson et al., 1968; Dunlop and Nemeroff, 2007; Schildkraut, 1965). Accordingly, rebalancing monoaminergic signalling with an antidepressant would tend to restore normal function in depressed patients.

Historically, the monoamine deficiency hypothesis evolved when antidepressant side effects in tuberculosis patients treated with iproniazid were observed and inhibitory action of iproniazid on the monoamine oxidase was detected, which increased the concentration of norepinephrine in the synaptic cleft by blocking the degradation of monoamines (Zeller et al., 1952). Additionally, the depressogenic side effects of reserpine, a blocker of the vesicular monoamine transporter, supported the involvement of monoamines in depression (Everett and Tolman, 1959). Later on it was shown that the administration of imipramine and imipramine-like agents, early members of the group of tricyclic antidepressants (TCAs), increased norepinephrine concentration in the rodent brain by blocking its cellular uptake (Glowinski and Axelrod, 1964). In the following years also inhibition of serotonin reuptake was shown for imipramine (Carlsson et al., 1968). Since then, several drugs with a tricyclic structure have received FDA approval, amongst them amitriptyline (AMT, doxepin (DXP) and clomipramine (CLP).

After to the promising results obtained with the MAOIs and TCAs, more selective reuptake-inhibitors for serotonin, norepinephrine and dopamine were identified. Finally in 1968, fluoxetine (FLX), one of the first selective serotonin reuptake inhibitors (SSRIs), became available on the market and achieved comparable antidepressant effects along with reduced side effects compared to TCAs (Montgomery, 1989). SSRIs are now the most widely prescribed group of antidepressants in many countries, typically used in the treatment of major depressive disorder and anxiety disorders (Preskorn et al., 2004). Most common SSRIs besides fluoxetine are citalopram (CTP), escitalopram, fluvoxamine, paroxetine (PRX) and sertraline.

In 1993, venlafaxine (VNF), the first non-tricyclic agent with dual serotonin and norepinephrine reuptake inhibition (SNRIs), was introduced to the US market (Gutierrez et al., 2003). The accessory inhibition of norepinephrine reuptake might be causative for the potential of venlafaxine to induce a rapid onset of action in contrast to MAOIs, TCAs, and SSRIs (Ruelas et al., 1997). Additionally to venlafaxine, the most commonly used SNRI, duloxetine, desvenlafaxine and milnacipran became approved members of the group of SNRIs. Recently, vortioxetine (VTX) has been shown to not only inhibit the serotonin reuptake but to also act as partial agonist of the 5-HT_{1A} receptor and antagonist of the 5-HT_3 and 5-HT_7 receptors (Mahableshwarkar et al., 2013). VTX has received FDA approval for the treatment of adults suffering from major depressive disorder in 2013.

The so called second-generation antidepressants with selective reuptake inhibition profiles for serotonin, norepinephrine and dopamine have since then gradually replaced first-generation antidepressants such as MAOIs and TCAs, mostly because of their improved tolerability and safety profile (Spina et al., 2008).

1.3.2 Treatment approaches beyond the monoamine system

It turned out that the monoamine deficiency hypothesis does not cover all the effects antidepressants exert in a biological system. For example the atypical antidepressant tianeptine (TNP), structurally belonging to the group of TCAs, decreases the extracellular monoamine concentration but coinstantaneously exerts antidepressant effects (Lôo et al., 2001). Furthermore, it remains unclear why not all drugs that enhance serotonergic or noradrenergic transmission are necessarily effective in the treatment of depression. Moreover, the monoamine deficiency hypothesis failed to provide reasonable models for the delayed beneficial effect in patients in contrast to the rapid boost in available monoamines within hours (Gardner and Boles, 2010).

Recently, non-monoaminergic biological systems have received increasing attention as potential drug targets in the treatment of mood disorders, amongst them aminoacid neurotransmitter receptors and transporters, neuropeptides and neurotrophic factors (Mathew et al., 2008). Especially the observation that the anaesthetic ketamine (KTM), an NMDA receptor antagonist, has potent antidepressant effects when administered in a single subanesthetic dose has driven attention to the glutamatergic and dopaminergic signalling (Duman et al., 2012; Zarate et al., 2006). Effort has been made to find more selective NMDA receptor antagonists and several substances are in clinical trials now. One of those substances, Lanicemine (LNC), can produce rapid antidepressant effects in subjects with treatment-resistant major depressive disorder without psychomimetic side effects like ketamine (Zarate et al., 2013).

A further class of drugs is used especially for the treatment of bipolar disorder, a subtype of depression characterised by periods of elevated mood and periods of depression. Already more than half a century ago, psychiatric patients were treated with lithium carbonate (LIT), which was reported to cease or reduce symptoms in manic patients (Cade, 1949). In parallel to the introduction of the first SSRIs in the late 1960s, clinical evidence was provided for the effectiveness of LIT therapy in bipolar affective disorder (Baastrup and Schou, 1967). Potential mechanism of LIT action include ion dysregulation, effects on neurotransmitter signalling, inhibition of glycogen synthase kinase 3 beta (GSK3β), interaction with the adenylyl cyclase system as well as inositol and protein kinase C signalling (Marmol, 2008).

Evidence has also been provided for the effectiveness of lamotrigine (LMT), a phenyltriazine derivative used for anticonvulsant medication as a mood stabiliser; LMT has been the first FDA approved drug for this purpose since the approval of LIT almost 30 years earlier (Goldsmith et al., 2003). Approved for treatment of mania in the US in 1995, valproate has since then surpassed LIT as the primary mood stabiliser prescribed for the treatment of bipolar disorder. Several mechanisms of action of valproate that may be relevant to its actions in bipolar disorders have been reported. These include inhibition of GSK3β and activation of extracellular signal-regulated kinase (ERK) (Einat et al., 2003; Yuan et al., 2001). Interestingly, several of these actions overlap with those observed for LIT (Harwood and Agam, 2003).

Moreover, VPA has been shown to modulate the epigenome by inhibiting histone deacetylases (HDACs) and DNA methyltransferase (DNMT) (Göttlicher et al., 2001; Zimmermann et al., 2012). Antidepressant-like effects have been found for HDAC inhibitors (Covington et al., 2009; Schroeder et al., 2007; Tsankova et al., 2006).

Reversal of dysfunctional epigenetic regulation associated with early life events might thus play a role in the mood stabilizing effects of VPA.

1.3.3 FKBP51 as modulator of antidepressant responsiveness

While psychopharmaca are widely prescribed to treat stress-related psychiatric disorders, response to medication is highly variable with only some patients responding to a particular treatment. Besides clinical heterogeneity, diagnostic uncertainty and environmental and social factors, the genetic and epigenetic configuration of individual patients might provide explanations for the poor drug-response rates.

First evidence for a role of FKBP5 in antidepressant treatment response came from a genetic study, which found association of three SNPs in this gene with antidepressant treatment outcome in depressed patients of two independent samples (Binder et al., 2004). Patients homozygous for the high-induction FKBP5 alleles responded faster to treatment with either TCAs or SSRIs. A meta-analysis including data from eight genetic association studies, however, could not validate the association between SNPs rs1360780 and rs3800373 with treatment response, but confirmed a significant association of SNP rs4713916 and response rate in patients with mood disorders (Zou et al., 2010).

The finding that reduced HPA axis hyperactivity after treatment in patients carrying the genotypes associated with faster response alleles combined with the observation that the high induction alleles associated with enhanced GR sensitivity in depressed patients hint to a mechanism where FKBP51 facilitates the normalization of HPA axis hyperactivity upon treatment.

Mechanistic evidence for an FKBP5 dependent treatment response beyond the hypothesised normalization of HPA axis hyperactivity is provided by two of our recent studies. We could show that the protein FKBP51 is required for the effects of both acute and chronic antidepressant treatment on behaviour and on autophagic pathways in mice (Gassen et al., 2014). Furthermore we identified the early stages of autophagy as FKBP5 modulated targets of antidepressants. In a second study we found that deletion of FKBP5 attenuated the behavioural effects of LIT treatment in mice (Gassen et al., 2015). Summarised, these findings point to a multifactorial role of FKBP51 in modulation of treatment response via several pathways targeted by antidepressant drugs.

1.4 Potential cellular pathways affected by FKBP5 and stress or antidepressants

Exposure to chronic stress has been shown to affect brain morphology, neurogenesis, synaptic transmission and structural plasticity, amongst other in the hippocampus (Joëls et al., 2008). Effort has been made to clarify the underlying pathways without gaining a clear picture up to now. At least some of the stress effects can be targeted with antidepressant treatment (Warner-Schmidt and Duman, 2006).

1.4.1 Transcriptional pathways

Transcriptional analysis in models of chronic stress consistently found modifications in the expression of brain-derived neurotrophic factor, cAMP-response-element binding protein, serotonin receptors, HPA axis components, synaptic proteins, transcription factors and proteins involved in neuronal growth and differentiation (Alfonso et al., 2005). Only a minority of the changes could be reversed by blockade of glucocorticoid receptor signalling (Datson et al., 2012). In general, however, these alterations could be reversed by treatment with antidepressants (Alfonso et al., 2005). The particular role of the stress induced protein FKBP51 in regulation of global gene expression, however, has not been addressed so far. At least in its function as a modulator of glucocorticoid induced transcription, FKBP51 should be a regulator of gene transcription.

1.4.2 GSK3β signalling

GSK3β is a serine-threonine kinase that was primarily identified as a glycogen synthase inhibiting enzyme, a key player in energy homeostasis (Cohen and Frame, 2001). Over the years, it became more and more evident that GSK3β plays an important role in developmental processes in the brain, including neurogenesis and neuroprotection (Hur and Zhou, 2010). Regulation of the processes involves the kinase activity of GSK3β onto its wide network of target proteins. GSK3β is a constitutively active kinase and becomes inactivated upon phosphorylation at its N-terminus at Ser-9 (Harwood, 2001). Several kinases including AKT, protein kinase A and protein kinase C as well as the two phosphatases protein phosphatase 2A and protein phosphatase 1 have been shown to control Ser-9 phosphorylation of GSK3β (Harwood, 2001).

Increased GSK3β activity is observed as a pathogenic factor and normalisation of GSK3β activity is considered as therapeutic means in bipolar disorder and schizophrenia (Emamian, 2012; Jope and Roh, 2006). In line, increased activity of GSK3β along with decreased activity of AKT, was found post-mortem in the ventral prefrontal cortex of subjects with major depression (Karege et al., 2007). Accordingly, several mood stabilisers, antidepressants and antipsychotics inhibit GSK3β (Li and Jope, 2010). Furthermore, we recently could show that FKBP51 inhibits GSK3β and auguments the effects of distinct psychotropic medications (Gassen et al., 2015).

A prominent target of GSK3β is β-catenin (BCAT), which primarily has been characterised as an intracellular signal transducer in the Wnt signaling pathway. In this regard, BCAT is phosphorylated by GSK3β at an ubiquitin ligase recognition motif, thereby promoting its proteasomal degradation (Xing et al., 2003). Interestingly, chronic treatment with lithium, a well-known inhibitor of GSK3β, has been shown to increase brain β-catenin levels in rodents (De Ferrari et al., 2003).

Another target of GSK3β is collapsin response mediator protein 2 (CRMP2), which plays an important role in neuronal polarization (Ip et al., 2014). In addition, activity of CRMP2 has been associated with psychiatric diseases and in particular with schizophrenia (Fallin et al., 2005; Yoshimura et al., 2005). Activity of CRMP2 is precisely regulated by phosphorylation status of CRMP2. GSK3β phosphorylates CRMP2 at the Thr-509 and Thr-514 sites in the presence of a priming phosphorylation at Ser-522 (Yoshimura et al., 2005). When phosphorylated at Thr-514, interaction of CRMP2 with tubulin is reduced, which leads to inhibition of neurite extension (Yoshimura et al., 2005).

1.4.3 Autophagy

An important pathway affected by antidepressants is autophagy (Rossi et al., 2009; Zschocke et al., 2011). It is an evolutionary conserved cellular process that controls the functional integrity of cells via the degradation of damaged cytoplasmic proteins and organelles (Mizushima and Komatsu, 2011). The subtype of autophagy reported to be affected by antidepressants is macroautophagy. It is characterised by the engulfment of autophagic cargo by membranous structures leading to the formation of autophagosomes, which subsequently fuse with a protease-providing lysosome.

The initiation of autophagy is mediated by the ULK1 complex, which serves as a hub for the integration of upstream signals to the downstream PI3K effector complex (Alers et

al., 2012). Activation of ULK1 results in the phosphorylation of Beclin-1 (BECN1) and a subsequent increase in the activity of the VPS34 complex (Russell et al., 2013). We recently could show, that the autophagy and apoptosis regulating phosphorylation of BECN1 by AKT is dependent on FKBP51 (Gassen et al., 2014; Wang et al., 2012).

Autophagosome formation is tightly controlled by a series of autophagy proteins (ATGs). Precursor vesicles containing a complex of ATG5 - ATG12 - ATG16L1 fuse to form a sac-like single membrane covered pre-autophagosomal structure called phagophore (Puri et al., 2013). Important for the recruitment of membrane to the growing phagophore is the incorporation and processing of microtubule-associated protein 1 light chain 3 (LC3) into the membrane. LC3 is, in a first step, cleaved to form LC3-I and in a second step conjugated to phosphatidylethanolamine to form LC3-II (Kabeya et al., 2000). LC3-II remains associated with the closing membrane globe that imbeds substrates for degradation. Furthermore LC3 plays a role in the recruitment of the adaptor protein p62 (Noda et al., 2008). Upon maturation and fusion of the autophagosomes with lysosomes, the autophagic substrates become digested and recycled.

An additional level of autophagy regulation is represented by transcriptional control of the ATG genes via members of the family of forkhead box O (FOXO) transcription factors. Especially FOXO3α is involved in promoting autophagy upon nutrient deprivation (Sengupta et al., 2009). Activity of FOXO3α is mainly regulated by phosphorylation, amongst others at Ser-256, Ser-318 and Ser-321 by AKT (Rena et al., 2002). When phosphorylated, FOXO3α is exported from the nucleus and thus becomes transcriptionally inactive.

1.4.4 ERK signalling

The Extracellular Signal-regulated Kinases ERK1 and ERK2 belong to the family of mitogen-activated protein kinases, that play a role in various cellular processes such as proliferation, differentiation, survival and apoptosis (Sun et al., 2015). Moreover, it was also reported that the ERK pathway plays a role in AMPK induced autophagy regulation via BECN1 (Wang et al., 2009). Recently, also an unconventional regulation of ERK phosphorylation by autophagic ATG proteins as cellular scaffolds was reported (Martinez-Lopez et al., 2013). Furthermore, ERK has been shown to inhibit FOXO3α via phosphorylation at Ser-294, Ser-344 and Ser-425 (Yang et al., 2008).

ERK activity itself is tightly regulated by the dual specificity mitogen-Activated Protein kinases 1 AND 2 via phosphorylation at Thr-202 and Thr-204 (Rubinfeld and Seger,

2005). Because of the high similarity of their sequences, it has long been a matter of debate whether ERK1 or ERK2 are functionally redundant (Lefloch et al., 2009).

In the last decade, ERK signalling has been implicated in depression (Duric et al., 2010; Dwivedi et al., 2001; Einat et al., 2003; Qi et al., 2009). Furthermore, differential effects of antidepressant treatment on ERK phosphorylation were reported (Di Benedetto et al., 2013; Fumagalli et al., 2005; Zassadowski et al., 2015). However, cell type, treatment duration and drug class appear to be important factors determining the changes in ERK phosphorylation.

1.5 Objective

FKBP51 is a major regulator of the GR and shapes its hormone affinity. This mechanism has been shown to be important for the regulation of the mammalian stress response and to be implicated in the pathophysiology of stress related psychiatric disorders. Effects of FKBP51 on kinases were also reported recently.

1.5.1 Does FKBP5 modulate transcription of risk genes?

The first objective of this thesis was to analyse FKBP5 dependent effects on global gene transcription in an unbiased approach. Differential transcriptional effects may be induced by FKBP51 either directly via regulation of GR mediated transcription or indirectly through yet largely unknown pathways, conceivably through the wide effects on kinase activity. The aim was to compare the expression profile of FKBP5-KO and FKBP5-WT mice and in the next step to characterise the regulation of differentially expressed genes. Those genes would be considered additional candidates potentially underlying the pathophysiology of psychiatric disorders.

1.5.2 Do different psychopharmaca affect overlapping pathways subjected to FKBP5?

In a second study, the impact of several psychopharmaca from different drug groups on selected pathways was to be analysed on the protein level. In order to unravel a potential effect of FKBP5 on the induction of the protein markers by those psychopharmaca, embryonal fibroblast cells deficient of FKBP5 as well as wild type equivalents were to be utilised.

Prior to this study, it was published that FKBP51 interacts with the kinase AKT and modulates its phosphorylation status by recruiting PHLPP phosphatase (Pei et al., 2009). Further evidence for a global role of FKBP51 in modulating kinase activity was provided by a screening experiment that showed that FKBP51 is present in several HSP90 dependent client complexes, in particular in HSP90:kinase complexes (Taipale et al., 2010). Given the clinical observation that FKBP5 impacts on the antidepressant response, molecular pathways affected both by FKBP5 and psychopharmaca were searched for. FKBP5 dependent action of psychopharmaca on molecular markers could provide a mechanism for the role of FKBP51 in antidepressant response. In two recent publication

we could show that the proteins AKT, BECN1 and GSK3β are convergently targeted by FKBP51 and the psychopharmaca PRX and LIT (Gassen et al., 2014, 2015). Interestingly, AKT as well as GSK3β have both already been discussed as psychopharmaca targets downstream of the D2 dopamine receptor (Beaulieu et al., 2009).

2 Material

2.1 Consumable supplies

Type	Manufacturer
Cell culture dishes, multi-well plates	TPP (Trasadingen, Switzerland)
Cell scrapers sterile	Peske (Aindlingen-Arnhofen)
Centrifugation tubes 50 mL, 15 mL	TPP (Trasadingen, Switzerland)
Cryotubes 2 mL	TPP (Trasadingen, Switzerland)
Electroporation cuvettes	Bio-Rad Laboratories (München)
Eppendorf reaction tubes 1.5 mL, 2 mL	TPP (Trasadingen, Switzerland)
Eppendorf reaction tubes 1.5 mL, low-binding	Eppendorf (Wesseling-Berzdorf)
Eppendorf reaction tubes 1.5 mL, safe-lock	Eppendorf (Wesseling-Berzdorf)
Filter paper 3 MM Whatman	Carl Roth (Karlsruhe)
Folded filter	Carl Roth (Karlsruhe)
Glass slides	Carl Roth (Karlsruhe)
Luminometer plate 96 well (white)	Nalgene Nunc International (USA)
Nitrocellulose membrane	GE Healthcare (Freiburg)
Pasteur pipettes 230 mm	Carl Roth (Karlsruhe)
Petri dishes unsterile	TPP (Trasadingen, Switzerland)
Pipette Stripette 1, 5, 10, 25 mL	Corning Inc. (Acton, USA)
Pipette tips 0.5-10 µL, 5-200 µL, 100-1000 µL	Corning Inc. (Acton, USA)
Plastic supplies for tissue culture	TPP (Trasadingen, Switzerland)
Serological pipettes 2, 5, 10, 25 mL	Peske (Aindlingen-Arnhofen)

Table 1: **List of consumable supplies.**

2.2 Chemicals and solutions

Type	Manufacturer
Acetic acid (CH3COOH)	Sigma-Aldrich (St. Louis, USA)
Acrylamide/Bis Solution, 37.5:1 (30% w/v)	Serva (Heidelberg)
Adenosine 5‘-triphosphate (ATP)	Sigma-Aldrich (St. Louis, USA)
Agar agar	Carl Roth (Karlsruhe)
Agarose	Biozym (Oldenburg)
AhR Inhibitor αNaphtovlavone	Sigma-Aldrich (St. Louis, USA)
Amitriptyline hydrochloride	Sigma-Aldrich (St. Louis, USA)
Ammonium sulfate	Carl Roth (Karlsruhe)
Ammonium persulfate (APS)	Carl Roth (Karlsruhe)
Ampicillin	Sigma-Aldrich (St. Louis, USA)
Antibiotic-antimycotic (100x)	Life Technologies (Carlsbad, USA)
Bafilomycin A1	Sigma-Aldrich (St. Louis, USA)
Bovine Serum Albumin (BSA)	Sigma-Aldrich (St. Louis, USA)
Brilliant blue G	Sigma-Aldrich (St. Louis, USA)
Bromophenol blue	Sigma-Aldrich (St. Louis, USA)
Calcium chloride (CaCl2 · 2 H2O)	Carl Roth (Karlsruhe)
Citalopram hydrobromide	Sigma-Aldrich (St. Louis, USA)
Clomipramine hydrochloride	Sigma-Aldrich (St. Louis, USA)
Coenzyme A	Sigma-Aldrich (St. Louis, USA)
Coomassie Brillant Blue G	Sigma-Aldrich (St. Louis, USA)
Deoxynucleotide triphosphates (dNTPs)	Peqlab (Erlangen)
Dexamethasone	Sigma-Aldrich (St. Louis, USA)
Dipotassium phosphate (K2HPO4 · 3 H2O)	Carl Roth (Karlsruhe)
Disodium phosphate (Na2HPO4)	Carl Roth (Karlsruhe)
DME medium	Life Technologies (Carlsbad, USA)
DMSO (dimethyl sulfoxide)	Sigma-Aldrich (St. Louis, USA)
Doxepine hydrochloride	Kemprotec (Cumbria, U.K.)
DTT (1,4-Dithiothreitol)	Carl Roth (Karlsruhe)
Ethanol absolute p.a.	Sigma-Aldrich (St. Louis, USA)
Ethidium bromide	Sigma-Aldrich (St. Louis, USA)
Ethylene glycol tetraacetic acid (EGTA)	Carl Roth (Karlsruhe)
Fetal bovine serum	Life Technologies (Carlsbad, USA)
Fluoxetine hydrochloride	Sigma-Aldrich (St. Louis, USA)
Gentamycine	Life Technologies (Carlsbad, USA)
Glucose	Carl Roth (Karlsruhe)
Glycerol	Merck Millipore (Darmstadt)

Type	Manufacturer
Glycin	Sigma-Aldrich (St. Louis, USA)
GSK3 Inhibitor CHIR99021	Merck Millipore (Darmstadt)
Hydrochloric acid (HCl)	Merck Millipore (Darmstadt)
IGEPAL	Sigma-Aldrich (St. Louis, USA)
Isopropyl alcohol	Sigma-Aldrich (St. Louis, USA)
Isopropyl-β-D-1-thiogalactopyranoside (IPTG)	Peqlab (Erlangen)
Ketamine	Sigma-Aldrich (St. Louis, USA)
Lamotrigine	Sigma-Aldrich (St. Louis, USA)
Lanicemine hydrochloride	Kemprotec (Cumbria, U.K.)
Lithium chloride	Sigma-Aldrich (St. Louis, USA)
Magnesium chloride (MgCl2)	Carl Roth (Karlsruhe)
Magnesium sulfate (MgSO4)	Merck Millipore (Darmstadt)
Methanol	Sigma-Aldrich (St. Louis, USA)
Milk powder	Carl Roth (Karlsruhe)
MTT dye	Sigma-Aldrich (St. Louis, USA)
Paraformaldehyde (PFA)	Carl Roth (Karlsruhe)
Paroxetine hydrochloride	Sigma-Aldrich (St. Louis, USA)
PBS (10x)	Life Technologies (Carlsbad, USA)
Phosphoric Acid, 85%	Sigma-Aldrich (St. Louis, USA)
PMSF (Phenylmethylsulfonyl fluoride)	Sigma-Aldrich (St. Louis, USA)
Poly-D-lysine	Sigma-Aldrich (St. Louis, USA)
Potassium acetate	Carl Roth (Karlsruhe)
Potassium chloride (KCl)	Carl Roth (Karlsruhe)
Potassium hydroxide (KOH)	Carl Roth (Karlsruhe)
Ribonuclease A	Sigma-Aldrich (St. Louis, USA)
S.O.C. medium	Life Technologies (Carlsbad, USA)
Sodium butyrate (BUT)	Sigma-Aldrich (St. Louis, USA)
Sodium chloride (NaCl)	Carl Roth (Karlsruhe)
Sodium dodecyl sulfate (SDS)	Fluka (USA)
Sodium hydroxide (NaOH)	Merck Millipore (Darmstadt)
Sodium pyruvate (100x)	Life Technologies (Carlsbad, USA)
TEMED (Tetramethylethylenediamine)	Carl Roth (Karlsruhe)
Tianeptine	Kemprotec (Cumbria, U.K.)
Trichostatin A (TSA)	Sigma-Aldrich (St. Louis, USA)
Tris-(hydroxymethyl)-aminomethane (Tris)	Riedel-de Haen (Seelze)
Triton X-100	Carl Roth (Karlsruhe)
Trypan blue (5x)	Carl Roth (Karlsruhe)
Trypsin-EDTA solution (10x)	Life Technologies (Carlsbad, USA)
Tween 20	Sigma-Aldrich (St. Louis, USA)

Type	Manufacturer
Valproic Acid	Sigma-Aldrich (St. Louis, USA)
Venlafaxine hydrochloride	Kemprotec (Cumbria, U.K.)
Vortioxetine hydrobromide	Sigma-Aldrich (St. Louis, USA)
β-Mercaptoethanol	Sigma-Aldrich (St. Louis, USA)

Table 2: **List of chemicals and solutions.**

2.3 Buffer and self-made media

Amaxa electroporation buffer

90 mM	Sodium phosphate
5 mM	KCl
0.15 mM	$CaCl_2$
50 mM	Hepes
	pH adjusted to 7.3

Bacterial freezing medium

50 %	Glycerol
50 %	LB medium

CoIP buffer

20 mM	Tris-HCl, pH 8.0
100 mM	NaCl
1 mM	EDTA
0.5 %	Igepal
1 x	Protease inhibitor cocktail (Sigma, P2714)

5 x DNA loading buffer

5 %	Glycerol
0.5 %	SDS
10 mM	EDTA
0.025 %	Bromophenol blue
0.025 %	Xylene cyanol

FLuc buffer (optimised)

40 mM	Tris-HCl
15 mM	$MgSO_4$
4 mM	EGTA
0.2 mM	Coenzyme A
2 mM	DTT
1 mM	ATP
0.2 mM	Luciferin
	pH adjusted to 7.8 with HCl

FLuc buffer (traditional)

3 mM	$MgCl_2$
2.5 mM	ATP
0.2 mM	Luciferin

Freezing medium

40 %	DMEM
50 %	FCS
10 %	DMSO

GenePulser electroporation buffer

50 mM	Potassium phosphate, pH 7.35
20 mM	KAc, pH 7.35
25 mM	$MgSO_4$, pH 6.7

PLP

0.2 %	Triton X-100
100 mM	Potassium phosphate, pH 7.8

solubilisation buffer

20 % (w/v)	SDS
50 % (v/v)	DMF
50 % (v/v)	H_2O
	pH adjusted to 2.0 with HCl

RLuc buffer

1.1 M	NaCl
2.2 mM	EDTA
220 mM	Potassium phosphate
0.44 g/l	BSA
5.72 µM	Coelenterazine
	pH adjusted to 5.1 with HCl

S1 buffer

50 mM	Tris-HCl
10 mM	EDTA, pH 8.0
100 µg/µl	RNase A

S2 buffer

200 mM	NaOH
1 %	SDS

S3 buffer

2.8 M	KAc, pH 5.1

TBE buffer

9 mM	Boric acid
0.25 mM	EDTA
9 mM	Tris-HCl
	pH adjusted to 8.3

TfB I

30 mM	KAc, pH 8.5
100 mM	RbCl
50 mM	$MnCl_2$
10 mM	$CaCl_2$
15 %	Glycerol
	pH adjusted to 5.8

TfB II	
10 mM	MOPS-KOH, pH 6.8
100 mM	RbCl
75 mM	$CaCl_2$
15 %	Glycerol
	pH adjusted to 6.5

2.4 Kits and ready-to-use materials

Type	Manufacturer
Albumin Standard	Thermo Scientific (Rockford, USA)
BCA Protein Assay	Thermo Scientific (Rockford, USA)
BSA (100x) for restriction of DNA	NEB (Frankfurt)
Dynabeads Protein G	Life Technologies (Frankfurt)
EndoFree Plasmid Maxi Kit	Qiagen (Hilden)
EZ-PCR Mycoplasma Test Kit	Biological Industries (Frankfurt)
GeneArt Site-Directed Mutagenesis System	Life Technologies (Frankfurt)
Genomic DNA from Tissue	Macherey-Nagel (Düren)
Immobilon ECL reagent	Merck Millipore (Darmstadt)
LDH Cytotoxicity Detection Kit	Clontech (Paris, France)
NEBuffers 1-4 for restriction of DNA	NEB (Frankfurt)
NucleoBond AX100 Columns	Macherey-Nagel (Düren)
peqGOLD DNA ladder mix	Peqlab (Erlangen)
peqGOLD Prestained Protein-Marker IV	Peqlab (Erlangen)
Protease inhibitor cocktail	Sigma-Aldrich (St. Louis, USA)
QIAquick Gel Extraction Kit	Qiagen (Hilden)
RNA isolation kit	Macherey-Nagel (Düren)

Table 3: **List of kits and ready-to-use materials.**

2.5 Cloning enzymes

Type	Manufacturer
Herculase II Fusion DNA Polymerase	Agilent Technologies (Santa Clara, USA)
Restriction Endonucleases	NEB (Frankfurt)
T4-DNA Ligase	NEB (Frankfurt)
Taq DNA Polymerase	Life Technologies (Frankfurt)

Table 4: **List of cloning enzymes.**

2.6 Antibodies

2.6.1 Primary antibodies

Type	Manufacturer
Anti-Actin	Santa Cruz Biotech. (Heidelberg)
Anti-Akt	Cell Signaling (Cambridge, U.K.)
Anti-BCAT	BD Biosciences (Franklin Lakes, USA)
Anti- BECN1	Cell Signaling (Cambridge, U.K.)
Anti-CRMP2	Cell Signaling (Cambridge, U.K.)
Anti-pCRMP2(T514)	Cell Signaling (Cambridge, U.K.)
Anti-ERK1	Cell Signaling (Cambridge, U.K.)
Anti-Fkbp51	Bethyl Laborat. (Montgomery, USA)
Anti-Fkbp52	Bethyl Laborat. (Montgomery, USA)
Anti-Flag	Biomol (Hamburg)
Anti-FoxO3a	Cell Signaling (Cambridge, U.K.)
Anti-Glo1	Santa Cruz Biotech. (Heidelberg)
Anti-GSK3b	Cell Signaling (Cambridge, U.K.)
Anti-HA	Roche (Basel, Switzerland)
Anti-Hsp90	Santa Cruz Biotech. (Heidelberg)
Anti-JunB	Cell Signaling (Cambridge, U.K.)
Anti-LC3	Cell Signaling (Cambridge, U.K.)
Anti-MEK1	Cell Signaling (Cambridge, U.K.)
Anti-Myc	Sigma-Aldrich (St. Louis, USA)

Type	Manufacturer
Anti-pAkt(S473)	Cell Signaling (Cambridge, U.K.)
Anti-pERK1/2(T202/Y204)	Cell Signaling (Cambridge, U.K.)
Anti-pFoxO3a(S318/S321)	Cell Signaling (Cambridge, U.K.)
Anti-pGR(S211)	Sigma-Aldrich (St. Louis, USA)
Anti-pGR(S226)	Sigma-Aldrich (St. Louis, USA)
Anti-pGSK3b(S9)	Cell Signaling (Cambridge, U.K.)
Anti-pJunB(S259)	Cell Signaling (Cambridge, U.K.)
Anti-pMSK1(T581)	Cell Signaling (Cambridge, U.K.)
Anti-pRSK1(T359/S363)	Merck Millipore (Darmstadt)
Anti-pSGTA(S305)	Cell Signaling (Cambridge, U.K.)

Table 5: **List of primary antibodies.**

2.6.2 Secondary antibodies

Type	Manufacturer
Donkey anti-goat Alexa Fluor 488	Life Technologies (Frankfurt)
Goat anti-mouse HRP	Santa Cruz Biotech. (Heidelberg)
Goat anti-rabbit HRP	Santa Cruz Biotech. (Heidelberg)

Table 6: **List of secondary antibodies.**

2.7 Bacterial clades

Type	Genetic description
E. coli BL21(DE3)pLysS	B F- dcm ompT hsdS(r B-;m B-) galß(DE3)[pLysS Cam`]
E. coli DH5α	F-Φ80LacZΔM15Δ(lacZYA-argF)U169 deoR recA1 endA1 hsdR17 (r k-;m r+) phoA supE44 thi-1gyrA96relA1

Table 7: List of bacterial clades

2.8 Cell lines

Type	origin
HEK-293	Human kidney cells
HeLa	Human cervix carcinoma cells
MEF	Mouse embryonal fibroblasts
MEF-FKBP51$^{-/-}$	Mouse embryonal fibroblasts from FKBP51$^{-/-}$ animals

Table 8: **List of cell lines.**

2.9 Oligonucleotides

Name	Sequence (5' – 3')	Purpose
actin 1as	CAGGTCCAGACGCAGGATGGC	qRT
actin 1s	CTACAATGAGCTGCGTGTGGC	qRT
Atg12_M_RT_1_fw	AACAAAGAAATGGGCTGTGGAGCG	qRT
Atg12_M_RT_1_rv	TTCCGAGGCCACCAGTTTAAGGAA	qRT
Becn1_M_RT_1_fw	TGAAATCAATGCTGCCTGGG	qRT
Becn1_M_RT_1_rv	CCAGAACAGTATAACGGCAACTCC	qRT
FKBP51_H_RT_f	CCATTGCTTTATTGGCCTCT	qRT
FKBP51_H_RT_r	GGATATACGCCAACATGTTCAA	qRT
Fkbp51-M-RT-for	TGCAGATCTCCATGTGCCAGAGG	qRT
Fkbp51-M-RT-for_2	AGCAACGGTAAAAGTCCACCT	qRT
Fkbp51-M-RT-rev	GCTCCTTCTACAGCCTTCTTGCTCC	qRT
Fkbp51-M-RT-rev_2	CCCAACAACGAACACCACATC	qRT
Fkbp51Ex2-fw	AAAGGACAATGACTACTGATGAGG	genotyping
Fkbp51Int2/3-re	AAGGAGGGGTTCTTTTGAGG	genotyping
Fkbp51WT-M-RT-f	CCATGACTGAGCAGGGTGAAG	qRT
Fkbp51WT-M-RT-r	CCAAACATTGGGGCCTCGTC	qRT
FKBP52_H_RT_f	CATTGCCATAGCCACCATGAA	qRT
FKBP52_H_RT_r	TCCAGTGCAACCTCCACGATA	qRT
FKBP5-HR-f_1	ACCAAAGAAAAACTGGAGCAGGC	qRT
FKBP5-HR-r_1	GTAGCACATGGCCAGGTTGAG	qRT
GAPDH_H_RT_f	AATGGGCAGCCGTTAGGAAA	qRT
GAPDH_H_RT_r	ACCAGAGTTAAAAGCAGCCC	qRT

Name	Sequence (5’ – 3’)	Purpose
GAPDH_M_RT_f	TCCATGACAACTTTGGCATTGTGG	qRT
GAPDH_M_RT_r	GTTGCTGTTGAAGTCGCAGGAGAC	qRT
LC3B_M_RT_1_fw	TCGCCGACCGCTGTAAG	qRT
LC3B_M_RT_1_rv	CTCGATGATCACCGGGATCT	qRT
GLO1-H-RT-f_1	TCCCCGCCATGATTCACATT	qRT
GLO1-H-RT-f_2	TCTTCCCCGCCATGATTCAC	qRT
GLO1-H-RT-r_1	AGCAGTACAAGCACGGTTGG	qRT
GLO1-H-RT-r_2	AGTACAAGCACGGTTGGCAT	qRT
GLO1-R-RT-f_1	TCTTGGACTGACGCTTCTCC	qRT
GLO1-R-RT-r_1	TGTCCTCTCCGTCTTGTCCT	qRT
GLO1-R-RT-r_2	GAGCTCCAGGGTAGCCTTTC	qRT
Glo1-RT-for	TGCCGTTCCTGATGTCTACAGTGCC	qRT
Glo1-RT-rev	TCCCCCATACCTCAAAGGCACATTC	qRT
GR_H_seq1_f	TACCACAGACCAAAGCACCTT	seq
GR_H_seq2_r	TCCGGTAAAATGAGAGGCTT	seq
GR1-515_pEGFP_f	CTACAGGAGTCTCACAAGAAACCTCTGAAAATCCT TGAGGTACCGCGGGCCCGGGATCCACCGGATCTAG	cloning
GR1-515_pEGFP_r	CTAGATCCGGTGGATCCCGGGCCCGCGGTACCTCA AGGATTTTCAGAGGTTTCTTGTGAGACTCCTGTAG	cloning
GR1-515_pRK7_f	CTACAGGAGTCTCACAAGAAACCTCTGAAAATCCT TGACTGCCTTAATAAGAATGGTTGCCTTAAAGAAA	cloning
GR1-515_pRK7_r	TTTCTTTAAGGCAACCATTCTTATTAAGGCAGTCAA GGATTTTCAGAGGTTTCTTGTGAGACTCCTGTAG	cloning
GR-A211_f	AGGTCTGATCTCCAAGGAGCCTCATTCGTCTCTTTA C	mutation
GR-A211_r	GTAAAGAGACGAATGAGGCTCCTTGGAGATCAGAC CT	mutation
GR-A226_new_f	TTCTCCCGCCAGAGGAGCAAGCAAACAGTTTTCAT C	mutation
GR-A226_new_r	GATGAAAACTGTTTGCTTGCTCCTCTGGCGGGAGA A	mutation
GR-E211_f	AGGTCTGATCTCCAAGGCTCCTCATTCGTCTCTTTA C	mutation
GR-E211_r	GTAAAGAGACGAATGAGGAGCCTTGGAGATCAGA CCT	mutation
GR-E226_f	TTCTCCCGCCAGAGGCTCAAGCAAACAGTTTTCATC	mutation
GR-E226_r	GATGAAAACTGTTTGCTTGAGCCTCTGGCGGGAGA A	mutation
HPRT R+M as	CCTGTATCCAACACTTCGAG	qRT
HPRT R+M s	AACGGGGGACATAAAAGTTA	qRT
HPRT_H_RT_f	TTGCTTTCCTTGGTCAGGCA	qRT

Name	Sequence (5’ – 3’)	Purpose
HPRT_H_RT_r	TTCGTGGGGTCCTTTTCACC	qRT
NPSR1-CNV_f	CAGCTGCTGCCCCGGCTAAC	gDNA
NPSR1-CNV_r	GGTTGGCTGGCATGGCTCAGG	gDNA
GLO1-CNV_f	CTCTGCCCCAGAGAACAGTC	gDNA
GLO1-CNV_r	TGATAGAGGCCACACAGCAG	gDNA
ULK1_M_RT_1_fw	TGCCCTTGATGAGATGTTCC	qRT
ULK1_M_RT_1_rv	AGTCTCCTCTCAATGCACAGC	qRT
VPS34_M_RT_1_fw	TGTCAGATGAGGAGGCTGTG	qRT
VPS34_M_RT_1_rv	CCAGGCACGACGTAACTTCT	qRT

Table 9: **List of oligonucleotides.**

2.10 Plasmids

Name	Feature	Source	Backbone
ERK1-HA	expression of HA-tagged ERK1 in mammalian cells	Plasmid obtained from addgene.org	pMT
FHRE-FLuc	FLuc under control of Foxo3a responsive promoter	Plasmid obtained from addgene.org	
FKBP51-FLAG	expression of FLAG-tagged FKBP51 in mammalian cells	Plasmid obtained from addgene.org	
Gaussia-KDEL	SV40-driven gaussia luciferase reporter plasmid	Plasmid obtained from G. Wochnik	pRK5
GR(A211)-GFP	expression of point-mutated GFP-tagged GR in mammalian cells	subcloned from GR-GFP	pEGFP
GR(A211)-HA	expression of point-mutated HA-tagged GR in mammalian cells	subcloned from GR-HA	pRK7
GR(A211,A226)-GFP	expression of point-mutated GFP-tagged GR in mammalian cells	subcloned from GR-GFP	pEGFP
GR(A211,A226)-HA	expression of point-mutated HA-tagged GR in mammalian cells	subcloned from GR-HA	pRK7
GR(A211,E226)-GFP	expression of point-mutated GFP-tagged GR in mammalian cells	subcloned from GR-GFP	pEGFP
GR(A211,E226)-HA	expression of point-mutated HA-tagged GR in mammalian cells	subcloned from GR-HA	pRK7
GR(A226)-GFP	expression of point-mutated GFP-tagged GR in mammalian cells	subcloned from GR-GFP	pEGFP

Name	Feature	Source	Backbone
GR(A226)-HA	expression of point-mutated HA-tagged GR in mammalian cells	subcloned from GR-HA	pRK7
GR(E211)-GFP	expression of point-mutated GFP-tagged GR in mammalian cells	subcloned from GR-GFP	pEGFP
GR(E211)-HA	expression of point-mutated HA-tagged GR in mammalian cells	subcloned from GR-HA	pRK7
GR(E211,A226)-GFP	expression of point-mutated GFP-tagged GR in mammalian cells	subcloned from GR-GFP	pEGFP
GR(E211,A226)-HA	expression of point-mutated HA-tagged GR in mammalian cells	subcloned from GR-HA	pRK7
GR(E211,E226)-GFP	expression of point-mutated GFP-tagged GR in mammalian cells	subcloned from GR-GFP	pEGFP
GR(E211,E226)-HA	expression of point-mutated HA-tagged GR in mammalian cells	subcloned from GR-HA	pRK7
GR(E226)-GFP	expression of point-mutated GFP-tagged GR in mammalian cells	subcloned from GR-GFP	pEGFP
GR(E226)-HA	expression of point-mutated HA-tagged GR in mammalian cells	subcloned from GR-HA	pRK7
GR-GFP	expression of GFP-tagged GR in mammalian cells	Plasmid obtained from G. Wochnik	pEGFP
GR-HA	expression of HA-tagged GR in mammalian cells	Plasmid obtained from G. Wochnik	pRK7
MMTV-FLuc	FLuc under control of MMTV promoter	Plasmid obtained from G. Wochnik	
pRK5-SV40-MCS	Cloning vector for protein expression in mammalian cells.	Plasmid obtained from G. Wochnik	pRK5
TCF/LEF-FLuc	FLuc under control of TCF/LEF responsive promoter	Plasmid obtained from addgene.org	

Table 10: **List of plasmids.**

2.11 Instruments

Name	Manufacturer
Allegra 21	Beckman (Krefeld)
Allegra X-22R	Beckman (Krefeld)
Axioplan 2	Carl Zeiss (Jena)
Balance Voyager 50187	Ohaus (Giessen)
Biofuge pico	Heraeus (Mannheim)

Name	Manufacturer
Centro Luminometer	Berthold Tech. (Bad Wildbad)
ChemiDoc Imaging System	Bio-Rad Laboratories (München)
CK30	Olympus (Hamburg)
Electroporation System, Gene Pulser II	Bio-Rad Laboratories (München)
High-voltage power supply PowerPac 400	Bio-Rad Laboratories (München)
Incubator CB210	Binder (Tuttlingen)
IX50	Olympus (Hamburg)
J2 MC (Rotor JA-14)	Beckman (Krefeld)
LSM FV1000	Olympus (Hamburg)
Magnetic stirrer RCT basic IKAMAG	Labortechnik (Staufen)
Microplate reader MR 7000	Dynatech (Denkendorf)
Mini Trans-Blot Cell	Bio-Rad Laboratories (München)
Mini-PROTEAN Electrophoresis system	Bio-Rad Laboratories (München)
Overhead stirrer Rotamix	ELMI (Latvia)
pH meter pH538	WTW (Weilheim)
Pipettes PIPETMAN	Gilson (Middletown, USA)
Refrigerated centrifuge (5417 R)	Eppendorf (Wesseling-Berzdorf)
Refrigerated centrifuge (5804 R)	Eppendorf (Wesseling-Berzdorf)
Sonicator, Cell Disruptor B15	Branson (USA)
Spectrophotometer DU 640	Beckman (Krefeld)
Stirrer DUOMAX 1030/POLYMAX1040	Heidolph (Schwabach)
Supplies for agarose gels	Bio-Rad Laboratories (München)
Thermocycler Primus 25	Peqlab (Erlangen)
Thermocycler Tgradient	Biometra (Göttingen)
Thermomixer comfort	Eppendorf (Wesseling-Berzdorf)
TriStar LB941 Luminometer	Berthold Tech. (Bad Wildbad)
TSC SP5	Leica (Solms)
Ultracentrifuge LB-70M (Rotor: SW 60 Ti)	Beckman (Krefeld)
UV-Transilluminator	Stratagene (La Jolla, USA)
UV-Transilluminator GelDoc	Bio-Rad Laboratories (München)
Varifuge 3.0R	Heraeus (Mannheim)
Vortexer MS2 IKA	Labortechnik (Staufen)
Voyager 50228 (Precision balance)	Ohaus (Giessen)
Water bath type 1008	Ges. f. Labortechnik (Burgwedel)

Table 11: **List of instruments.**

2.12 Software

Name	Application
Adobe Acrobat 8.0	Creating and editing pdf-files
Gimp 2.8	Image processing
Image Lab 5.0	Device control and data analysis for ChemiDoc imaging system
Inkscape 0.48	Vector graphic design
MikroWin 2013	Device control and data analysis for Tristar plate reader
MS Office 2013	Office suite for desktop application
Sigma Plot 12.5	Statistical analysis

Table 12: **List of software.**

3 Methods

3.1 Bacterial culture

3.1.1 Culturing and storage of bacteria

Escherichia coli (*E. coli*) bacteria of the clades DH5α and BL21 were streaked on agar plates with semi-solid medium to generate discrete colonies. Antibiotics ampicillin or kanamycin was added to the medium in a final concentration of 100 μg/ml or 25 μg/ml respectively in order to select for cells containing the plasmid of choice. Liquid cultures containing antibiotics were inoculated with a single colony or directly from glycerol stocks and cultured on a shaker at 200 rpm. Bacteria were cultured in LB medium at 37 °C. Optical density of liquid cultures was measured in a photometer at 550 nm to determine bacteria concentration. Cells were harvested at 3200 g at 4 °C for 10 min. Storage of bacteria was achieved by re-suspending the pellet of a fresh 5 ml overnight culture in 1 ml bacterial freezing medium. The glycerol stocks were stored at -80 °C.

3.1.2 Preparation of competent cells

Competent cells are needed for incorporation of plasmid DNA. Chemically competent bacterial cells of the strain DH5α were generated as follows: Cells were grown in 5 ml LB medium overnight. 5 ml pre-culture was transferred into 400 ml LB medium and cultivated until an optical density of 0.48 was reached. Cells were harvested by centrifugation at 3200 g at 4 °C for 5 min and re-suspended in 10 ml TfB I buffer. After 10 min incubation cells were again harvested at 5000 rpm at 4 °C for 5 min. Cells were subsequently re-suspended in 2 ml TfB II buffer, aliquoted and frozen in liquid nitrogen. Cells were stored at -80 °C.

3.1.3 Transformation of competent cells

Transformation of competent DH5α was carried out by the heat shock method. 15 µl of ligation reaction or 5 to 25 ng plasmid DNA was added to 50 µl of competent bacteria solution thawed on ice before. The mixture was incubated on ice for 30 min. Afterwards heat shock was applied at 42 °C for 45 s followed by cooling on ice for 10 min. Bacteria were rescued in SOC medium for 60 min at 37 °C under constant shaking of 400 rpm. Finally bacteria were streaked on agar plates containing antibiotic selecting for transformed bacteria and incubated at 37 °C overnight.

3.1.4 Isolation of plasmid DNA from bacteria

Preparation of plasmid DNA from bacteria was performed in two scales: with 5 ml overnight bacterial cultures for mini preparation scale and 50 ml for midi preparation scale. Both protocols were performed with alkaline lysis of the bacteria.

For mini preparation 2 ml of a fresh overnight culture was centrifuged for 5 min at 5000 rpm. Pellet cells were re-suspended in 200 µl buffer S1. Cells were lysed by addition of 200 µl buffer S2, inverting the tube 6 times and incubation at room temperature for 5 min. 200 µl of neutralisation buffer S3 was added, the solution was mixed by inverting the tube 6 times and incubated on ice for 5 min. Cell debris and genomic DNA was separated from the plasmid DNA by centrifugation for 30 min at 13000 rpm. Plasmid-containing supernatant was transferred to a new tube, 500 µl of isopropanol was added and the mixture was centrifuged 5 min at 13.000 rpm in order to precipitate plasmid DNA. Plasmid DNA was washed by addition of 1 ml 70 % ethanol and centrifugation 5 min at 13000 rpm. Ethanol was removed and the pellet was air-dried for about 30 min. plasmid DNA was re-suspended in 50 µl dH2O and stored at -20 °C.

For midi preparations of plasmid DNA a fresh overnight culture was lysed and the plasmid DNA was clarified using anion-exchange columns (Macherey-Nagel, Düren) following the manufacturer´s instructions. Plasmid DNA pellet was re-suspended in about 100 µl dH2O and stored at -20 °C.

3.2 Cloning

3.2.1 Polymerase chain reaction (PCR)

In-vitro amplification of DNA fragments was carried out via polymerase chain reaction (PCR). All fragments required for cloning were amplified by Herculase II fusion DNA polymerase exhibiting proofreading activity. For analytical purposes fragments were amplified by Taq polymerase without proofreading function.

For sub-cloning, the PCR reaction was prepared in a total reaction volume of 50 µl with the following components: 20 ng vector DNA template, 20 pmol of each primer, 200 µM of each dNTP, and 2.5 U Herculase II in 1 x reaction buffer. The temperature program for the PCR reaction catalysed by Herculase II was performed as follows: After an initial denaturation step, where the PCR mix was heated for 2 min at 95 °C, a three-stage temperature cycle was started and repeated for 25 to 30 times. This temperature cycle consisted of first a 30 s denaturation step at 95 °C, second a 30 s primer annealing step 5 °C below the melting temperature of primers and third an elongation step at 68 °C. The duration of the elongation step was determined by the length of the fragments. At the very end a 5 min lasting elongation step at 68 °C was carried out to elongate incomplete fragments.

For analytical purposes, vector DNA was amplified in 25 µl reaction volume with the following components: 10 ng DNA template, 10 pmol of each primer, 200 µM each dNTP, 5 mM MgCl2, and 1 U Taq polymerase in 1 x reaction buffer. The temperature program for PCR reaction catalysed by Taq polymerase fusion was performed as follows: After an initial denaturation, where the PCR mix was heated for 5 min at 95 °C, a three stage temperature cycle was started and repeated 30 times. This temperature cycle consisted first of a 60 s denaturation step at 95 °C, second a 60 s primer annealing step 5 °C below the melting temperature of the primers and third an elongation step at 72 °C, whose duration was determined by the length of the fragment. Finally, a 5 min elongation step at 72 °C was carried out.

3.2.2 Agarose gel electrophoresis

Linear DNA fragments were separated according to their size by agarose gel electrophoresis. The size of the fragments was determined by comparison with a DNA ladder running on the same gel.

For gel preparation 1 to 1.5 g/l agarose was melted in 1 x TBE buffer by heating. After cooling down to about 40 °C, 0.1 µg/ml ethidium bromide was added. The solution was poured into a gel tank and a comb was inserted. To run the electrophoresis, the polymerised gel was transferred into the electrophoresis tank filled with TBE buffer. The DNA samples were mixed with 5x DNA loading buffer and carefully loaded into the wells. Electrophoresis was performed at 100 V until DNA fragments were separated. Afterwards the gels were analysed and dissected under UV irradiation of 302 nm in a UV-trans-illuminator (Stratagene).

3.2.3 Purification of DNA from agarose gels

In order to isolate particular DNA fragments separated by gel electrophoresis, gel bands containing the DNA were cut out from the gel on a UV-trans-illuminator with a scalpel. The DNA was purified from the gel with the QIAquick Gel Extraction Kit, subsequently eluted in 30 to 50 µl dH2O and stored at -20 °C.

3.2.4 Enzymatic restriction of DNA

For preparing the ends of DNA fragments for ligation or for vector analysis, plasmid DNA was cut using restriction endonucleases. The reaction was carried out under appropriate buffer conditions. BSA was added as recommended by NEB guidelines. For preparative restriction, 50 µl PCR product was reacted for 3 h at 37 °C in a 200 µl reaction volume containing 20 U of restriction endonucleases in the appropriate buffer conditions. For vector analysis, 5 µg of DNA was restricted for 90 min at 37 °C in a 25 µl reaction volume containing 10 U of restriction endonucleases in the appropriate buffer conditions.

3.2.5 Ligation of DNA fragments

Linear DNA fragments with complementary overhangs were ligated using T4 DNA ligase. Ligation was performed in a total reaction volume of 20 µl containing 0.025 pmol vector DNA, 0.075 pmol insert DNA and 1 µl T4 DNA ligase in 1 x reaction buffer at 16 °C overnight. Subsequently, the product was immediately transformed into bacteria or stored at -20 °C.

3.2.6 Measurement of DNA concentration

The concentration of nucleic acids was determined photometrically by measuring the absorbance at 260 nm in a quartz crystal cuvette. Potential protein contaminations was excluded by measuring the ratio of absorbance at 260 nm to 280 nm.

3.2.7 Plasmid DNA sequencing

The coding sequence as well as parts of the vector backbone was sequenced by Microsynth (Lindau). For this, the DNA was adjusted with dH2O to a concentration of 80 ng/µl in a final volume of 10 µl. Primers were added in 20 pmol if needed.

3.3 Cell line culture

3.3.1 Culturing of eukaryotic cell lines

All cell lines used in this work were cultured as adherent cells in sterile tissue culture dishes or flasks. HEK-293 cells, HeLa cells or MEF cells were cultured in high glucose DMEM supplemented with 10 % FCS, 1 % sodium pyruvate and 1 % antibiotic-antimycotic (penicillin-streptomycin) if not denoted differently. Cells were cultured in an incubator at 37 °C and under an atmosphere containing 5 % CO_2.

For maintenance, cells were passaged as soon as they had grown to an approximately 90 % confluent population. For this, the adherent cells from a t-75 flask were carefully washed with 5 ml pre-warmed PBS once, then detached off the surface by incubating in 2 ml pre-warmed trypsin-EDTA not more than 5 min. 3 ml DMEM were added to inactivate trypsin-EDTA. Cells were flushed from the surface and transferred to a sterile falcon tube. To remove the trypsin-EDTA, the cells were pelleted 4 min at 150 g and re-suspended in an appropriate volume of fresh medium to split in the desired ratio.

3.3.2 Storage of eukaryotic cell lines

For the long-term storage of cell lines, the cell pellet of a confluent T-75 flask was re-suspended in 1 mL freezing medium. The cell suspension was transferred to a cryo-tube and frozen overnight at -80 °C. For long term storage, the cells were placed in a liquid nitrogen tank at the next day.

In order to take frozen cells into culture, the cells were thawed rapidly in a 37 °C water bath. The freezing medium was removed by centrifugation for 4 min at 150 g and re-suspension in fresh culture medium. The cells were then transferred to a T-75 flask, incubated at 37 °C overnight and passaged on the next day.

3.3.3 Transfection of eukaryotic cell lines

For transfection of HEK-293 cells by electroporation, 5×10^6 cells were trypsinated, washed with PBS and electroporated with 10 µg plasmid DNA in 400 µl of GenePulser electroporation buffer using a GenePulser (Bio-Rad) at 350 V / 700 µF and cultivated as desired.

For chemo-transfection of HEK-293 cells in 96 well format, 10000 cells per well were seeded out 24 prior to transfection. For transfection of cells in one well, pre-mixes of 300 ng plasmid DNA in 15 µl serum-free DMEM and 1 µl polyethylenimine (PEI, kindly provided by Dr. Heinrich Leonhardt, LMU, Munich) in 15 µl serum-free DMEM were mixed and transferred onto cells after an incubation step for 30 min at room temperature.

For transfection of MEF cells by electroporation, $2x10^6$ cells were trypsinated, washed with PBS and electroporated with 2 µg plasmid DNA in 100 µl of Amaxa electroporation buffer using the Amaxa Nucleofactor (Lonza) at T-020 setting and cultivated as desired.

3.3.4 Genotyping of FKBP5 deficient MEF cells

To obtain DNA, cells were trypsinated, pelleted by centrifugation for 4 min at 150 g and frozen at -20 °C if necessary. Next, 100 µl of 50 mM NaOH was added to the cell pellet and the mixture was boiled at 99°C for 30 min. The lysate was neutralised with 30 µl of 1 M Tris-HCl with a pH of 7 and stored at -20 °C if not used immediately. Finally, genotypes were determined by PCR using primers surrounding the deleted region.

3.4 DNA-analytical methods

3.4.1 Isolation of total RNA from tissues or cells

Total RNA was isolated using an RNA isolation kit (Machery-Nagel) following the manufacturers instruction. Isolation of RNA based on cell lysis and RNase inactivation in a solution containing large amounts of chaotropic ions and adsorption of RNA to a silica membrane. Co-adsorbed DNA was removed by rDNAse dependent degradation. After washing and elution from the silica membrane, RNA was stored at -80 °C or immediately used for reverse transcription.

3.4.2 Reverse transcription of RNA

A reverse transcriptase was used to transcribe RNA from tissue or cells into coding DNA (cDNA). Reverse transcription reaction mix in a total volume of 20 µl was set up from 400 ng RNA template, 2 µl 10x Omniscript RT-buffer (Qiagen), 500 nM each dNTP, 2.5 µM random hexa-primers (Promega), 10 U RNase inhibitor and 4 U Omniscript reverse transcriptase (Qiagen). Reverse transcription was performed at 37 °C for 60 min. cDNA solution was stored at -20 °C.

3.4.3 Isolation of genomic DNA from cooked mouse tails

Isolation of genomic DNA from cooked mouse tails was performed using the Genomic DNA from Tissue kit (Macherey Nagel) as follows. Mouse tails were transferred to 96 well plates, cooked in 100 µl 50 mM NaOH for 30 min and neutralised with 30 µl 1 M Tris-HCl, pH7.0. 50 µl supernatant was transferred to a new reaction tube. Cell lysis, DNA binding to the column, washing and elution was performed exactly to the manufacturer's instructions.

3.4.4 Quantitative transcriptional real time PCR

Gene expression was quantified using quantitative transcriptional real time PCR (qRT-PCR). Sections of interest in cDNA were amplified during PCR and synthesised double stranded DNA was quantified in real time as a measure of fluorescence light

emitted from the DNA intercalating fluorescent dye SYBR Green. Gene expression of a gene of interest was then calculated as the mean cycle number from exponential fluorescence signal increase and normalised to the same measure derived from analysis of a housekeeping genes.

PCR reaction mix in a total volume of 10 µl was set up from 5 µl 2x QuantiFast SYBR Green PCR Master Mix (Qiagen), 10 pmol of forward and reverse primer and 2 µl of 1:10 diluted cDNA. Reaction mixes were transferred to glass capillaries, centrifuged and analysed in a LightCycler 2.0 (Roche) in technical duplicates. The PCR programme started with 5 min incubation at 95 °C followed by 40 cycles of amplification (10 s at 95 °C, 20 s at 60 °C). The fluorescence signal after each cycle was stimulated at 494 nm and measured at 521 nm. Specificity of the amplification was controlled by the existence of a single peak in the melting curve of the PCR product.

3.4.5 Quantitative genomic real time PCR

Quantitative genomic real time PCR was used to identify the copy number of a genomic region of interest, in this case a region suspected to be duplicated. The duplicated region was amplified during PCR with primers located in close proximity of the duplication boundary. Newly synthesised double stranded DNA was quantified in real time as a measure of fluorescence light emitted from the DNA intercalating fluorescent dye SYBR Green. The copy number was then calculated as mean cycle number of exponential fluorescence signal increase in section of interest relatively to the signal increase in a section of a housekeeping gene.

PCR reaction mix in a total volume of 10 µl was set up from 5 µl 2x QuantiFast SYBR Green PCR Master Mix (Qiagen), 10 pmol of forward and reverse primer and 40 ng genomic DNA. Reaction mixes were transferred to glass capillaries, centrifuged and analysed in a LightCycler 2.0 (Roche) in technical duplicates. PCR programme started with 5 min incubation at 95 °C followed by 40 cycles of amplification (10 s at 95 °C, 20 s at 60 °C). The fluorescence signal after each cycle was stimulated at 494 nm and measured at 521 nm. Specificity of the amplification was controlled by the existence of a single peak in the melting curve of the PCR product.

3.5 Protein-biochemical methods

3.5.1 BCA assay for measurement of protein concentration

Protein concentration was determined using a commercially available BCA kit (Thermo Scientific) and used according to the manufacturer´s instructions. The BCA reaction is a combination of the Biuret reaction where Cu^{2+} is reduced to Cu^{1+} in the presence of protein in an alkaline solution. Highly specific detection of Cu^{1+} in purple complexes with bichinonic acid (BCA) is used for absorbance photometry. Estimation of protein concentration is based on the comparison with BCA reacted in the presence of different amounts of bovine serum albumin (BSA) as standard.

Samples as well as standards were pipetted into a 96-microtiter plate in triplicates. All samples and standards were mixed with the BCA reagent according to the manufacturer´s protocol and incubated at 60 °C for 20 min. The absorbance was measured at 550 nm in a microplate reader (Bio-Rad).

3.5.2 SDS-Polyacrylamide gel electrophoresis

SDS-polyacrylamide gel electrophoresis (SDS-PAGE) is used to separate proteins according to their molecular weight. Proteins are denatured and masked with the anionic detergent SDS, which carries a negative charge. By this, proteins are charged according to their size and can be separated in an electric field. To achieve optimal resolving conditions a discontinuous gel electrophoresis was used.

Gels were poured in a gel caster (Bio-Rad) with a thickness of 1 mm. First, the resolving gel was poured into the apparatus and covered with a thin layer of isopropanol. After 20-30 min isopropanol was removed, the stacking gel was poured onto the resolving gel and a comb was placed to form the slots. Polymerised gels were stored at 4 °C in a humid atmosphere.

Protein solutions were boiled in Laemmli loading buffer at 95 °C for 5 min and subsequently loaded on the gel placed in the running chamber and filled with Laemmli running buffer.

Electrophoresis was performed at 80 V for 20-30 min until the proteins were focused at the gel interface and at 150 V until the running front reached the end of the resolving gel.

After SDS-PAGE, the gels were used for subsequent detection of proteins in gel or western blotting on nitrocellulose membrane.

3.5.3 Western Blotting

Proteins separated by SDS-PAGE were immobilised on a nitrocellulose membrane by western blotting. For wet blotting, the transfer apparatus was assembled with the following components from cathode to anode in a sandwich manner: a sponge, three Whatman filter papers, gel, the nitrocellulose membrane, three Whatman papers and a sponge. All components were equilibrated in wetblot transfer buffer and the entire stack was placed into a blotting chamber filled with wetblot buffer. The transfer reaction was performed at 100 V for 90 min at 4 °C.

3.5.4 Western Detection

Proteins immobilised on a membrane were visualised by immuno-detection. If not denoted differently, two antibodies were used sequentially for this purpose. The primary antibody bound specifically to the target protein, while the secondary antibody, which was either coupled to the horseradish peroxidase (HRP) or a fluorescent dye, recognised the constant region of the primary antibody.

Western detection was either carried out by a chemo-luminescent reaction catalysed by the HRP or by fluorescence derived from the coupled dye. For the sooner, HRP catalysed the oxidation of its substrate luminol in the presence of H_2O_2 resulting in a striking blue glow. For the latter, the fluorescent signal was measured. Both chemo-luminescence as well as fluorescence were detected in the ChemiDoc imaging system (Bio-Rad).

Prior to the incubation with antibodies, non-specific binding sites on the nitrocellulose membrane were blocked by incubation in TBS-T supplemented with 5 % (w/v) milk powder for 1 h at room temperature. Subsequently, the membrane was incubated with the primary and secondary antibody. The membrane was incubated with primary antibodies diluted in TBS-T at 4 °C over night and with secondary antibodies diluted in TBS-T supplemented with 2 % (w/v) milk powder for 4 h at room temperature. After each antibody incubation the membrane was washed at least three times for 5 min with TBS-T.

3.6 Cellular assays

3.6.1 MTT cytotoxicity assay

Cytotoxicity was measured in a colorimetric assay determining cell metabolic activity. Viable, metabolically active cells produce reduction equivalents that reduce the 3-(4,5-dimethylthiazol-2-yl)-2,5-diphenyltetrazolium (MTT) dye to its insoluble, purple formazan salt, which shows an absorbance maximum near 570 nm. The quantity of formazan is presumably directly proportional to the number of viable cells and was measured by recording absorbance at 570 nm.

Cells were seeded and treated in 96 well plates with 150 µl medium per well. For analysis of cytotoxicity 75 of cell culture medium was removed and 25 µl MTT dye (2 mg/ml in PBS) was added to the adherent cells covered with 75 µl remaining cell culture medium and incubated for 6 hours at 37 °C. Formazan salt was solubilised by incubation with 100 µl solubilisation buffer per well over night in a dark place at room temperature. Formazan dependent absorption was measured at 570 nm.

3.6.2 LDH cytotoxicity assay

Cytotoxicity can also be measured as a means of membrane integrity. The release of the widely expressed intracellular enzyme lactate dehydrogenase (LDH) into the cell culture medium is quantified by a coupled enzymatic reaction. In a first step, LDH catalyses the conversion of lactate to pyruvate via reduction of NAD+ to NADH. Second, NADH dehydrogenase uses NADH to reduce a tetrazolium salt to a red formazan product. The quantity of formazan is presumably directly proportional to the amount of released LDH and was measured by recording absorbance at 490 nm.

Cells were seeded and treated in 96 well plates in 150 µl per well cell culture medium supplemented with only 1 % serum. Maximal cytotoxicity as reference value was achieved by incubation with 1 % Triton X-100. For analysis of cytotoxicity 75 µl of cell culture medium from treated cells was transferred to a new 96 well plate and mixed with 75 µl LDH substrate (LDH Cytotoxicity Detection Kit, Clontech). After light protected incubation for 30 min at room temperature absorbance was measured at a wavelength of 490 nm.

3.6.3 Dual luciferase assay in MEF cells

MEF cells were transfected by electroporation and seeded out into 64 wells of a 96 well plate per electroporation cuvette. For TCF/LEF responsive reporter gene assays, the amounts of transfected plasmids electroporation cuvette were 1.2 µg luciferase based TCF/LEF responsive reporter plasmid TOPFlash, 0.6 µg FLAG-tagged FKBP51 expression plasmid, and 0.2 µg of Gaussia-KDEL expression vector as control plasmid. For FoxO responsive reporter gene assays, the amounts of transfected plasmids electroporation cuvette were 1.0 µg luciferase based FoxO responsive reporter plasmid FHRE, 0.8 µg FLAG-tagged FKBP51 expression plasmid, and 0.2 µg of Gaussia-KDEL expression vector as control plasmid. 24 h after transfection, cells were cultured for 48 h in fresh medium supplemented with drugs as indicated or DMSO as control.

To measure reporter gene activity cells were washed once with PBS and lysed in 50 µl passive lysis buffer (PLP). Firefly and Gaussia luciferase activities were measured in the same aliquot using an automatic luminometer equipped with an injector device (Tristar, Berthold). Firefly activity was measured first by adding 50 µl FLuc buffer (optimised) to 10 µl lysate in white microtiter plates. By adding 50 µl RLuc buffer the firefly reaction was quenched and Gaussia luminescence was measured after a 5 s delay. Firefly activity data represent the ratio of background corrected Firefly to Gaussia luminescence values.

3.6.4 Co-immunoprecipitation

Co-immunoprecipitations (CoIPs) were performed in HEK-293 cells. 72 hours after transfection by electroporation, cells were lysed in CoIP buffer. This was followed by incubation on an overhead shaker for 20 min at 4 °C. The lysate was cleared by centrifugation for 20 min at 13000 g at room temperature. 1.2 mg of lysate was incubated with 2.5 µg of the target directed antibody overnight at 4 °C on an overhead rotator. 20 µl of BSA-blocked Protein G Dynabead slurry (Invitrogen, 100-03D) was added to the lysate-antibody mix, followed by 3 h of incubation at 4 °C. The beads were washed three times with PBS, and protein-antibody complexes were eluted with an excess of antigen peptide in CoIP buffer for 30 min at 4°C. 5 to 15 µg of the cell lysates or 2.5 µl of the immunoprecipitates were separated by SDS-PAGE and analysed by western detection.

4 Results

4.1 Transcriptional regulation by FKBP51

FKBP5 is a mediator of the stress response system and plays an important role in the development of stress-related diseases. To elucidate the role of FKBP5 in an animal model, a knockout mouse had been constructed (Touma et al., 2011). These mice had been generated following the well-established technique of replacing the endogenous allele by a non-functional allele employing *in vitro* homologous recombination in stem cells isolated from a blastocyst, a procedure herein referred to as conventional gene knockout. Offspring homozygous for the FKBP5 deletion showed an enhanced negative glucocorticoid feedback at the HPA axis in response to a chronic stress paradigm, indicative of an increased sensitivity of the GR (Hartmann et al., 2012). On the behavioural level, they displayed more active coping behaviour upon either chronic or acute stress (Hartmann et al., 2012; Touma et al., 2011). To elucidate the effects of FKBP5 deletion on molecular pathways the expression profile of stressed mice deficient for FKBP5 (FKBP5-KO) and their wild type litter mates (FKBP5-WT) was compared.

4.1.1 Expression analysis in FKBP5-KO mice

For this purpose, six FKBP5-WT and six FKBP5-KO mice were treated with dexamethasone for three hours by intraperitoneal injection of 2 mg/kg. mRNA expression of whole brain lysates were analysed on two Illumina gene expression arrays, covering 45281 gene probes.

Within a 95 % confidence interval, four genes were detected differentially expressed between dexamethasone treated FKBP5-KO mice and their dexamethasone treated FKBP-WT litter mates (Figure 1). Besides downregulation of FKBP5, increased expression of the three genes RNA binding motif protein 12 (RBM12), glyoxalase 1 (GLO1) and faciogenital dysplasia 2 (FGD2) was detected.

The first gene, RBM12, codes for a protein of unknown function. The protein contains five distinct RNA binding motifs, two proline-rich regions and several putative transmembrane domains (Stover et al., 2001).

Gene	FC	Adj.P.Val
FKBP5	-2.1	0.00004
RBM12	1.6	0.0285
GLO1	1.7	0.0313
FGD2	1.9	0.0428

Figure 1: **Specification of the four top genes across the FKBP5 genotype contrast as detected by the microarray expression analysis.** Genes with adjusted *p*-values smaller than 0.05 are listed.

The second gene, GLO1, is a ubiquitously expressed enzyme that catalyses the isomerization of hemithioacetal adducts. Thus, GLO1 is a key player in the detoxification of methylglyoxal, when methylglyoxal spontaneously forms a hemithioacetal with glutathione (Thornalley, 2008). Methylglyoxal is a toxic by-product of glycolysis that glycates proteins, nucleotides and basic phospholipids (Thornalley, 2008). Besides leading to apoptosis, methylglyoxal also influences anxiety behaviour when acting as a $GABA_A$ receptor agonist (Distler et al., 2012; Thornalley, 2008). GLO1 has been linked to diabetic complications, anxiety disorders, schizophrenia, seizure susceptibility, pain, cancer and aging (Distler and Palmer, 2012; Thornalley, 2008).

The third gene, FGD2, is a member of the FGD gene family. FGD genes encode a group of guanine nucleotide exchange factors, which, by specifically activating Cdc42, control cytoskeleton-dependent membrane rearrangements (Buchsbaum, 2007; Huber et al., 2008; Rossman et al., 2005; Snyder et al., 2002).

4.1.2 Examination of differential GLO1 expression in brain tissue and cell culture

In line with the upregulation of GLO1 mRNA detected upon loss of FKBP5 by the microarray, the upregulation of GLO1 mRNA was confirmed via quantitative RT-PCR in brain lysates from FKBP5-KO and wild type mice used for the microarray (Figure 2A). Upregulation of RBM12 could not be verified by quantitative RT-PCR in this sample (Figure 2B). Upregulation of GLO1 mRNA was accompanied by a corresponding increase in GLO1 protein (Figure 2C). Verification of FGD2 upregulation on mRNA

level was not possible due to experimental limitations. With GLO1 being associated with psychiatry related phenotypes, the focus was set on the further characterisation of GLO1 regulation.

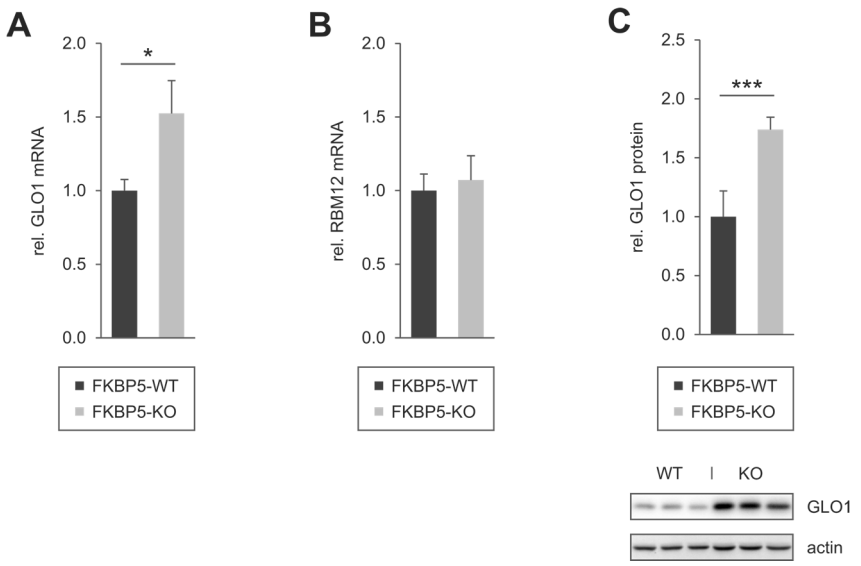

Figure 2: **Examining the expression of GLO1 and RBM12 in tissue from mice that were mRNA-profiled on the microarray.** Bars show the mean value and error bars represent the standard error of the mean. Statistical significances were calculated by a simple t-test and are depicted as follows: * for $p \leq 0.05$, ** for $p \leq 0.01$ and *** for $p \leq 0.001$. **A** GLO1 mRNA upregulation by loss of FKBP5 was replicated by qRT-PCR using the RNA preparations analysed on the microarray. GLO1 mRNA expression normalised to actin mRNA expression in tissue from FKBP5-KO animals relative to wild type tissue was calculated based on the results from three animals of each genotype. **B** Using the same RNA preparations, upregulation of RBM12 mRNA could not be verified by qRT-PCR. RBM12 mRNA expression normalised to actin mRNA expression in tissue from FKBP5-KO animals relative to wild type tissue was calculated. **C** GLO1 protein upregulation was detected by western analysis in brain lysates from the same mice that were analysed on the microarray. A representative western blot showing GLO1 and actin expression is attatched. Upregulation of GLO1 protein expression in FKBP5-KO tissue normalised to the expression of actin in comparison to wild type tissue was calculated from six biological replicates.

In a next step, the differential expression of GLO1 was verified in a second sample of FKBP5-KO mice and in mouse embryonal fibroblasts (MEFs) derived from the FKBP5-KO mouse model. Increased expression of GLO1 protein in FKBP5-KO mice was confirmed in brain tissue from a second sample of mice by western analysis (Figure 3A). Consistent with this, an approximately two times upregulated expression of GLO1 protein was detected in MEFs derived from the FKBP5-KO mice compared to MEFs derived from wild type litter mates by western analysis (Figure 3B).

For further analysis of the underlying mechanism of the seemingly FKBP5 dependent GLO1 expression, efforts were taken to establish a cellular model that would reflect the FKBP5 induced regulation of GLO1 expression. Extrapolating from the GLO1 upregulation in FKBP5-KO mice, ectopic overexpression of FKBP5 in cell culture should decrease GLO1 levels. To test this, FKBP5 was overexpressed in HEK-293 cells by transient transfection. Surprisingly, increased levels of FKBP51 did not lead to downregulation of GLO1 protein as indicated by western analysis (Figure 3C).

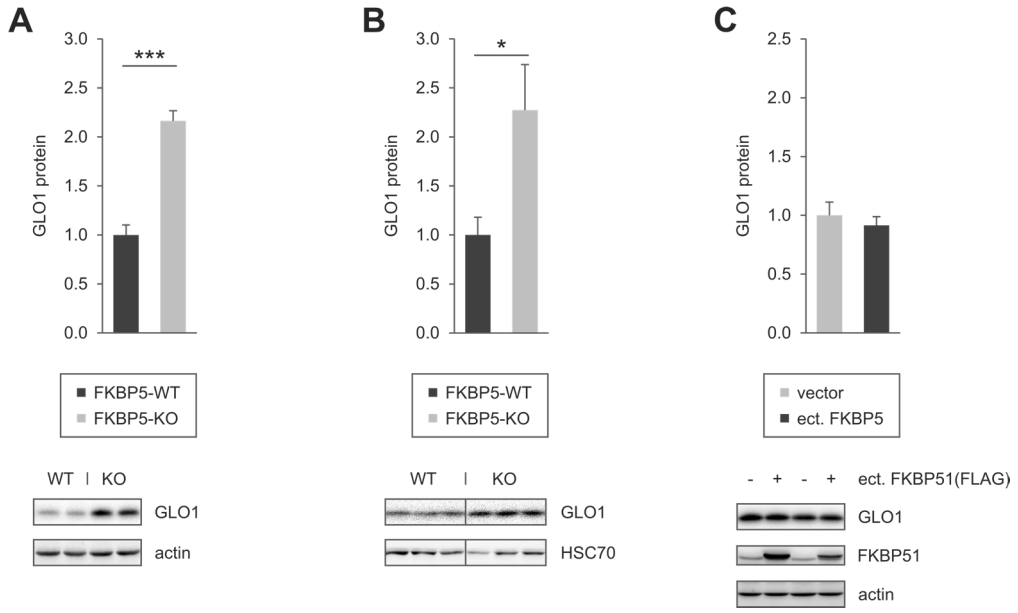

Figure 3: **Analysing the GLO1 regulation by modulating FKBP5 in cell culture.** Bars show the mean value and error bars represent the standard error of the mean. Statistical significances were calculated by a t-test and are depicted follows: * for $p \leq 0.05$, ** for $p \leq 0.01$ and *** for $p \leq 0.001$. Representative western blots are attatched. **A** Upregulation of GLO1 protein was detected in brain tissue from FKBP5-KO mice by western analysis. Upregulation of GLO1 expression in FKBP5-KO tissue normalised to the expression of actin in comparison to wild type tissue was calculated from twelve biological replicates. **B** Upregulation of GLO1 protein was detected in MEF cell lysate by western analysis. Upregulation of GLO1 expression in FKBP5-KO MEFs normalised to the expression of HSC70in comparison to wild type MEFs was calculated from three biological replicates. **C** GLO1 protein is not regulated by ectopic expression of FKBP5 in HEK-293 cells. GLO1 expression normalised to actin expression in cells transfected with FLAG-tagged FKBP5 compared to vehicle transfected cells was calculated from six biological replicates.

4.1.3 GLO1 gene duplication in FKBP5 knockout mice

The discovery of a recurrent spontaneous copy number variation of GLO1 in several laboratory mouse inbred lines provided a first hint to a genetic cause for GLO1

upregulation (Egan et al., 2007; Shafie et al., 2014). An approximately 475 kb tandem duplication on chromosome 17 that includes Glo1 (30,174,390-30,651,226 Mb; mouse genome build 36) forms the genetic basis of the duplication of the locus spanning GLO1 (Williams et al., 2009). This duplication at the GLO1 locus was observed in 23 of 71 tested inbred mouse strains (Williams et al., 2009).

As a matter of fact, the genes coding for GLO1 and FKBP51 are both located on mouse chromosome 17, separated by only approximately 2 mega bases (Mb). Therefrom, a GLO1 copy number variance in the FKBP5 mouse model was considered.

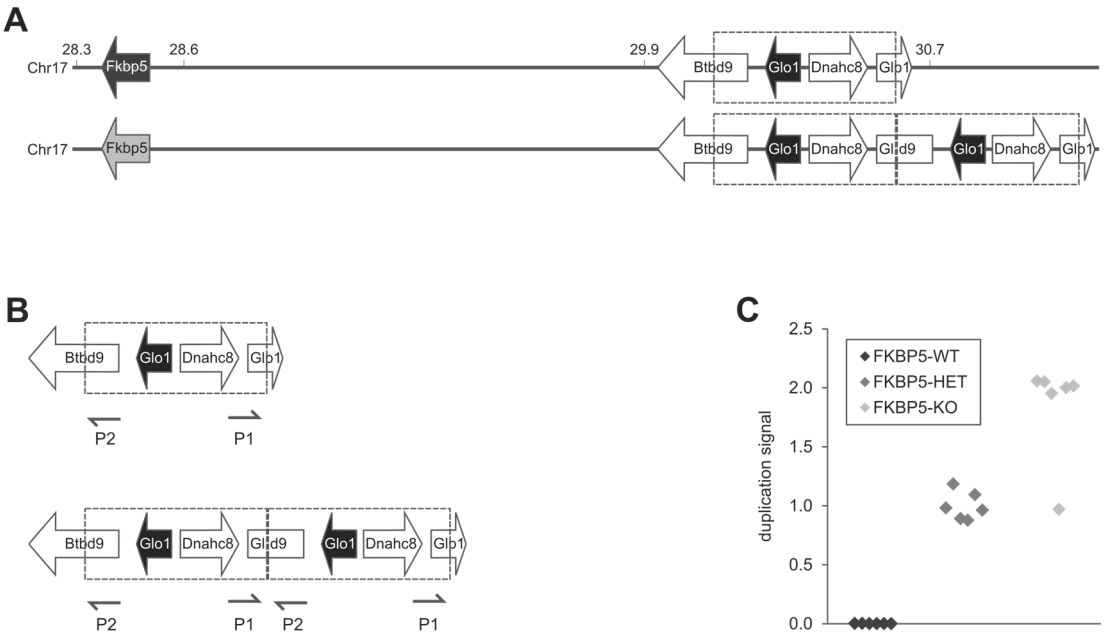

Figure 4: **Co-inheritance of a GLO1 gene duplication with the FKBP5-KO allele in FKBP5-KO mice. A** The genomic arrangement of mouse chromosome 17 with the FKBP5-WT allele compared to the FKBP5-KO allele is sketched schematically. Genetic distances on chromosome 17 are marked in Mb. **B** Primer (P1: GLO1-CNV_f and P2: GLO1-CNV_r) complementary to sequences in close proximity to the duplication boundary yield a PCR product only in presence of a template providing the duplication. **C** The relative allelic frequency of the GLO1 gene in genomic DNA purified from FKBP5-WT, FKBP5-HET and FKBP5-KO animals was quantified in a qPCR with the primer pair spanning the duplication boundary. GLO1 gene duplication signal in qPCR was normalised to qPCR signal for the NPSR1 genomic DNA on chromosome 7, which served as a reference gene coded on a singular locus. Duplication signal in probes from FKBP5-HET animals was set to 1.

With embryonal stem cell donor mice and back crossing foster mice exhibiting differential genetic background FKBP5-KO mice might carry a genetic duplication of GLO1, whereas wild type mice might carry a single copy of the GLO1 gene (Figure 4A). Moreover, FKBP5 and GLO1 alleles would be co-inherited and the GLO1 copy number

variance would be co-selected with the FKBP5 genotype due to their close genetic proximity.

These hypotheses were substantiated by the investigation of the genetic background of the FKBP5 mouse model. The FKBP5 deletion was constructed in embryonal stem cells derived from 129SvJ mice. Later on, the resulting mice were crossed with C57BL/6 mice. In contrast to C57BL/6 mice, 129SvJ mice were reported to be carriers of the GLO1 gene duplication (Williams et al., 2009).

Finally, experimental evidence for these hypotheses was provided by the quantification of the relative frequency of the duplicated section. Therefore, a primer pair spanning the duplication boundary was utilised in a PCR, which exclusively yields a PCR product in the presence of a template providing the duplication (Figure 4B). Genomic DNA from mice homozygous and heterozygous (FKBP5-HET) for the FKBP5 deletion as well as from their wild type litter mates was purified. Using this primer pair in a quantitative PCR setup, genomic samples from the three genotypes were probed for the GLO1 duplication (Williams et al., 2009). Indeed, no GLO1 duplication was detectable in FKBP5-WT mice, whereas the PCR signal in FKBP5-KO mice was clearly detectable and twice as high as in FKBP5-HET mice (Figure 4C).

This finding is in line with the hypothesis that FKBP5-KO mice carry two deleted FKBP5 alleles, each of them co-segregated with a duplicated GLO1. FKBP5-WT mice, hence, carry two functional FKBP5 alleles, each of them co-segregated with a single copy of GLO1. FKBP5-HET mice carry one deleted FKBP5 allele co-segregated with a duplicated GLO1, and one functional FKBP5 allele co-segregated with a single copy of GLO1.

Therefore, the higher levels of mRNA and protein of GLO1 in FKBP5-KO mice compared with wild type litter mates are very likely due to the doubled GLO1 gene dose in these mice.

These results have been published (Kollmannsberger et al., 2013).

4.2 Pathway modulation by FKBP51 and psychopharmaca

As published in two recent publications, we found that AKT and GSK3β as well as downstream targets are convergently affected by FKBP51 and the antidepressants PRX and LIT (Gassen et al., 2014, 2015). As part of this thesis, potential convergent effects of thirteen psychopharmaca and FKBP51 on the kinases GSK3β, AKT and ERK as well as their downstream targets were analysed.

4.2.1 Definition of a cellular system and determination of drug treatment

For this purpose, MEF cells were chosen as cellular model for loss of FKBP51 function. Before starting these experiments and additionally in the course of the experiments, the existence and purity of the FKBP5 deletion on both DNA and protein level was verified.

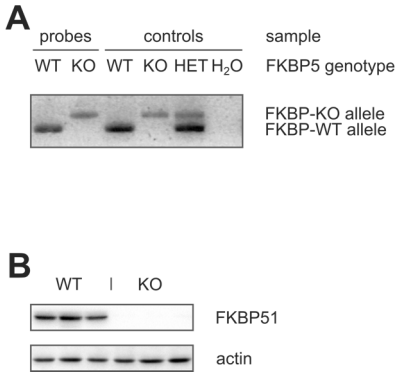

Figure 5: **Verification of the FKBP5 deletion in MEF cells. A** Cell lysate from MEF cells and control mouse tissue was probed for the presence of the FKBP5-KO allele as well as the FKBP5-WT allele by PCR. A representative agarose gel is shown. **B** Cell lysate from MEF cells was checked for the expression of the FKBP51 protein by western detection. A representative western blot is shown.

Hence, genotype of cells coding for functional and deleted FKBP5 were determined by PCR using primers specific for the wildtype (363 nt product) or mutant (530 nt product) alleles (Figure 5A). Tissue from mice heterozygous for the FKBP5 deletion generates two bands both for the wildtype and the mutant alleles. The same pattern would be expected for a mixed population of MEF cells derived from FKBP5-KO and FKBP5-WT cultures. PCR product for FKBP5-WT MEF cells, indeed, exclusively showed a band derived from the FKBP5-WT allele, whereas the PCR product for FKBP5-KO MEF cells showed exclusively a band derived from the FKBP5-KO allele.

Absence of the FKBP51 protein in MEF cells with deleted FKBP5 was verified by western detection (Figure 5B). No signal in immune-detection of FKBP51 was obtained in FKBP5-KO cells, whereas a distinct signal was found in FKBP5-WT cells.

CTP	Citalopram	10 µM
FLX	Fluoxetine	3 µM
PRX	Paroxetine	3 µM
VTX	Vortioxetine	3 µM
VNF	Venlafaxine	10 µM
AMT	Amitriptyline	10 µM
DXP	Doxepin	30 µM
CLP	Clomipramine	10 µM
TNP	Tianeptine	10 µM
VPA	Valproate	5 mM
LMT	Lamotrigine	10 µM
LIT	Lithium	10 mM
KTM	Ketamine	100 µM
LNC	Lanicemine	100 µM
CHI	CHIR-99021	3 µM

Figure 6: **Table of psychopharmaca and additional substances used for pathway modulation screen.** Depicted are the abbreviation code, the substance name and the concentration used for treatment in cell culture, if not described otherwise.

In addition to PRX and LIT applied in our two recent studies, eleven further psychopharmaca of different classes and suspected mode of action well as two additional substances were included in this study (Figure 6). CTP and FLX together with PRX completed the class of SSRIs. With VTX and VNF, two serotonin and noradrenaline modulating drugs were used here. In addition, three drugs with tricyclic structure, AMT, DXP and CLP, were included in this study. Furthermore, TNP, an atypical antidepressant, was utilised. Moreover, the structurally diverse group of mood stabilisers was represented by VPA, LMT and LIT. Moreover, the anaesthetic KTM, which exerts antagonistic action on the NMDA receptor, was added to the list of psychopharmaca. Finally, two additional substances included LNC, a further drug with antagonistic action on the NMDA receptor, and the GSK3β inhibitor CHIR-99021 (CHI).

Most importantly, cytotoxic effects of high drug concentrations had to be excluded. Therefore, two orthogonal toxicity tests in MEF cells were performed with all substances for the three incubation times 12 hours, 24 hours, and 48 hours. In the first toxicity test, the MTT test, some aspect of general metabolism as a marker of cell viability was measured. In the second toxicity test, the LDH test, the egression of a cytosolic enzyme into the cell culture medium as a marker of cell membrane integrity was measured.

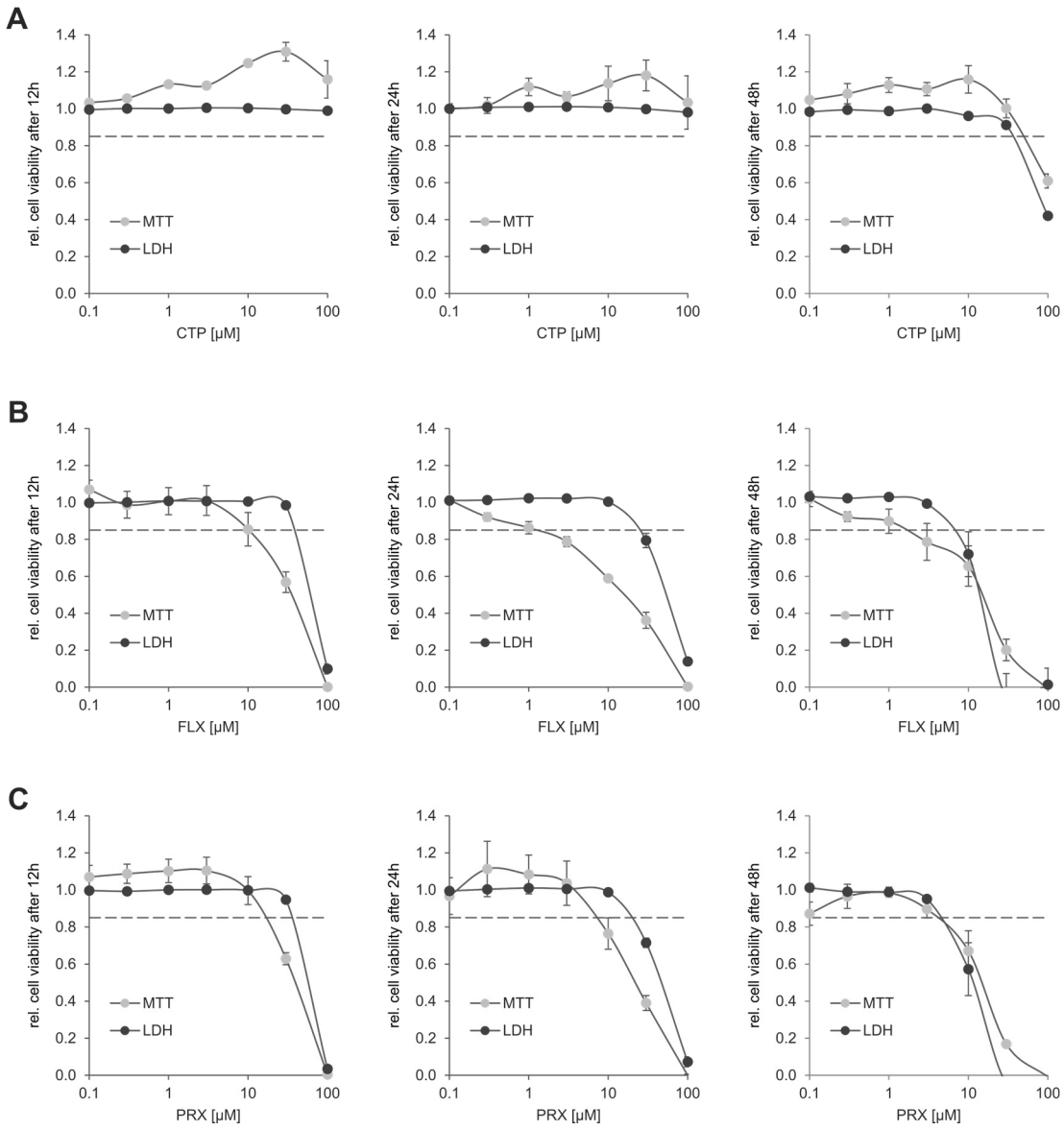

Figure 7: **Toxicity of selected SSRIs.** Cell viability was analysed after 12 hours, 24 hours and 48 hours drug treatment and normalised to viability of control treated cells in two assays. Cell viability was detected as a measure of general metabolism in the MTT assay and as a measure of cell membrane integrity in the LDH assay. Viability rate of 85%, which was defined as toxicity limit, is indicated by the dashed line. Cell viability was measured upon treatment with 0.1 µM to 100 µM CTP (**A**), 0.1 µM to 100 µM FLX (**B**), or 0.1 µM to 100 µM PRX (**C**). Dots show the mean value and error bars represent the standard error of the mean.

When depressive patients are pharmacologically treated, improvement of symptoms in response to treatment with classical antidepressants is found with a delay of weeks. In order to mimic a chronic treatment in cell culture, 48 hours incubation time with drugs was chosen. Appropriate drug concentrations for the treatment were selected based on two criteria: limits of toxicity in the viability assays in MEF cells and drug

concentrations used in recent publications. Toxicity limit in response to drug treatment was set to 85% viability rate. If the MTT and the LDH assays indicated different viability at a given concentration, viability data from the LDH assay were considered more reliable.

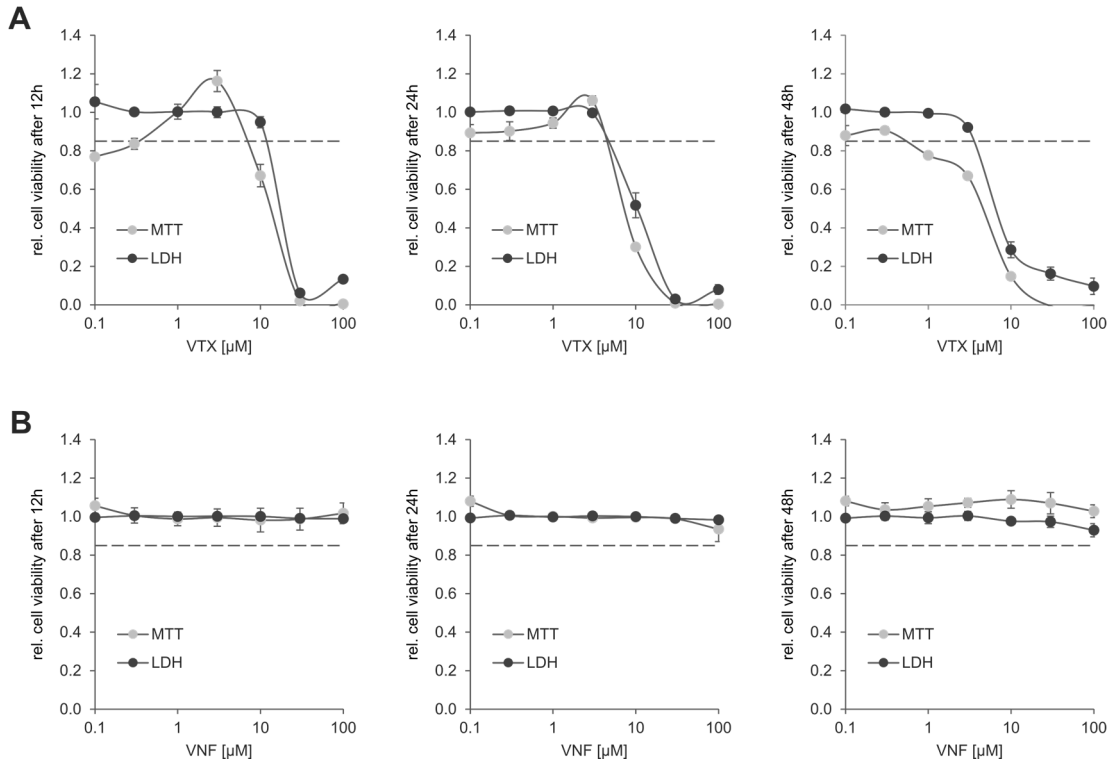

Figure 8**: Toxicity of selected SSNRIs.** Cell viability was analysed after 12 hours, 24 hours and 48 hours drug treatment and normalised to viability of control treated cells in two assays. Cell viability was detected as a measure of general metabolism in the MTT assay and as a measure of cell membrane integrity in the LDH assay. Viability rate of 85%, which was defined as toxicity limit, is indicated by the dashed line. Cell viability was measured upon treatment with 0.1 µM to 100 µM VTX (**A**) or 0.1 µM to 100 µM VNF (**B**). Dots show the mean value and error bars represent the standard error of the mean.

CTP did not induce cytotoxic effects up to a maximal concentration of 30 µM (Figure 7A). Administered at 100 µM, cytotoxic effects became apparent after 48 hours as detected both in the MTT and LDH assay. Interestingly, subtoxic concentrations of CTP led to enhanced MTT signals, especially after the short exposure time. FLX, the second SSRI, was slightly more cytotoxic than CTP (Figure 7B). Already 10 µM FLX induced cytotoxic effects after 48 hours as detected both in the MTT and LDH assay. Cytotoxicity evoked by treatment with PRX was comparable to cytotoxicity evoked by treatment with FLX, with cytotoxic effects starting at concentrations of 10 µM PRX after 48 hours

(Figure 7C). Treatment with 3 µM PRX for 48 hours did not induce cytotoxic effects. Therefore, 10 µM CTP, 3 µM FLX and 3 µM PRX were used for our following experiments if not declared otherwise.

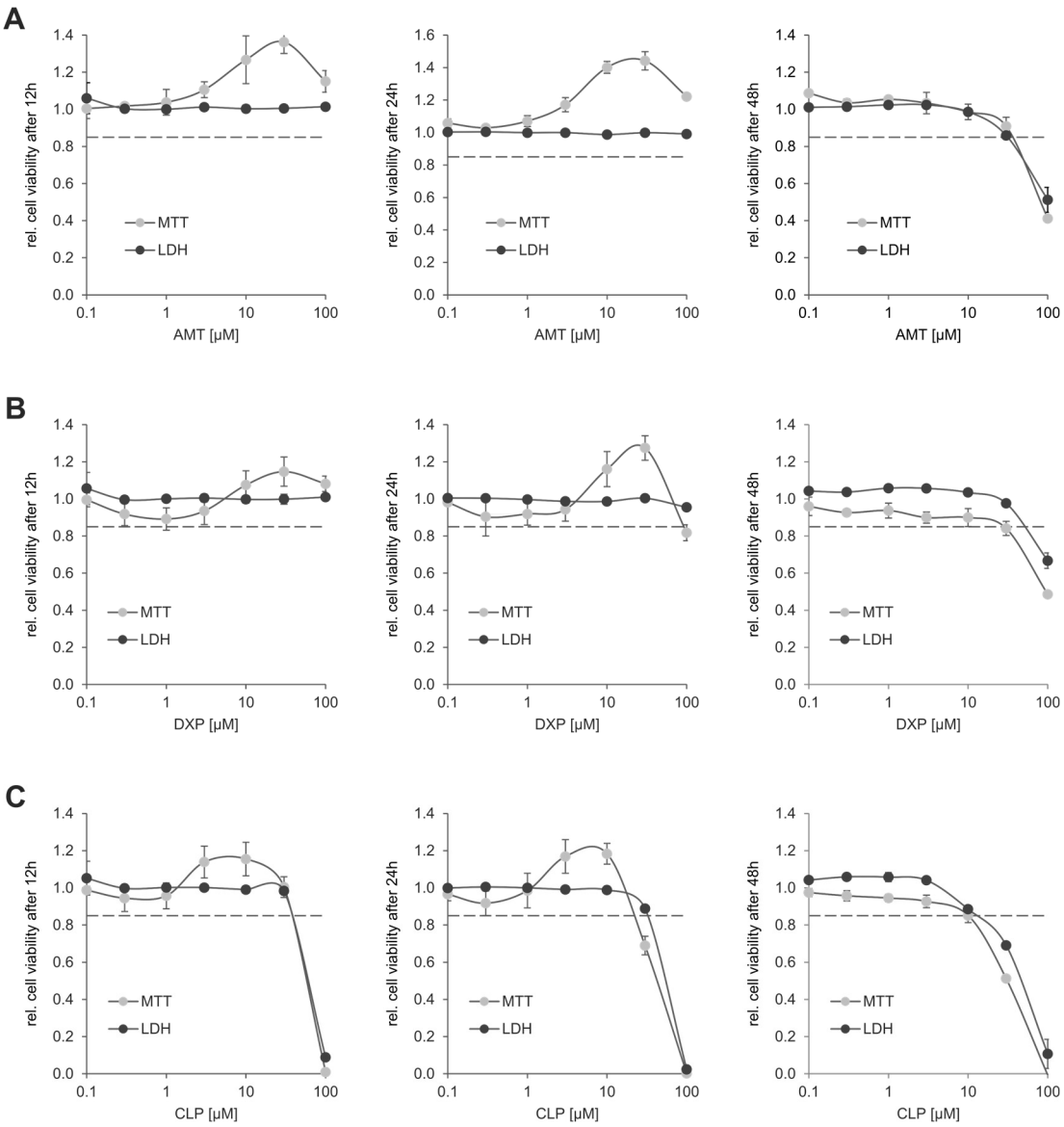

Figure 9: **Toxicity of selected TCAs.** Cell viability was analysed after 12 hours, 24 hours and 48 hours drug treatment and normalised to viability of control treated cells in two assays. Cell viability was detected as a measure of general metabolism in the MTT assay and as a measure of cell membrane integrity in the LDH assay. Viability rate of 85%, which was defined as toxicity limit, is indicated by the dashed line. Cell viability was measured upon treatment with 0.1 µM to 100 µM AMT (**A**), 0.1 µM to 100 µM DXP (**B**), or 0.1 µM to 100 µM CLP (**C**). Dots show the mean value and error bars represent the standard error of the mean.

VTX, the most recently approved antidepressant, was starting to induce cytotoxic effects at concentrations of 10 µM after 48 hours with slightly more toxic effects measured in the MTT than in the LDH assay (Figure 8A). No cytotoxic effects were observed upon treatment with VNF in concentrations up to 100 µM in either MTT or LDH assay (Figure 8B). Therefore, the maximal non-toxic concentration of VTX, i.e. 3 µM, and the subtoxic concentration of 10 µM VNF were chosen for further experiments if not declared otherwise.

Cytotoxic effects in response to treatment with 100 µM of the TCA AMT appeared not earlier than after 48 hours in either MTT or LDH assay (Figure 9A). No cytotoxic effects, but increased MTT signal upon treatment with 30 µM AMT after 12 hours and 24 hours were observed with AMT treatment. A similar picture was found for treatment with DXP (Figure 9B). Cytotoxic effects were only found with 100 µM DXP after 48 hours treatment. Moreover, treatment with 30 µM DXP resulted in a signal induction in the MTT assay after 12 hours and even more pronounced after 24 hours. The third TCA, CLP, was slightly more toxic (Figure 9C). Cytotoxic effects after 48 hours treatment were observed in response to CLP concentrations starting at 30 µM. The typical shoulder of signal induction in MTT signal after 12 hours and 24 hours treatment peaked at a concentration of 10 µM CLP. Therefore, the concentrations of 10 µM AMT, 30 µM DXP and 10 µM CLP were chosen for further experiments if not declared differently.

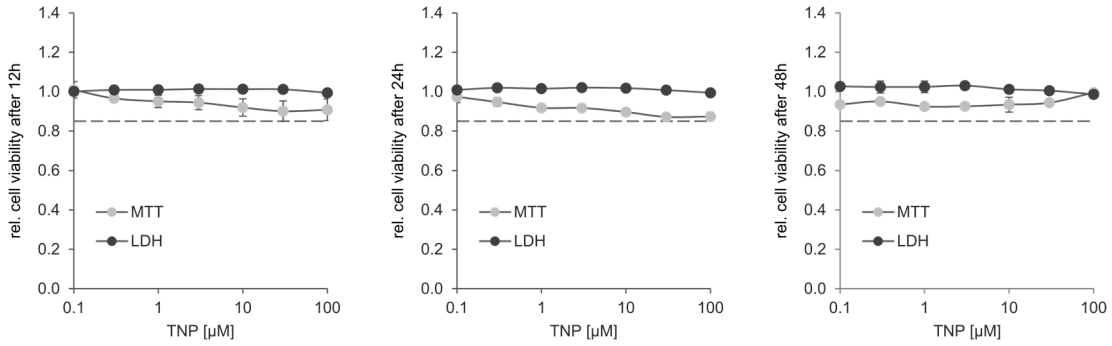

Figure 10: **Toxicity of the atypical antidepressant TNP.** Cell viability was analysed after 12 hours, 24 hours and 48 hours drug treatment and normalised to viability of control treated cells in two assays. Cell viability was detected as a measure of general metabolism in the MTT assay and as a measure of cell membrane integrity in the LDH assay upon treatment with 0.1 µM to 100 µM TNP. Dots show the mean value and error bars represent the standard error of the mean. Viability rate of 85%, which was defined as toxicity limit, is indicated by the dashed line.

No cytotoxic effects were found in response to treatment with the atypical antidepressant TNP up to 100 µM in either assay (Figure 10). A signal induction in the MTT assay after 12 hours and 24 hours, which was found in treatment with CTP and the three TCAs

AMT, DXP, and CLP, did not emerge in response to treatment with TNP. Finally, a concentration of 10 µM TNP was selected for further experiments.

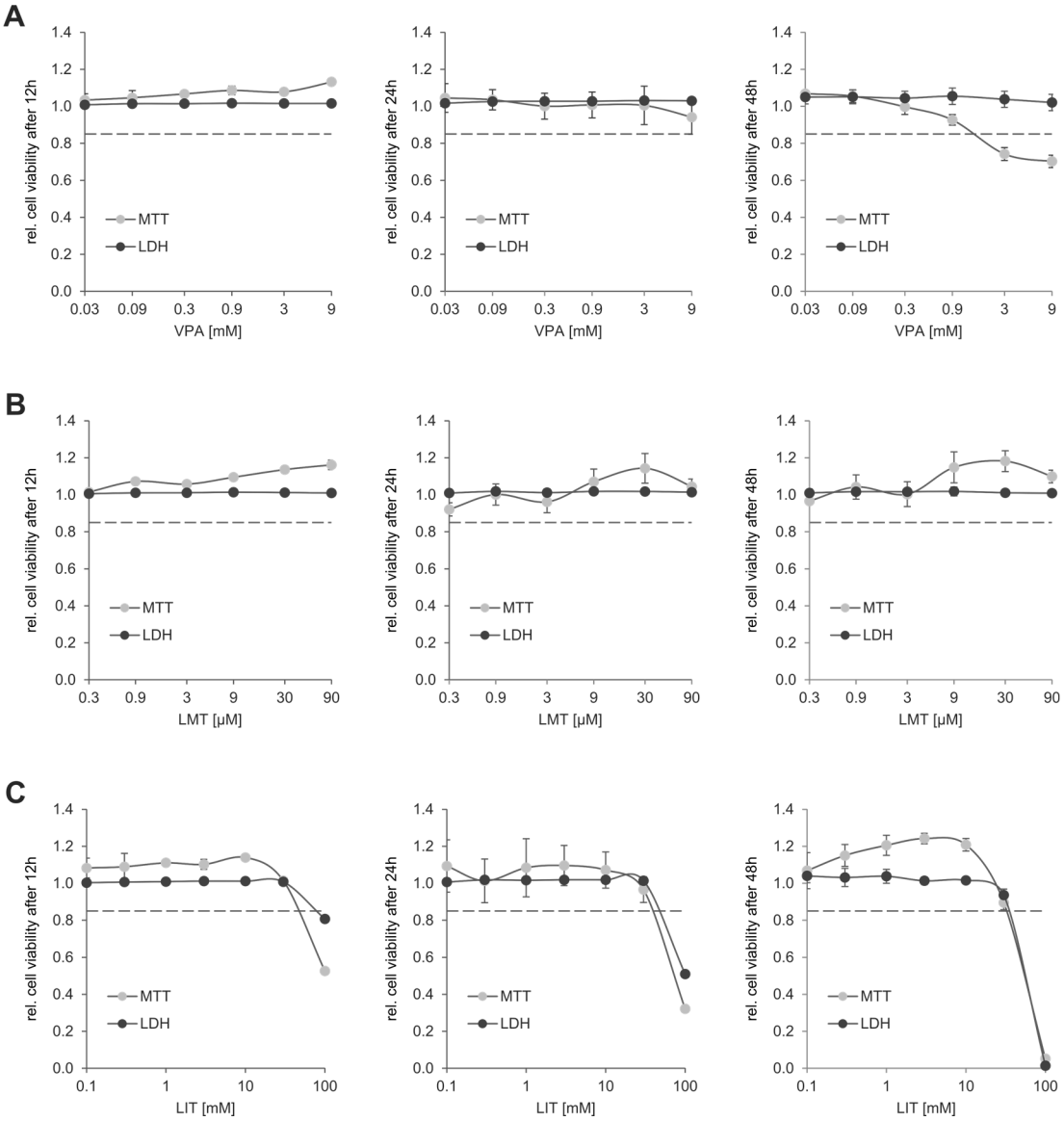

Figure 11: **Toxicity of selected mood stabilisers.** Cell viability was analysed after 12 hours, 24 hours and 48 hours drug treatment and normalised to viability of control treated cells in two assays. Cell viability was detected as a measure of general metabolism in the MTT assay and as a measure of cell membrane integrity in the LDH assay. Viability rate of 85%, which was defined as toxicity limit, is indicated by the dashed line. Cell viability was measured upon treatment with 0.03 mM to 9 mM VPA (**A**), 0.3 µM to 90 µM LMT (**B**), or 0.1 mM to 100 mM LIT (**C**). Dots show the mean value and error bars represent the standard error of the mean.

Different toxicity profiles were observed for the structurally diverse group of mood stabilisers (Figure 11). VPA, which was administered up to 9 mM, did not evoke

cytotoxicity in the LDH assay and the MTT assay indicated only slightly induced cytotoxicity after 48 hours at concentrations starting from 3 mM (Figure 11A). No cytotoxicity was observed in response to treatment with the second mood stabiliser LMT in either assay at a concentration up to 90 mM (Figure 11B). An induction of signal solely in the MTT assay emerged, however, with LMT at all three time points and peaked at a concentration of 30 µM. The third mood stabiliser, LIT, started to induce cytotoxic effects detected in both assays when administered above 30 µM at all time points. An induction of signal solely in the MTT assay was visible after 48 hours incubation peaking at a concentration of 3 mM LIT. Hence, 5 µM VPA, 10 µM LMT and 10 mM LIT were selected for treatment in further experiments if not declared differently.

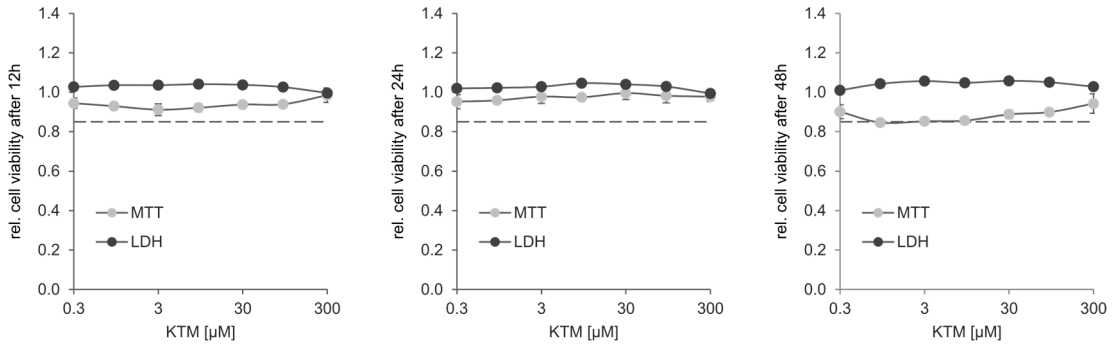

Figure 12: **Toxicity of the NMDA receptor antagonists KTM.** Cell viability was analysed after 12 hours, 24 hours and 48 hours drug treatment and normalised to viability of control treated cells in two assays. Cell viability was detected as a measure of general metabolism in the MTT assay and as a measure of cell membrane integrity in the LDH assay. Viability rate of 85%, which was defined as toxicity limit, is indicated by the dashed line. Cell viability was measured upon treatment with 0.3 µM to 300 µM KTM. Dots show the mean value and error bars represent the standard error of the mean.

The NMDA receptor antagonist KTM did not induce cytotoxicity over the entire range of drug concentrations (Figure 12). A concentration of 100 µM KTM was chosen for treatment in further experiments.

Neither assay indicated cytotoxicity in response to treatment with the NMDA receptor antagonist LNC (Figure 13A). Treatment with the GSK3β inhibitor CHI also did not evoke cytotoxic effects as indicated by the MTT and the LDH assay up to a concentration of 30 µM (Figure 13B). An induction of signal solely in the MTT assay in response to treatment with CHI started to emerge at concentrations above 10 µM. Hence, 3 µM CHI was chosen for treatment in further experiments.

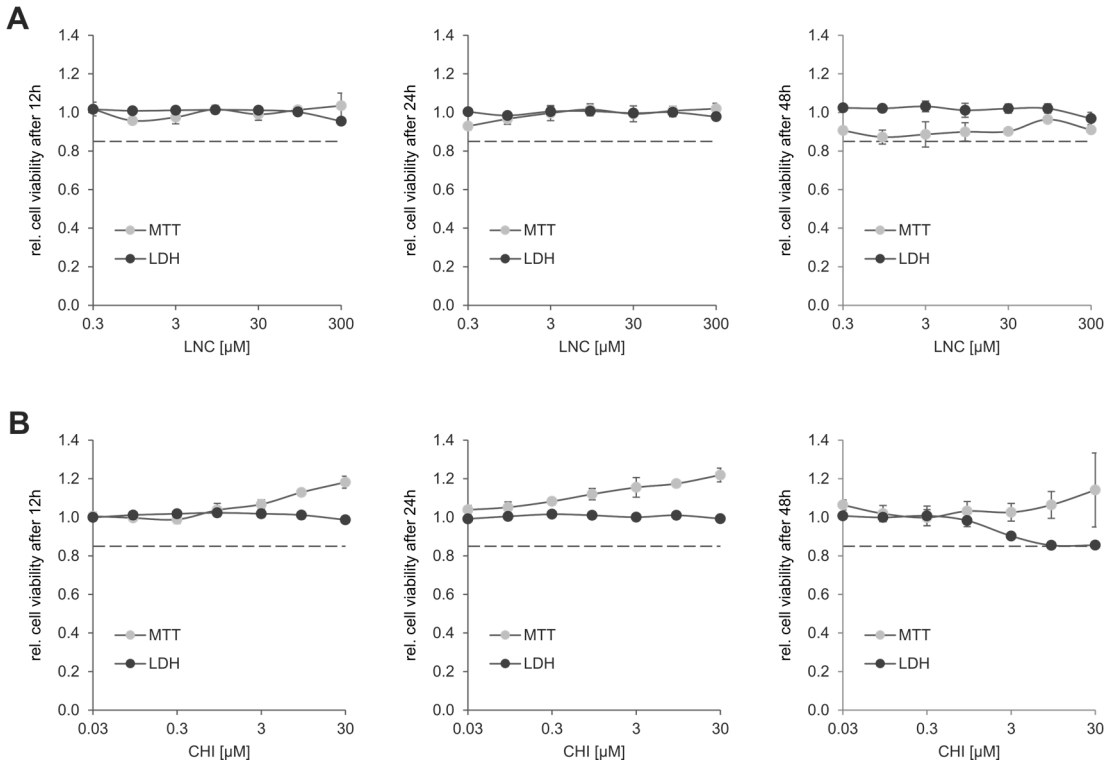

Figure 13: **Toxicity of the experimental substances LNC and CHI.** Cell viability was analysed after 12 hours, 24 hours and 48 hours drug treatment and normalised to viability of control treated cells in two assays. Cell viability was detected as a measure of general metabolism in the MTT assay and as a measure of cell membrane integrity in the LDH assay. Viability rate of 85%, which was defined as toxicity limit, is indicated by the dashed line. Cell viability was measured upon treatment with 0.3 nM to 300 nM LNC (**A**) or 0.03 µM to 30 µM CHI (**B**). Dots show the mean value and error bars represent the standard error of the mean.

4.2.2 Effect of FKBP5 deletion on protein markers previously linked to antidepressants

Next, a potential differential activity-indicating phosphorylation of the kinases GSK3β, AKT and ERK2 as well as selected presumptive downstream targets in MEF cells with and without the FKBP5 deletion was assessed.

No difference in the inhibitory phosphorylation of GSK3β at Ser-9 was detected upon normalization to the housekeeping protein actin (Figure 14A). Upon normalization to the total expression level of GSK3β, however, an increased fraction of phosphorylated GSK3β was found in FKBP5-KO cells (Figure 14B). Combining those two findings, there was a decrease of the unphosphorylated GSK3β in FKBP5-KO cells, which is the active form of the kinase. BCAT is a substrate of GSK3β and becomes phosphorylated by GSK3β when pre-phosphorylated at priming sites. Final phosphorylation by GSK3β

leads to the destruction of BCAT. Less GSK3β activity in FKBP5-KO cells, however, was not reflected by a significant increase in BCAT levels (Figure 14C). The second target of GSK3β analysed here was CRMP2, which has been reported to be inactivated by GSK3β upon phosphorylation at Thr-514 (Yoshimura et al., 2005). In line with lowered GSK3β activity, decreased phosphorylation of CRMP2 in FKBP5-KO cells was detected (Figure 14D).

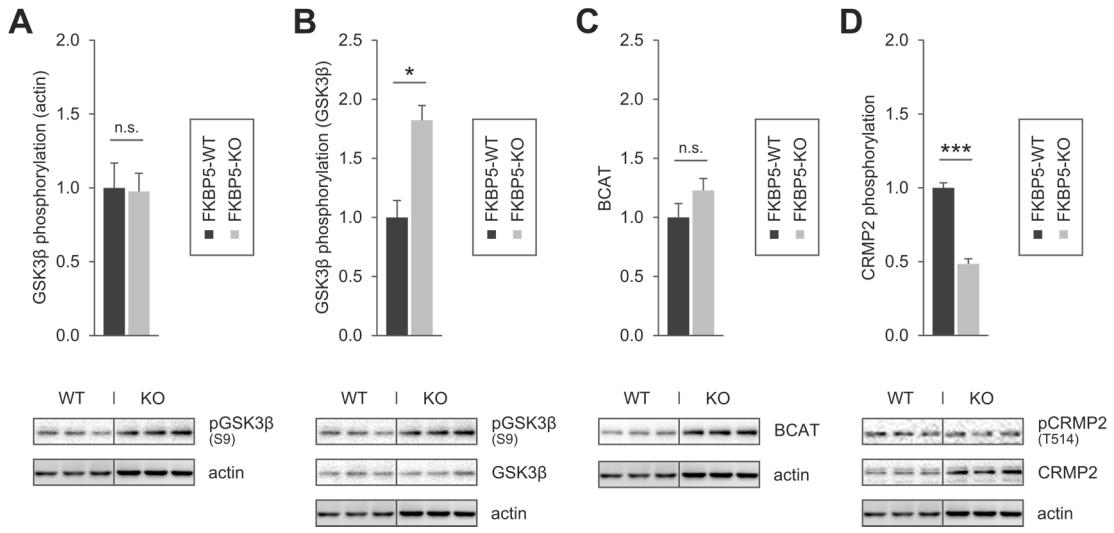

Figure 14: **Effect of FKBP5 deletion on selected markers of the GSK3β pathway**. The protein status of selected markers in MEF cells with and without FKBP5 deletion was analysed by western detection. Bars show the mean value and error bars represent the standard error of the mean. Statistical significances were calculated by a simple t-test and are depicted as follows: n.s. for $p>0.05$, * for $p\leq0.05$, ** for $p\leq0.01$ and *** for $p\leq0.001$. **A** Phosphorylation of GSK3β at Ser-9 was quantified and normalised to the level of actin from three biological replicates on one western blot. **B** Phosphorylation of GSK3β at Ser-9 was quantified and normalised to the total level of GSK3β from three biological replicates on one western blot. **C** Level of BCAT was quantified and normalised to the level of actin from three biological replicates on one western blot. **D** Phosphorylation of CRMP2 at Thr-514 was quantified and normalised to the total level of CRMP2 from three biological replicates on one western blot.

A marked increase in phosphorylation of AKT at Ser-473 was found in MEF cells with deleted FKBP5 (Figure 15A). This reflects the finding of increased AKT phosphorylation due to the absence of FKBP51 mediated formation of the AKT:PHLPP phosphatase complex (Pei et al., 2009). Slightly increased levels of the autophagy regulator BECN1 were found in cells with the FKBP5 deletion (Figure 15B). In those cells, increased levels of BECN1 were accompanied by increased lipidation of LC3, both markers of increased autophagy (Figure 15C). No difference in phosphorylation of CRMP2 at Ser-

318 and Ser-321, an assumed target of FKBP51, was detected in cells with deleted FKBP5 compared to cells with functional FKBP5 (Figure 15D).

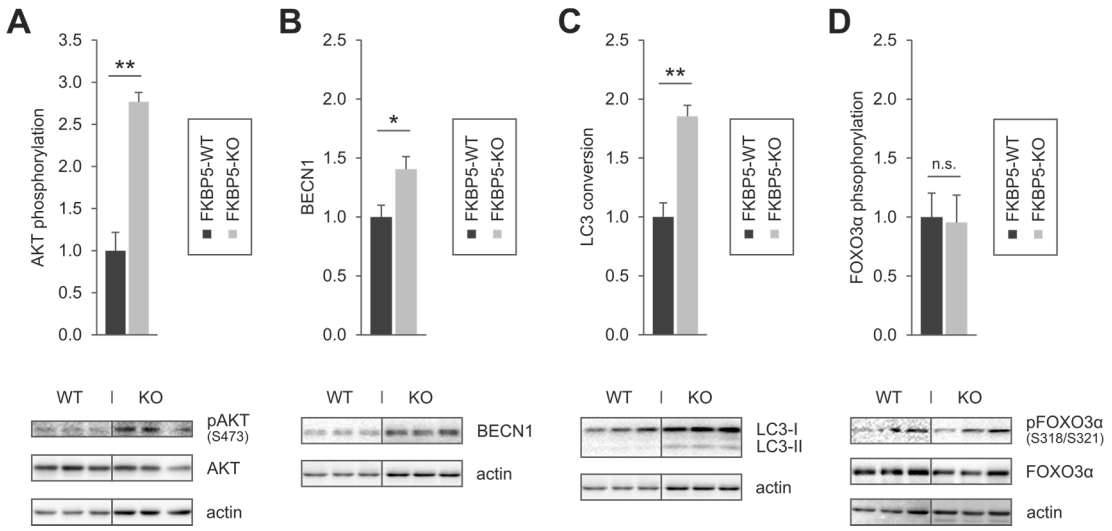

Figure 15: **Effect of FKBP5 deletion on selected markers of the AKT and autophagy pathway.** The protein status of selected markers in MEF cells with and without FKBP5 deletion was analysed by western detection. Bars show the mean value and error bars represent the standard error of the mean. Statistical significances were calculated by a simple t-test and are depicted as follows: n.s. for $p>0.05$, * for $p\leq0.05$, ** for $p\leq0.01$ and *** for $p\leq0.001$. **A** Phosphorylation of AKT at Ser-473 was quantified and normalised to the total level of AKT from three biological replicates on one western blot. **B** The level of BECN1 was quantified and normalised to the level of actin from three biological replicates on one western blot. **C** Conversion of LC3-I to LC3-II was calculated as the ratio of quantified LC3-II to LC3-I from three biological replicates on one western blot. **D** Phosphorylation of FOXO3α at Ser-318 and Ser-321 was quantified and normalised to the total level of FOXO3α from three biological replicates on one western blot.

With both FKBP51 and ERK being responsive to stress on the one hand and ERK being regulated by the HSP90 complex on the other hand, a potential physical interaction of FKBP51 with ERK was tested initially (Dou et al., 2005). FLAG-tagged FKBP51 and HA-tagged ERK1 was expressed in HEK-293 cells to assess their interaction by co-immunoprecipitation. Indeed, ERK1 displayed binding to FKBP51 and FKBP51 displayed binding to ERK1, respectively (Figure 16A).

Based on the interaction of FKBP51 with ERK1, next a potential differential phosphorylation of ERK in the presence or absence of FKBP51 was assessed. Indeed, increased phosphorylation of both ERK1 and ERK2 at Thr-202 and Tyr-204 was detected in MEF cells with deleted FKBP5, with similarly increased phosphorylation in both ERK isoforms (Figure 16B).

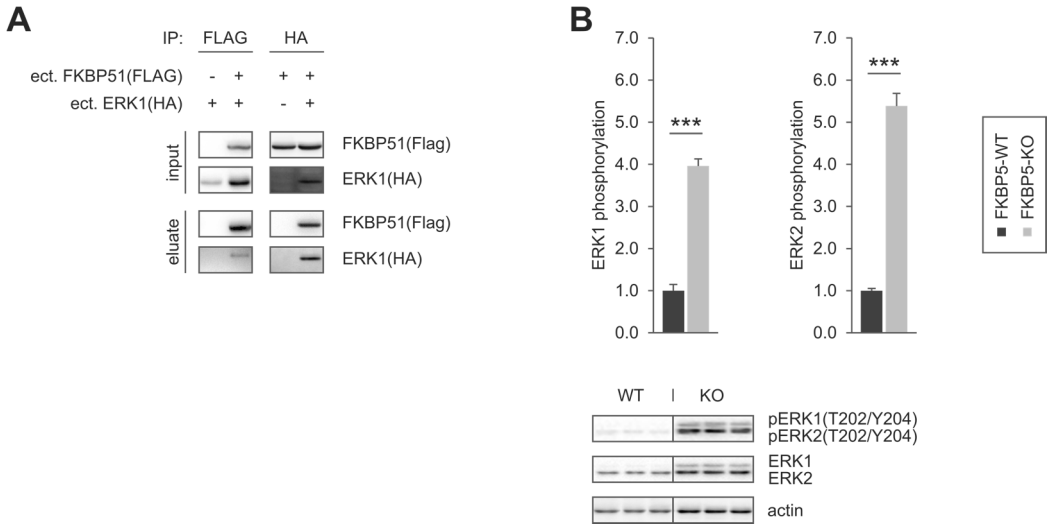

Figure 16: **Interaction of FKBP51 with ERK and effect of FKBP5 deletion on ERK phosphorylation. A** FKBP5 interacts with ERK. HEK-293 cells were transfected either with ERK1(HA) in combination with vector control or FKBP51(FLAG) expressing plasmids (lanes 1 and 2) or with FKBP51(FLAG) in combination with vector control or ERK1(HA) expressing plasmids (lanes 3 and 4). Cells were lysed 72 h after transfection. Proteins from lysates were immunoprecipitated with FLAG antibody (lanes 1 and 2) or HA antibody (lanes 3 and 4) and analysed by western detection. **B** ERK phosphorylation in MEF cells with and without FKBP5 deletion was analysed by western detection. Phosphorylation of ERK1 and ERK2 at Thr-202 and Tyr-204 was quantified and normalised to the total level of ERK1 and ERK2, respectively, from three biological replicates on one western blot. Bars show the mean value and error bars represent the standard error of the mean. Statistical significances were calculated by a simple t-test and are depicted as follows: n.s. for $p>0.05$, * for $p\leq0.05$, ** for $p\leq0.01$ and *** for $p\leq0.001$.

4.2.3 Responsiveness of selected protein markers to psychopharmaca treatment

FKBP5 was originally selected as a candidate gene for genetic analyses in depression and antidepressant responsiveness (Binder et al., 2004). Focusing on the protein level, the aim of this work was to analyse the responsiveness of pathways relevant to psychiatric diseases. MEF cells with and without a functional FKBP5 were treated with psychopharmaca and utilised as a cellular model for FKBP5-dependent effects.

GSK3β phosphorylation

As a first marker, the responsiveness in activity of GSK3β to treatment with psychopharmaca and experimental substances was analysed. Several psychopharmaca

increased the phosphorylation of GSK3β at Ser-9 normalised to the expression of the housekeeping protein actin and therefore inhibited GSK3β activity (Figure 17A).

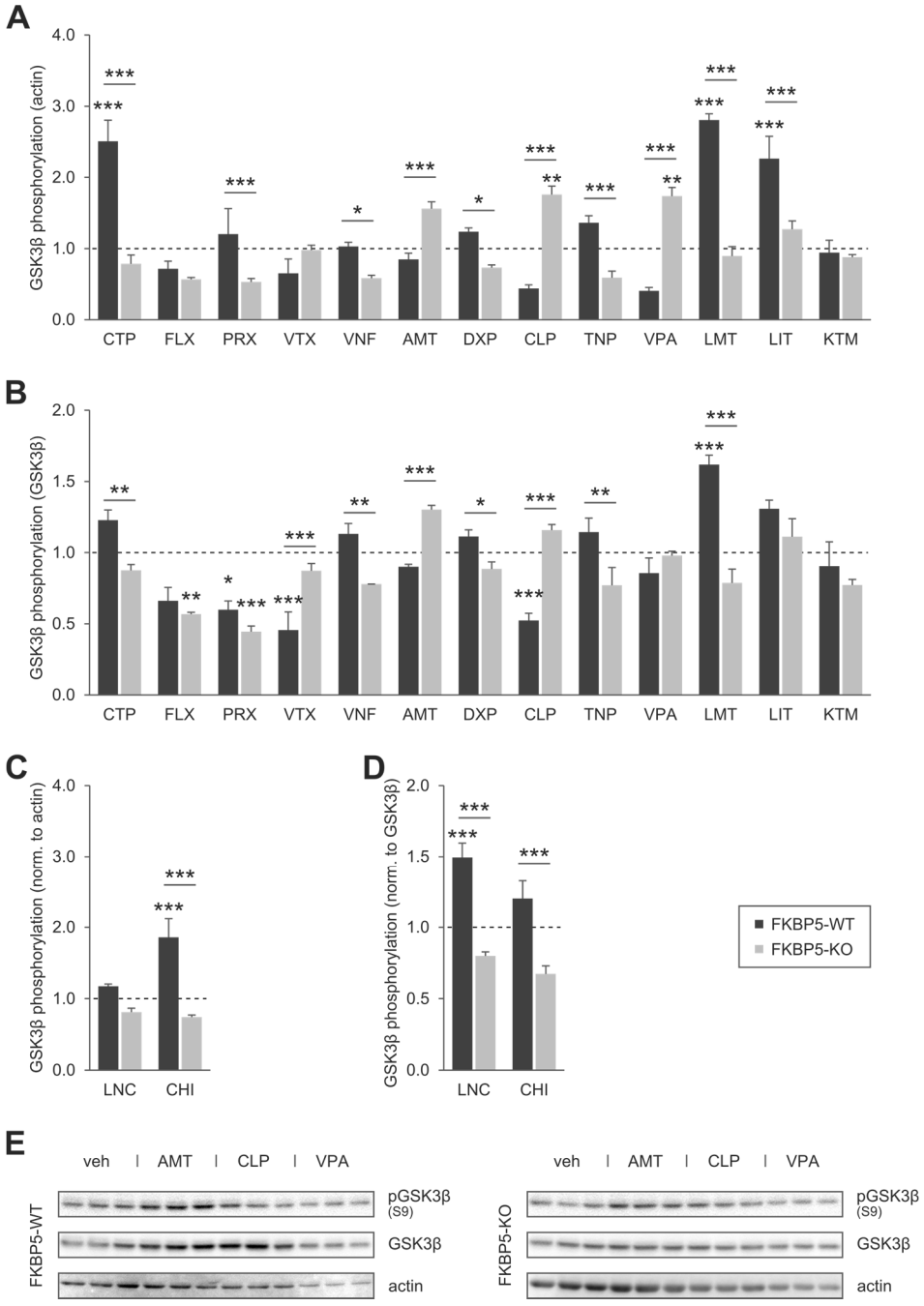

Figure 17: **Responsiveness of GSK3β phosphorylation to treatment with psychopharmaca.** GSK3β phosphorylation at Ser-9 in MEF cells with and without FKBP5 deletion was analysed by western detection after treatment with the indicated drugs for 48 hours. GSK3β phosphorylation was quantified and normalised to the level of actin or GSK3β as indicated from three biological replicates. Responsiveness to treatment in MEF cells with and without the FKBP5 deletion was calculated as ratio of values upon treatment divided by value upon control treatment in the respective cell line, which was thereby set to 1 and is indicated by the dashed line.

Bars show the mean value and error bars represent the standard error of the mean. Statistical significances were calculated by a two-way analysis of variance combined with a Bonferroni post-hoc test and are depicted as follows: * for p≤0.05, ** for p≤0.01 and *** for p≤0.001. **A** Responsiveness to treatment with psychopharmaca of GSK3β phosphorylation normalised to actin was assessed. **B** Responsiveness to treatment with psychopharmaca of GSK3β phosphorylation normalised to GSK3β was assessed. **C** Responsiveness to treatment with experimental substances of GSK3β phosphorylation normalised to actin was assessed. **D** Responsiveness to treatment with experimental substances of GSK3β phosphorylation normalised to GSK3β was assessed. **E** Exemplary western signals for vehicle, AMT, CLP and VPA treatment of cells with and without the FKBP5 deletion are depicted.

CTP, LMT and LIT significantly increased GSK3β phosphorylation in MEF cells with functional FKBP5, whereas CLP and VPA significantly increased GSK3β phosphorylation in MEF cells with deleted FKBP5. Moreover, the GSK3β inhibitor CHI significantly increased GSK3β phosphorylation exclusively in MEF cells with functional FKBP5 (Figure 17C). No significant decrease in GSK3β phosphorylation was observed in response to treatment with any of the psychopharmaca. Significant FKBP5 dependent effects with exclusive or at least higher responsiveness in MEF cells with functional FKBP5 were evoked by treatment with drugs from all subclasses including CTP, PRX, VNF, DXP, TNP, LMT, LIT and CHI. Increased or exclusive responsiveness in MEF cells with deleted FKBP5 was observed for treatment with AMT, CLP and VPA.

Interestingly, the increase in phosphorylated GSK3β in response to treatment generally appeared slightly attenuated when normalising to total GSK3β level (Figure 17B and Figure 17D). This is due to the observation that treatment with psychopharmaca tended to increase the level of total GSK3β compared to actin. When normalised to total GSK3β levels, significant decrease in GSK3β phosphorylation was detected in MEF cells with functional FKBP5 treated with PRX, VTX and CLP as well as in MEF cells with deleted FKBP5 treated with FLX and PRX. Increased phosphorylation was detected in MEF cells with functional FKBP5 upon treatment with LMT and LNC.

Significant FKBP5 dependency with exclusive or at least higher responsiveness in MEF cells with functional FKBP5 was observed in response to treatment with drugs from all subclasses including CTP, VNF, DXP, TNP, LMT, LNC, CHI. Increased or exclusive responsiveness in MEF cells with deleted FKBP5 was noted for treatment with VTX, AMT and CLP.

BCAT

GSK-3β plays an important role in regulating BCAT levels. Inhibition of GSK-3β has been shown to result in BCAT accumulation, due to a decrease in the rate of BCAT

protein degradation (Nishimura et al., 1999). While significant accumulation of BCAT to treatment was only observed for PRX in MEF cells with deleted FKBP5, increased degradation of BCAT was detected in MEF cells with functional FKBP5 treated with CLP, VPA and LMT as well as in MEF cells with deleted FKBP5 treated with LMT and CHI (Figure 18A, Figure 18B). Treatment with PRX actually increased BCAT levels.

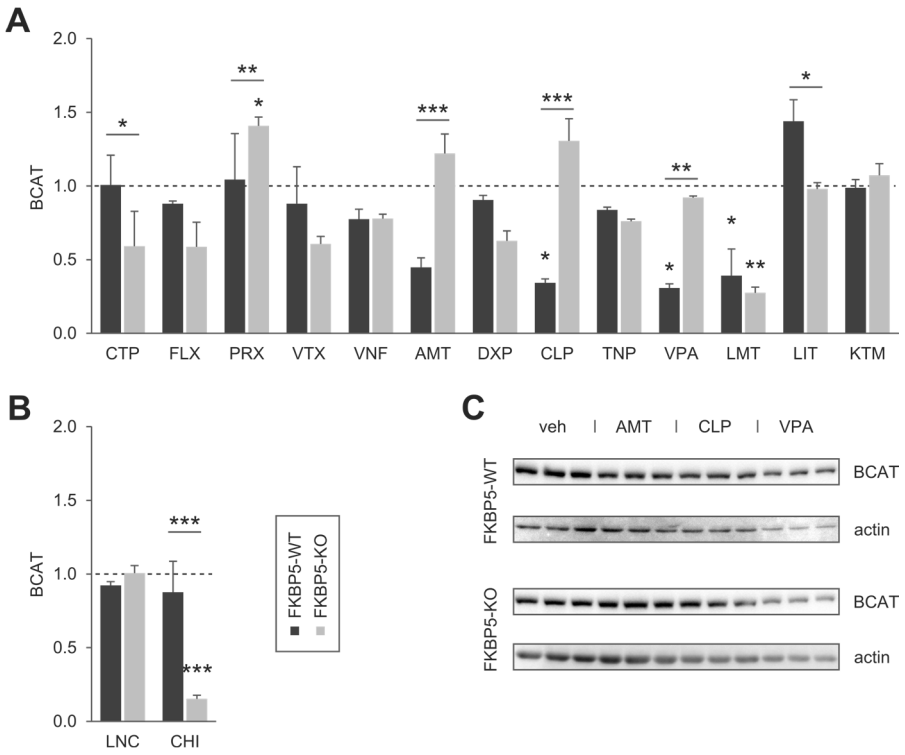

Figure 18: **Responsiveness of BCAT stability to treatment with psychopharmaca.** BCAT expression in MEF cells with and without FKBP5 deletion was analysed by western detection after treatment with the indicated drugs for 48 hours. Level of BCAT was quantified and normalised to the level of actin from three biological replicates. Responsiveness to treatment in MEF cells with and without the FKBP5 deletion was calculated as ratio of values upon treatment divided by value upon control treatment in the respective cell line, which was thereby set to 1 and is indicated by the dashed line. Bars show the mean value and error bars represent the standard error of the mean. Statistical significances were calculated by a two-way analysis of variance combined with a Bonferroni post-hoc test and are depicted as follows: * for $p \leq 0.05$, ** for $p \leq 0.01$ and *** for $p \leq 0.001$. **A** Responsiveness of BCAT expression level to treatment with psychopharmaca was assessed. **B** Responsiveness of BCAT expression level to treatment with experimental substances was assessed. **C** Exemplary western signals for vehicle, AMT, CLP and VPA treatment of cells with and without the FKBP5 deletion are depicted.

Significant FKBP5 dependent effects with exclusive or at least higher responsiveness in MEF cells with functional FKBP5 were evoked in response to treatment with CTP, LIT

and CHI. Increased or exclusive responsiveness in MEF cells with deleted FKBP5 was observed in response to treatment with PRX, AMT and CLP.

CRMP2 phosphorylation

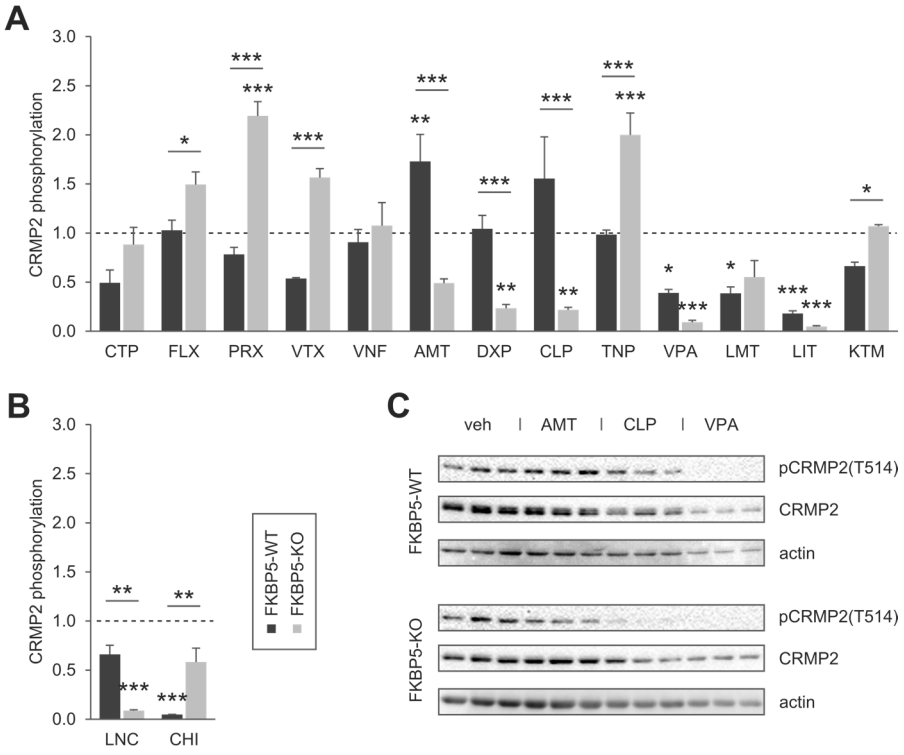

Figure 19: **Responsiveness of CRMP2 phosphorylation to treatment with psychopharmaca.** CRMP2 phosphorylation at Thr-514 in MEF cells with and without FKBP5 deletion was analysed by western detection after treatment with the indicated drugs for 48 hours. Level of CRMP2 phosphorylation was quantified and normalised to the total level of CRMP2 from three biological replicates. Responsiveness to treatment in MEF cells with and without the FKBP5 deletion was calculated as ratio of values upon treatment divided by value upon control treatment in the respective cell line, which was thereby set to 1 and is indicated by the dashed line. Bars show the mean value and error bars represent the standard error of the mean. Statistical significances were calculated by a two-way analysis of variance combined with a Bonferroni post-hoc test and are depicted as follows: * for $p \leq 0.05$, ** for $p \leq 0.01$ and *** for $p \leq 0.001$. **A** Responsiveness of CRMP2 phosphorylation to treatment with psychopharmaca was assessed. **B** Responsiveness of CRMP2 phosphorylation to treatment with experimental substances was assessed. **C** Exemplary western signals for vehicle, AMT, CLP and VPA treatment of cells with and without the FKBP5 deletion are depicted.

A further target of GSK3β and a protein associated with psychiatric diseases is CRMP2, which is phosphorylated by GSK3β at Thr-509 and Thr-514 Thus, the responsiveness of CRMP2 phosphorylation at Thr-509 and Thr-514 to treatment with psychopharmaca and experimental drugs was analysed (Figure 19A and Figure 19B). Both increase and

decrease in CRMP2 phosphorylation was observed in response to treatment. Interestingly, a distinct pattern in responsiveness to treatment was observed with regard to class subgroups. Decreased phosphorylation was observed in response to treatment with the three mood stabiliser VPA, LMT and LIT as well as the GSK3β inhibitor CHI in cells with functional FKBP5. This is, at least for three out of four drugs, in line with inhibited GSK3β activity, which was observed in response to treatment with CTP, LMT, LIT and CHI. In cells with deleted FKBP5, however, decreased phosphorylation was observed in response to treatment with the TCAs DXP and CLP and the mood stabiliser VPA and LIT. On the other hand, a significant increase in CRMP2 phosphorylation was found in response to treatment with AMT in cells with functional FKBP5 as well as in response to treatment with PRX and TNP in cells with deleted FKBP5.

Differential effects with regard to the presence or absence of functional FKBP5 were observed for all three TCAs AMT, DXP and CLP as well as the NMDA receptor antagonist LNC with lower CRMP2 phosphorylation in cells with deleted FKBP5. Opposite effects with lower CRMP2 phosphorylation in cells with functional FKBP5 were detected in response to treatment with the SSRIs FLX and PRX, the SSNRI VTX, the atypical antidepressant TNP, the NMDA receptor antagonist KTM and the GSK3β inhibitor CHI.

AKT phosphorylation

Next, the responsiveness of AKT phosphorylation at Ser-473 to treatment with psychopharmaca (Figure 20A) and experimental drugs (Figure 20B) in cells with either functional or deleted FKBP5 was analysed. Treatment with several drugs, including CTP, PRX AMT and LMT, significantly increased the phosphorylation of AKT in cells with functional FKBP5. In cells with deleted FKBP5 a significant increase in AKT phosphorylation was observed in response to treatment with the TCAs AMT and CLP.

Differential effects of loss of FKBP51 function were observed for all three SSRIs CTP, FLX and PRX, as well as for two mood stabiliser LMT and LIT with higher AKT phosphorylation in cells with functional FKBP5. Opposite effects with lower AKT phosphorylation in cells with functional FKBP5 were detected in response to treatment with CLP.

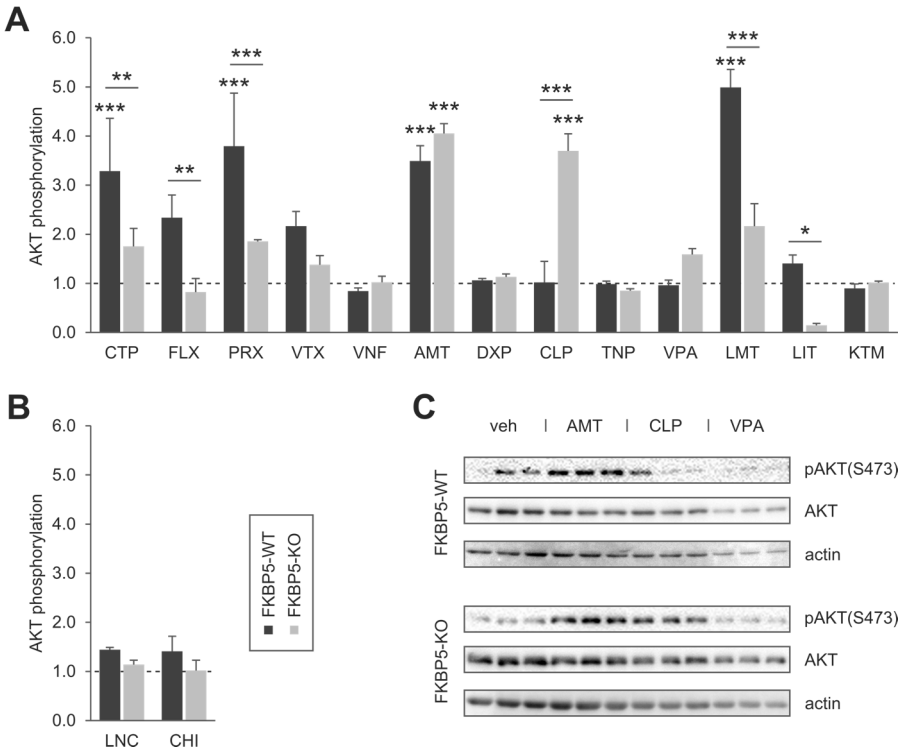

Figure 20: **Responsiveness of AKT phosphorylation to treatment with psychopharmaca.** AKT phosphorylation at Ser-473 in MEF cells with and without FKBP5 deletion was analysed by western detection after treatment with the indicated drugs for 48 hours. Level of AKT phosphorylation was quantified and normalised to the total level of AKT from three biological replicates. Responsiveness to treatment in MEF cells with and without the FKBP5 deletion was calculated as ratio of values upon treatment divided by value upon control treatment in the respective cell line, which was thereby set to 1 and is indicated by the dashed line. Bars show the mean value and error bars represent the standard error of the mean. Statistical significances were calculated by a two-way analysis of variance combined with a Bonferroni post-hoc test and are depicted as follows* for $p \leq 0.05$, ** for $p \leq 0.01$ and *** for $p \leq 0.001$. **A** Responsiveness of AKT phosphorylation to treatment with psychopharmaca was assessed. **B** Responsiveness of AKT phosphorylation to treatment with experimental substances was assessed. **C** Exemplary western signals for vehicle, AMT, CLP and VPA treatment of cells with and without the FKBP5 deletion are depicted.

BECN1

In order to unravel a potential effect of psychopharmaca on the initiation of autophagy, the expression levels of BECN1, a regulator of the VPS34 complex in response to treatment with psychopharmaca and experimental drugs were analysed (Figure 21A and Figure 21B). A significant accumulation of BECN1 was detected in response to treatment with CLP in cells with functional FKBP5 as well as in response to treatment with CTP and LMT in cells with deleted FKBP5. A significant decrease in the expression level of BECN1 in response to treatment was not observed.

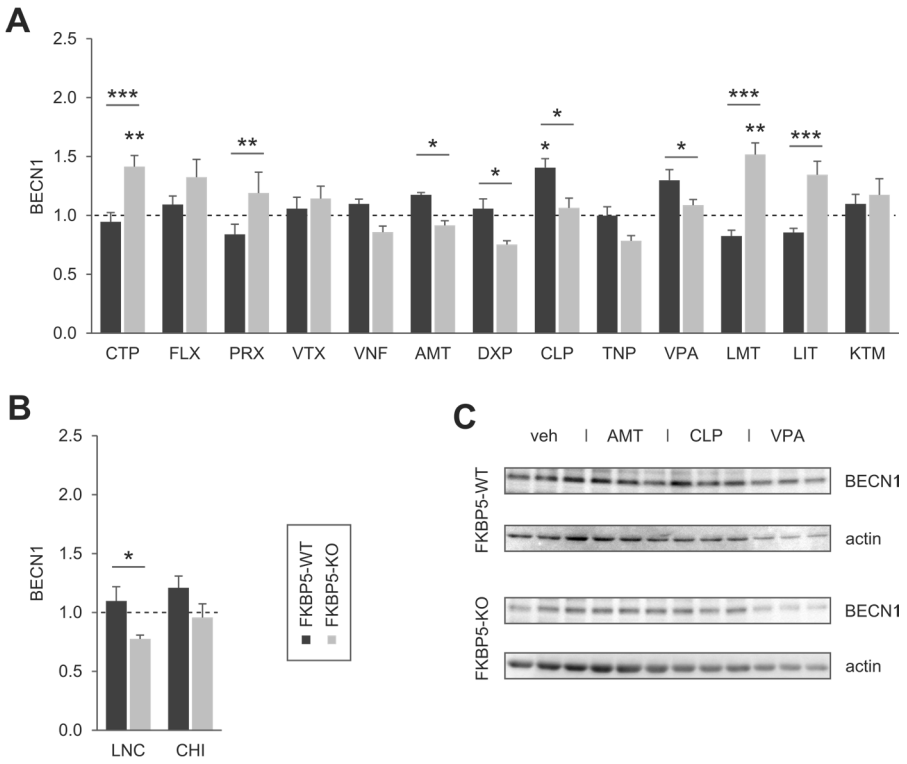

Figure 21: **Responsiveness of BECN1 stability to treatment with psychopharmaca.** BECN1 expression in MEF cells with and without FKBP5 deletion was analysed by western detection after treatment with the indicated drugs for 48 hours. Level of BECN1 was quantified and normalised to the level of actin from three biological replicates. Responsiveness to treatment in MEF cells with and without the FKBP5 deletion was calculated as ratio of values upon treatment divided by value upon control treatment in the respective cell line, which was thereby set to 1 and is indicated by the dashed line. Bars show the mean value and error bars represent the standard error of the mean. Statistical significances were calculated by a two-way analysis of variance combined with a Bonferroni post-hoc test and are depicted as follows: * for $p \leq 0.05$, ** for $p \leq 0.01$ and *** for $p \leq 0.001$. **A** Responsiveness of BECN1 expression level to treatment with psychopharmaca was assessed. **B** Responsiveness of BECN1 expression level to treatment with experimental substances was assessed. **C** Exemplary western signals for vehicle, AMT, CLP and VPA treatment of cells with and without the FKBP5 deletion are depicted.

Differential effects of loss of FKBP51 function were observed for all three TCAs AMT, DXP, and CLP as well as VPA and LNC with higher BECN1 levels in cells with functional FKBP5. Higher BECN1 levels in cells with deleted FKBP5 were detected in response to treatment with the two SSRIs CTP and PRX as well as the two mood stabiliser LMT and LIT.

LC3 conversion

Next, it was analysed if psychopharmaca increased autophagy indicated by LC3-II to LC3-I conversion (Figure 22A and Figure 22B). Increased conversion of LC3 in cells with functional FKBP5 was observed in response to treatment with the SSRIs FLX and PRX, the SNRI VTX and the SSRIs DXP and CLP. In cells with deleted FKBP5, increased conversion of LC3 was measured in response to treatment with FLX, VTX and all three TCAs AMT, DXP, and CLP.

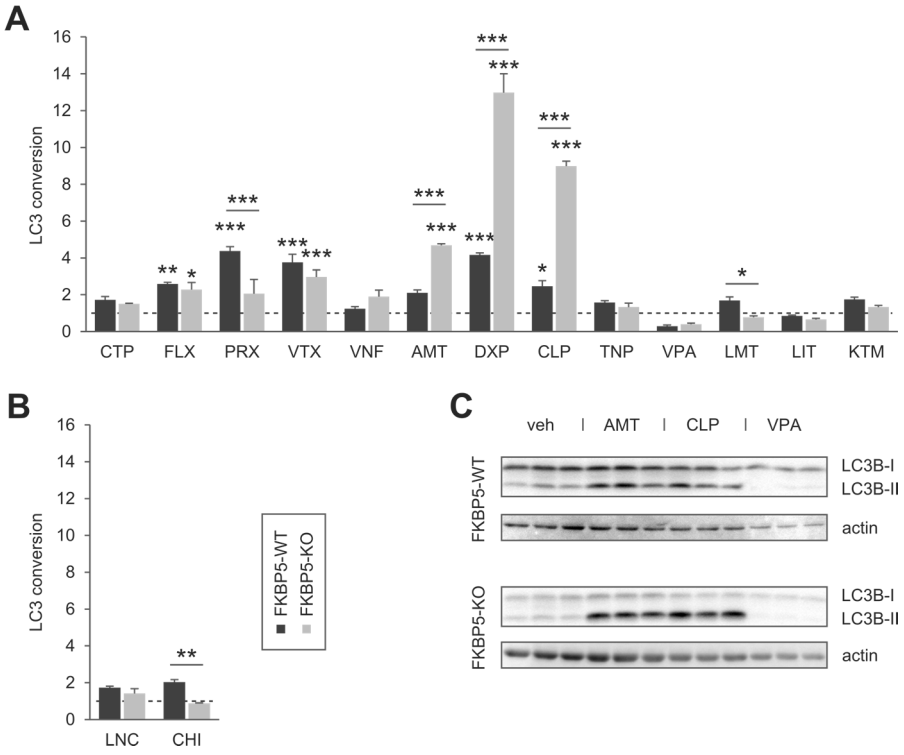

Figure 22: **Responsiveness of LC3 conversion to treatment with psychopharmaca.** LC3 conversion in MEF cells with and without FKBP5 deletion was analysed by western detection after treatment with the indicated drugs for 48 hours. Level of LC3-II was quantified and normalised to the level of LC3-I from three biological replicates. Responsiveness to treatment in MEF cells with and without the FKBP5 deletion was calculated as ratio of values upon treatment divided by value upon control treatment in the respective cell line, which was thereby set to 1 and is indicated by the dashed line. Bars show the mean value and error bars represent the standard error of the mean. Statistical significances were calculated by a two-way analysis of variance combined with a Bonferroni post-hoc test and are depicted as follows: * for $p \leq 0.05$, ** for $p \leq 0.01$ and *** for $p \leq 0.001$. **A** Responsiveness of LC3 conversion to treatment with psychopharmaca was assessed. **B** Responsiveness of LC3 conversion to treatment with experimental substances was assessed. **C** Exemplary western signals for vehicle, AMT, CLP and VPA treatment of cells with and without the FKBP5 deletion are depicted.

Differential effects of FKBP5 deletion were observed in response to treatment with PRX, LMT and CHI with higher LC3 conversion in cells with functional FKBP5. On the other hand, higher LC3 conversion in cells with deleted FKBP5 was detected in response to treatment with all three TCAs AMT, DXP, and CLP. Interestingly, decreased LC3-II to LC3-I conversion was exclusively observed in response to treatment with the mood stabiliser VPA in cells with either functional or deleted FKBP5, which was, however, not significant.

FOXO3α phosphorylation

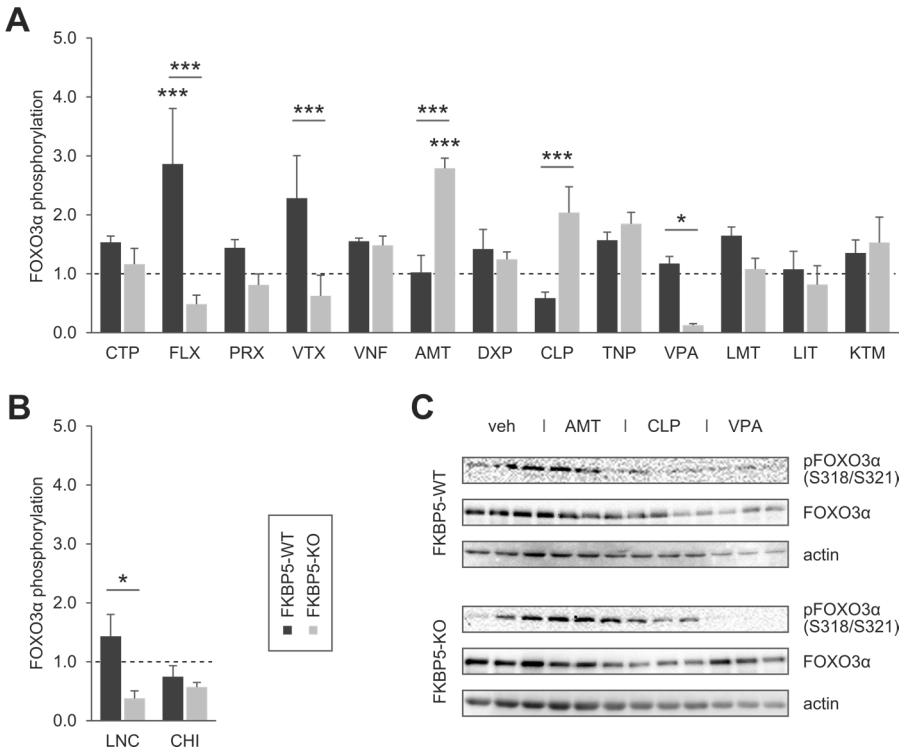

Figure 23: **Responsiveness of FoxO3α phosphorylation to treatment with psychopharmaca.** FOXO3α phosphorylation at Ser-318 and Ser-321 in MEF cells with and without FKBP5 deletion was analysed by western detection after treatment with the indicated drugs for 48 hours. Level of FOXO3α phosphorylation was quantified and normalised to the total level of FOXO3α from three biological replicates. Responsiveness to treatment in MEF cells with and without the FKBP5 deletion was calculated as ratio of values upon treatment divided by value upon control treatment in the respective cell line, which was thereby set to 1 and is indicated by the dashed line. Bars show the mean value and error bars represent the standard error of the mean. Statistical significances were calculated by a two-way analysis of variance combined with a Bonferroni post-hoc test and are depicted as follows: * for $p \leq 0.05$, ** for $p \leq 0.01$ and *** for $p \leq 0.001$. **A** Responsiveness of FOXO3α phosphorylation to treatment with psychopharmaca was assessed. **B** Responsiveness of FOXO3α phosphorylation to treatment with experimental substances was assessed. **C** Exemplary western signals for vehicle, AMT, CLP and VPA treatment of cells with and without the FKBP5 deletion are depicted.

A potential link between AKT and regulation of autophagy may be provided by the transcription factor FOXO3α, whose activity is, amongst others, regulated by AKT via phosphorylation at Ser-318 and Ser-321 (Rena et al., 2002). Therefore, the responsiveness of FOXO3α phosphorylation to treatment with psychopharmaca (Figure 23A) and experimental drugs (Figure 23B) was analysed in cells with functional or deleted FKBP5. Indeed, significantly increased FOXO3α phosphorylation was detected in response to treatment with FLX and VTX in cells with functional FKBP5. In cells with deleted FKBP5, increased FOXO3α phosphorylation was detected in response to treatment with AMT. Differential effects in regard to FKBP5 were observed in response to treatment with FLX, VTX, VPA and LNC with higher FOXO3α phosphorylation in cells with functional FKBP5. Increased FOXO3α phosphorylation in cells with deleted FKBP5 was detected in response to treatment with the two TCAs AMT and CLP.

ERK2 phosphorylation

It was recently reported that antidepressant treatment equally affects the activation of one of the two isoforms, ERK1 and ERK2, with respect to the other (Di Benedetto et al., 2013). In respect to a similar effect in ERK1 and ERK2 phosphorylation in MEF cells with deleted FKBP5, the analysis of ERK phosphorylation in response to treatment with psychopharmaca and experimental drugs was focused on ERK2, which was higher abundant and thus could be more reliably determined (Figure 24A and Figure 24B). In cells with functional FKBP5, treatment with CTP, VNF, TNP, VPA, LMT, KTM and CHI significantly increased phosphorylation of ERK2. ERK2 phosphorylation in cells with deleted FKBP5, however, did not significantly respond to treatment. Significant differential responsiveness in cells with functional FKBP5 compared to cells with deleted FKBP5 was observed in the treatment with CTP, VNF, TNP, KTM and CHI. Markedly, treatment with any of the three mood stabilisers VPA, LMT and LIT provoked a significantly difference in responsiveness in cells with functional FKBP5 compared to cells with deleted FKBP5.

Strikingly, a general FKBP5 dependent responsiveness in the phosphorylation of ERK2 to treatment with psychopharmaca was observed. A marked increase in ERK2 phosphorylation in response to average drug treatment in cells with functional FKBP5 was detected, which was not reflected in cells with deleted FKBP5.

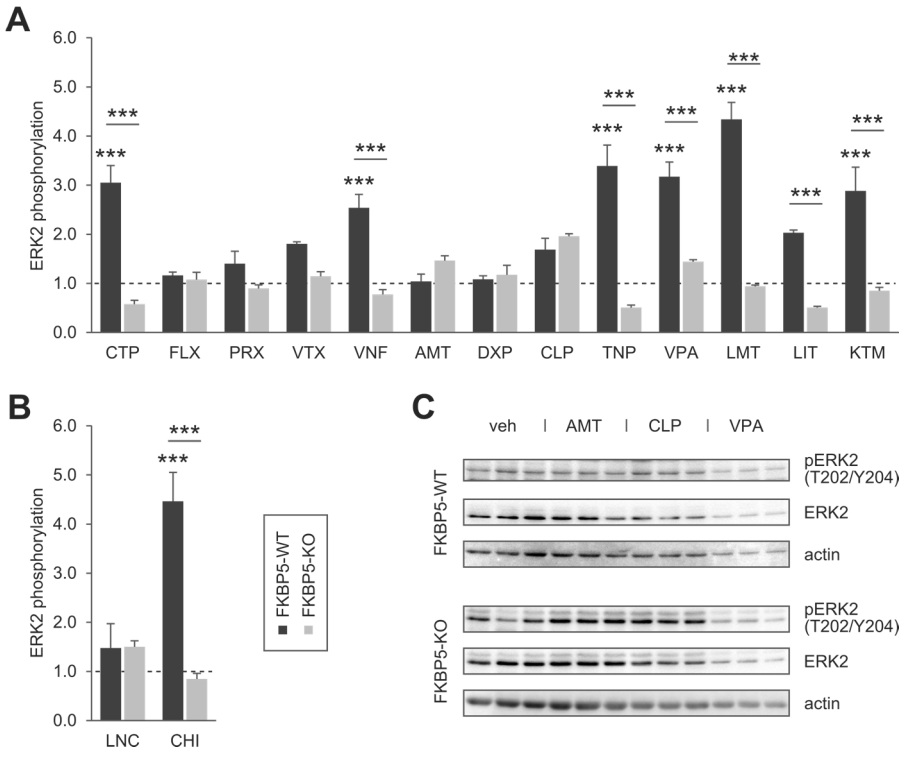

Figure 24: **Responsiveness of ERK2 phosphorylation to treatment with psychopharmaca.** ERK2 phosphorylation at Thr-202 and Tyr-204 in MEF cells with and without FKBP5 deletion was analysed by western detection after treatment with the indicated drugs for 48 hours. Level of ERK2 phosphorylation was quantified and normalised to the total level of ERK2 from three biological replicates. Responsiveness to treatment in MEF cells with and without the FKBP5 deletion was calculated as ratio of values upon treatment divided by value upon control treatment in the respective cell line, which was thereby set to 1 and is indicated by the dashed line. Bars show the mean value and error bars represent the standard error of the mean. Statistical significances were calculated by a two-way analysis of variance combined with a Bonferroni post-hoc test and are depicted as follows: * for $p \leq 0.05$, ** for $p \leq 0.01$ and *** for $p \leq 0.001$. **A** Responsiveness of ERK2 phosphorylation to treatment with psychopharmaca was assessed. **B** Responsiveness of ERK2 phosphorylation to treatment with experimental substances was assessed. **C** Exemplary western signals for vehicle, AMT, CLP and VPA treatment of cells with and without the FKBP5 deletion are depicted.

4.2.4 Modulation of transcription factor activity by psychopharmaca treatment

In addition to the analysis of expression and phosphorylation of proteins, the transcriptional activity of proteins, which are under control of pathways relevant for psychiatric diseases, was assesed.

TCF/LEF

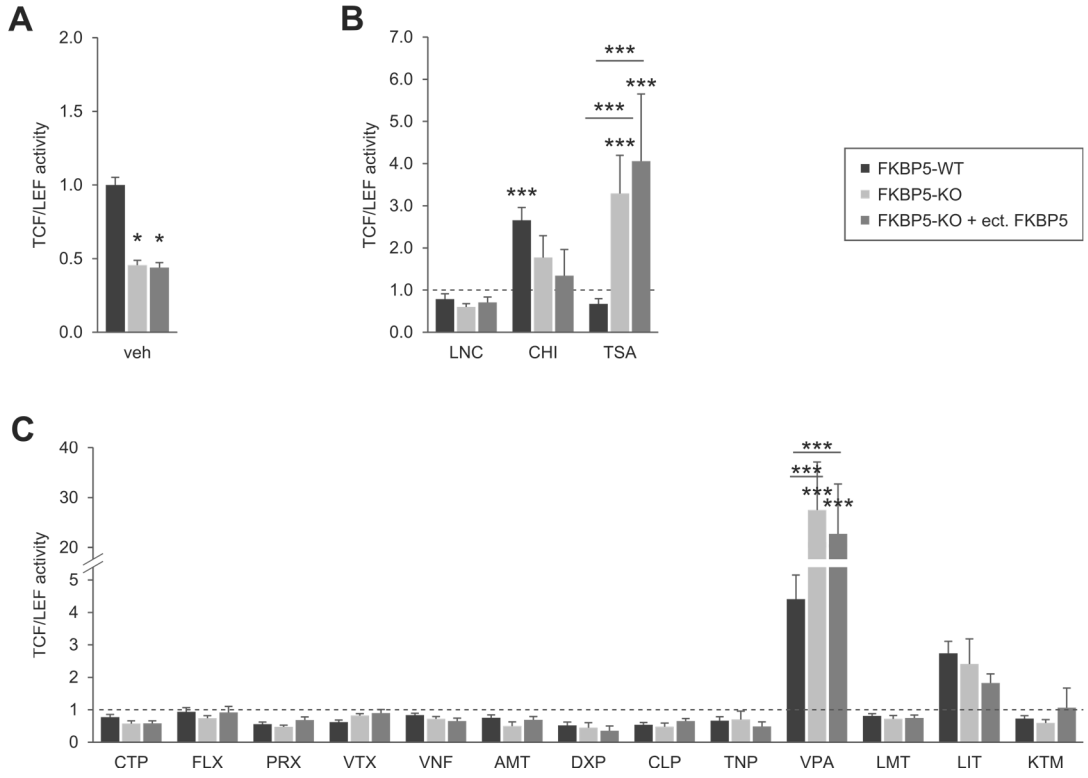

Figure 25: **Regulation of TCF/LEF activity by psychopharmaca and FKBP5.** Transcriptional activity of TCF/LEF was analysed in a dual luciferase based setup in MEF cells with and without the FKBP5 deletion. MEF cells were transfected with plasmids coding for firefly luciferase under control of a TCF/LEF dependent promoter, gaussia luciferase under control of a CMV promoter as well as FKBP51(FLAG) or control vector. Cells were treated 24 hours after transfection with the indicated drugs or vehicle for 48 hours. After cell lysis, light emission upon addition of firefly and gaussia substrate, subsequently, was measured. Firefly signal was normalised to gaussia signal. Bars show the mean value and error bars represent the standard error of the mean. Statistical significances were calculated by a two-way analysis of variance combined with a Bonferroni post-hoc test and are depicted as follows: * for $p \leq 0.05$, ** for $p \leq 0.01$ and *** for $p \leq 0.001$. **A** TCF/LEF activity was measured for each of the three FKBP5 conditions upon vehicle treatment and calculated as relative signal compared to signal from MEF cells without the FKBP5 deletion. **B** Responsiveness in TCF/LEF activity was measured for each of the three FKBP5 conditions upon treatment with experimental drugs and calculated as relative signal compared to signal from the respective FKBP5 condition in vehicle treated cells, which was thereby set to 1 and is indicated by the dashed line. **C** Responsiveness in TCF/LEF activity was measured for each of the three FKBP5 conditions upon treatment with psychopharmaca and calculated as relative signal compared to signal from the respective FKBP5 condition in vehicle treated cells, which was thereby set to 1 and is indicated by the dashed line.

T-cell factor/lymphoid enhancing factor (TCF/LEF) transcription factors present a group of transcription factors, which are controlled by GSK3β and BCAT in the Wnt signalling

pathway. In order to get a further readout for the ability of GSK3β to suppress downstream targets in response to FKBP5 deletion and treatment with psychopharmaca, the transcriptional activity of TCF/LEF was analysed in a dual luciferase based reporter construct in MEF cells with functional, deleted, or ectopic FKBP5.

Indeed, a significantly reduced transcriptional activity was detected in cells with deleted FKBP5 compared to cells with functional FKBP5 (Figure 25A). This reduction in transcriptional activity, however, could not be reversed by ectopic expression of FKBP5 in cells with deleted FKBP5 (Figure 25A).

In order to unravel the responsiveness of TCF/LEF activity to treatment, MEF cells with functional, deleted, or ectopic FKBP5 were treated with the experimental substances LNC, CHI or the HDAC inhibitor Trichostatin A (TSA) (Figure 25B). Treatment with CHI significantly increased the TCF/LEF activity in cells with functional FKBP5, but not in cells with deleted, or ectopic FKBP5. Treatment with TSA, however, significantly increased TCF/LEF activity in cells with deleted FKBP5 irrespectively of ectopic FKBP5 expression. In cells with functional FKBP5 no increase in TCF/LEF activity was observed in response to treatment with TSA.

No significant change in TCF/LEF activity was observed in response to treatment with most psychopharmaca (Figure 25C). Increase in TCF/LFE activity was solely measured in response to treatment with the mood stabilisers VPA and LIT. A non-significant increase in response to VPA treatment was detected in cells with functional FKBP5. A significant and even more pronounced increase in response to VPA treatment was detected in cells with deleted FKBP5 irrespectively of ectopic FKBP5 expression. Treatment with LIT non-significantly increased TCF/LEF activity in cells with either functional, deleted, or ectopic FKBP5.

Consecutively, begin of dose dependent treatment effects on TCF/LEF activity was analysed. Therefore, two concentrations of selected drugs from the groups of SSRIs, SSNRIs, TCAs and mood stabilisers were tested on their potential to modulate TCF/LEF activity in MEF cells with functional, deleted, or ectopic FKBP5.

In addition to 3 µM PRX, which was the concentration used in the preceding experiments, cells were treated with 10 µM PRX (Figure 26A). Treatment with 3 µM, but not 10 µM PRX significantly inhibited TCF/LEF activity in cells with functional FKBP5. In cells with deleted FKBP5, treatment with both 3 µM and 10 µM PRX inhibited TCF/LEF activity irrespectively of ectopic FKBP5 expression.

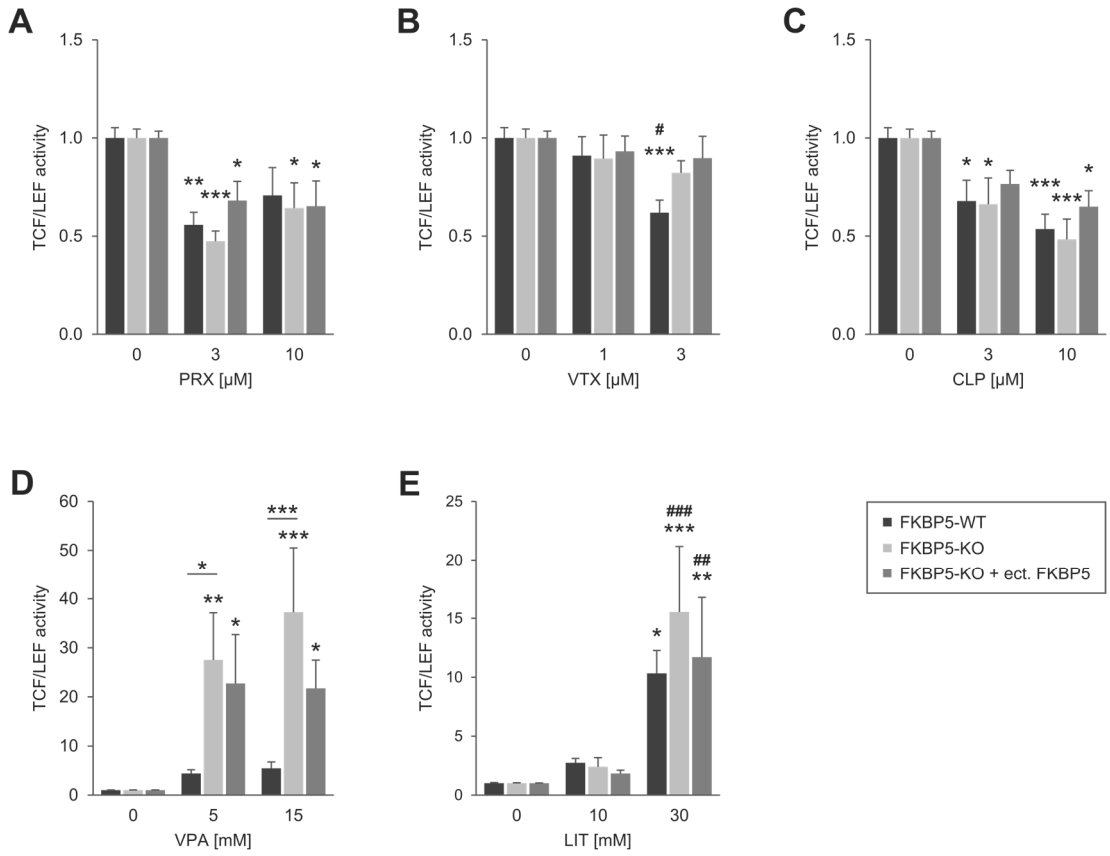

Figure 26: **Dose dependent effects of selected psychopharmaca on TCF/LEF activity.** Transcriptional activity of TCF/LEF was analysed in a dual luciferase based setup in MEF cells with and without the FKBP5 deletion. MEF cells were transfected with plasmids coding for firefly luciferase under control of a TCF/LEF dependent promoter, gaussia luciferase under control of a CMV promoter as well as FKBP51(FLAG) or control vector. Cells were treated 24 hours after transfection with the indicated drugs or vehicle for 48 hours. After cell lysis, light emission upon addition of firefly and gaussia substrate, subsequently, was measured. Firefly signal was normalised to gaussia signal. Responsiveness in TCF/LEF activity was measured for each of the three FKBP5 conditions upon treatment and calculated as relative signal compared to signal from the respective FKBP5 condition in vehicle treated cells. Bars show the mean value and error bars represent the standard error of the mean. Statistical significances were calculated by a two-way analysis of variance combined with a Bonferroni post-hoc test. Statistical significant differences compared to vehicle treatment are depicted with * and pairwise statistical differences with $^{\#}$ as follows: $^{*/\#}$ for $p \leq 0.05$, $^{**/\#\#}$ for $p \leq 0.01$ and $^{***/\#\#\#}$ for $p \leq 0.001$.

A dose dependent effect in response to treatment with the SNRI VTX was observed for TCF/LEF activity (Figure 26B). Treatment with 3 µM, but not 1 µM, VTX inhibited TCF/LEF activity in cells with functional FKBP5. In cells with deleted FKBP5, treatment with neither 1 µM nor 3 µM VTX modulated TCF/LEF irrespectively of ectopic FKBP5 expression.

Inhibition of TCF/LEF activity was observed in response to treatment with the TCA CLP with no significant difference between the two drug concentrations (Figure 26C). Treatment with 3 µM and 10 µM CLP dose dependently inhibited TCF/LEF activity in cells with functional FKBP5 as well as in cells with deleted FKBP5.

Treatment with 5 µM and 15 µM VPA generally increased TCF/LEF activity (Figure 26D). The increase in TCF/LEF activity in response to VPA treatment in cells with functional FKB5 was, however, not significant. Treatment with both concentrations of VPA markedly increased TCF/LEF activity in cells with deleted FKBP5 irrespectively of ectopic FKBP5 expression. There was a significant difference in responsiveness to VPA treatment between cells with deleted FKBP5 and functional FKBP5. This difference, however, was lost as a result of ectopic FKBP5 expression in cells with deleted FKBP5.

Treatment with LIT dose-dependently increased TCF/LEF activity (Figure 26E). A significant increase in TCF/LEF activity was observed in response to treatment with 30 mM, but not 10 mM, LIT. This effect, however, was not dependent on the FKBP5 status.

FOXO3α

The activity of a further transcription factor, FOXO3α, is controlled via its phosphorylation status, amongst others by AKT dependent phosphorylation at Ser-318 and Ser-321. As a further readout, the activity of FOXO3a was analysed in a dual luciferase based reporter construct in MEF cells with functional, deleted, or ectopic FKBP5.

No difference in FOXO3α activity was measured in cells with deleted or ectopic FKBP5 compared to cells with functional FKBP5 (Figure 27B). In order to unravel the responsiveness of FOXO3α activity to treatment, MEF cells with functional, deleted, or ectopic FKBP5 were treated with the experimental substances LNC, CHI or the AKT inhibitor triciribine (TCB) (Figure 27B) (Evangelisti et al., 2011). Treatment with LNC or CHI did not modulate FOXO3α activity. In line with inhibitory kinase activity of AKT on FOXO3α, treatment with TCB significantly increased FOXO3α activity in cells with functional FKBP5. This effect was even more pronounced in cells with deleted FKBP5. No marked reduction in FOXO3α activity in response to TCB treatment was observed by ectopic expression of FKBP5 in cells with deleted FKBP5.

No significant change in FOXO3α activity was observed in response to treatment with most psychopharmaca (Figure 27C). Increase in TCF/LFE activity was solely measured in response to treatment with the mood stabiliser VPA. A significant increase in response

to VPA treatment was detected in cells with functional FKBP5. A significantly more pronounced increase in response to VPA treatment was detected in cells with deleted FKBP5 irrespectively of ectopic FKBP5 expression.

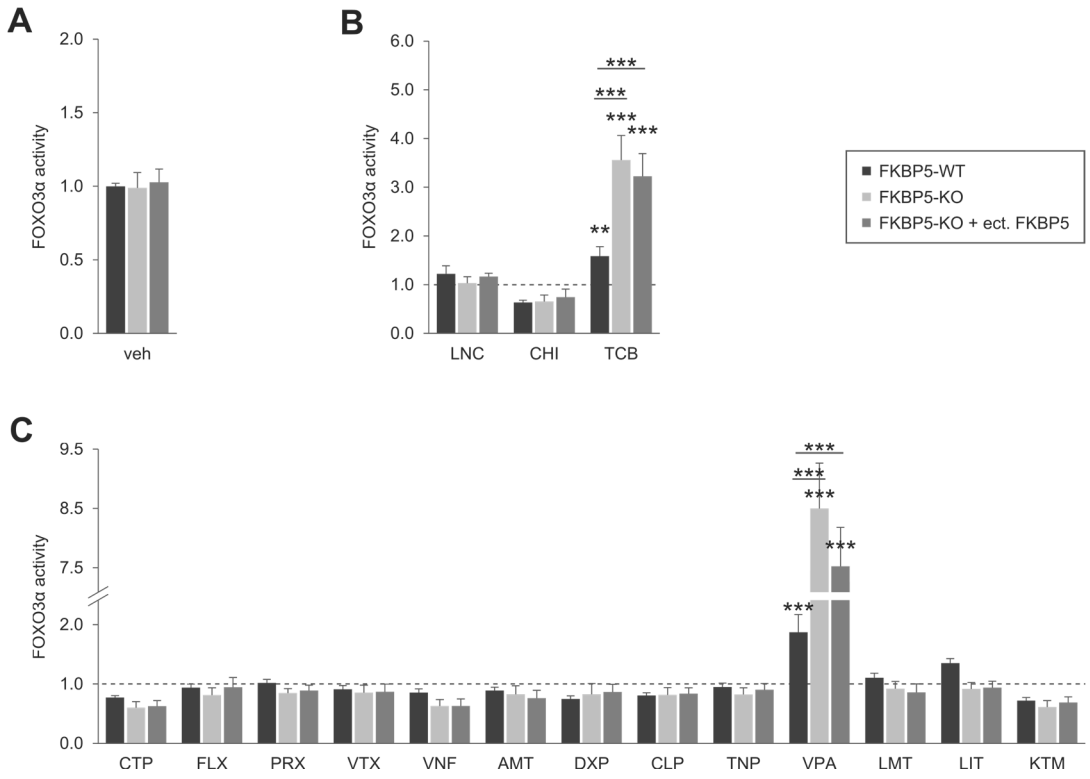

Figure 27: **Regulation of the FoxO3α activity by psychopharmaca and FKBP5.** Transcriptional activity of FOXO3α was analysed in a dual luciferase based setup in MEF cells with and without the FKBP5 deletion. MEF cells were transfected with plasmids coding for firefly luciferase under control of a FOXO3α dependent promoter, gaussia luciferase under control of a CMV promoter as well as FKBP51(FLAG) or control vector. Cells were treated 24 hours after transfection with the indicated drugs or vehicle for 48 hours. After cell lysis, light emission upon addition of firefly and gaussia substrate, subsequently, was measured. Firefly signal was normalised to gaussia signal. Bars show the mean value and error bars represent the standard error of the mean. Statistical significances were calculated by a two-way analysis of variance combined with a Bonferroni post-hoc test and are depicted as follows: * for $p \leq 0.05$, ** for $p \leq 0.01$ and *** for $p \leq 0.001$. **A** FOXO3α activity was measured for each of the three FKBP5 conditions upon vehicle treatment and calculated as relative signal compared to signal from MEF cells without the FKBP5 deletion. **B** Responsiveness in FOXO3α activity was measured for each of the three FKBP5 conditions upon treatment with experimental drugs and calculated as relative signal compared to signal from the respective FKBP5 condition in vehicle treated cells, which was thereby set to 1 and is indicated by the dashed line. **C** Responsiveness in FOXO3α activity was measured for each of the three FKBP5 conditions upon treatment with psychopharmaca and calculated as relative signal compared to signal from the respective FKBP5 condition in vehicle treated cells, which was thereby set to 1 and is indicated by the dashed line.

Consecutively, begin of dose dependent treatment effects on TCF/LEF activity was analysed. In order to answer this question, two concentrations of selected drugs from the groups of SSRIs, SSNRIs, TCAs and mood stabilisers were tested on their potential to modulate FOXO3α activity in MEF cells with functional, deleted, or ectopic FKBP5.

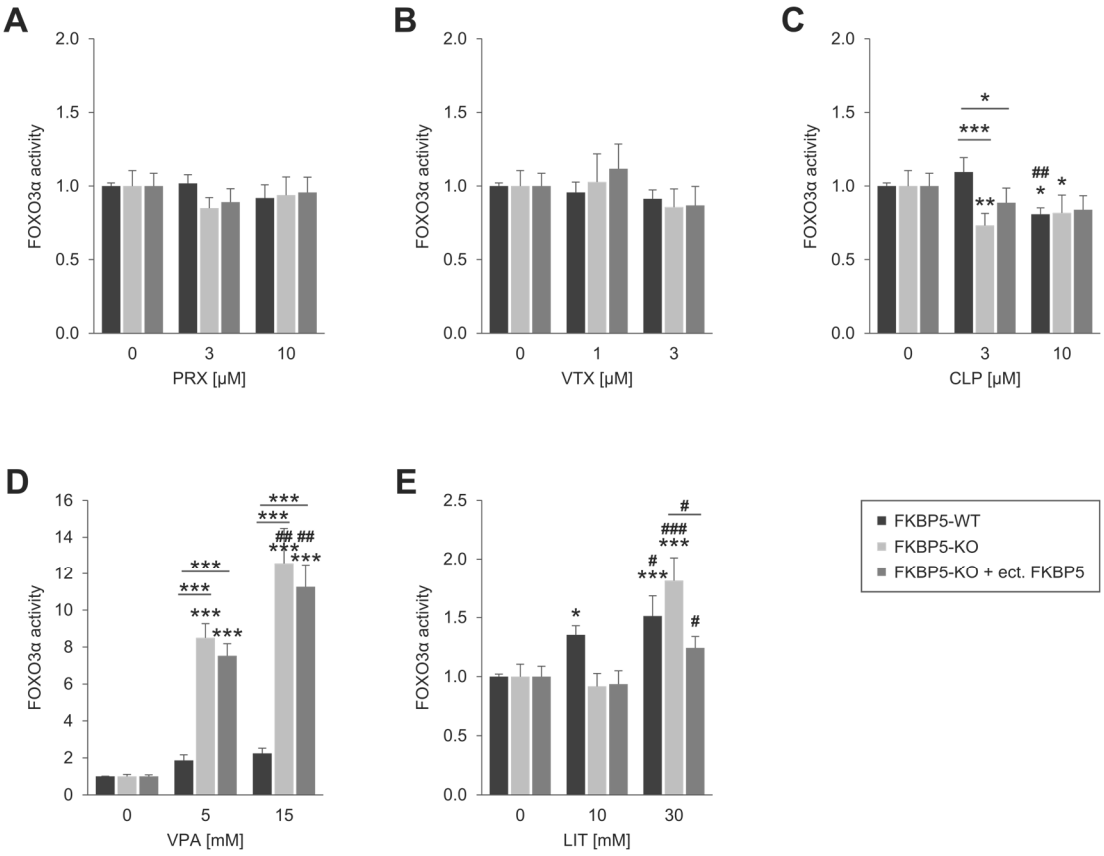

Figure 28: **Dose dependent effects of selected psychopharmaca on FOXO3α activity.** Transcriptional activity of FOXO3α was analysed in a dual luciferase based setup in MEF cells with and without the FKBP5 deletion. MEF cells were transfected with plasmids coding for firefly luciferase under control of a FOXO3α dependent promoter, gaussia luciferase under control of a CMV promoter as well as FKBP51(FLAG) or control vector. Cells were treated 24 hours after transfection with the indicated drugs or vehicle for 48 hours. After cell lysis, light emission upon addition of firefly and gaussia substrate, subsequently, was measured. Firefly signal was normalised to gaussia signal. Responsiveness in FOXO3α activity was measured for each of the three FKBP5 conditions upon treatment and calculated as relative signal compared to signal from the respective FKBP5 condition in vehicle treated cells. Bars show the mean value and error bars represent the standard error of the mean. Statistical significances were calculated by a two-way analysis of variance combined with a Bonferroni post-hoc test. Statistical significant differences compared to vehicle treatment are depicted with * and pairwise statistical differences with # as follows: $*^{/\#}$ for $p \leq 0.05$, $**^{/\#\#}$ for $p \leq 0.01$ and $***^{/\#\#\#}$ for $p \leq 0.001$.

Neither 3 µM nor 10 µM PRX modulated FOXO3α activity in MEF cells with functional, deleted, or ectopic FKBP5 (Figure 28A). Likewise, no modulation of FOXO3α activity in MEF cells with functional, deleted, or ectopic FKBP5 was observed in response to treatment with 1 µM or 3 µM VTX (Figure 28B).

Inhibition of FOXO3α activity was measured in response to treatment with CLP (Figure 28C). Treatment with 10 µM but not 3 µM CLP significantly inhibited FOXO3α activity in cells with functional FKBP5. Inhibition was also observed in cells with deleted FKBP5 in response to treatment with either 3 µM or 10 µM CLP. This inhibitory effect in response to treatment with CLP in cells with deleted FKBP5 was lost when FKBP5 was expressed ectopically.

A pronounced FOXO3α activating effect was observed in response to treatment with 5 mM and 15 mM VPA (Figure 28D). The increase in FOXO3α activity in response to VPA treatment in cells with functional FKB5 was, however, not significant. In cells with deleted FKBP5, treatment with both concentrations of VPA markedly increased FOXO3α activity irrespectively of ectopic FKBP5 expression. There was a significant difference in responsiveness to VPA treatment between cells with deleted FKBP5 and functional FKBP5.

Treatment with 10 mM and 30 mM LIT dose dependently increased FOXO3α activity (Figure 28E). In cells with functional FKBP5, treatment with both 10 mM and 30 mM LIT significantly increased FOXO3α activity. In cells with deleted FKBP5, however, no increase in FOXO3α activity was observed in response to treatment with 10 mM LIT. Only at a concentration of 30 mM LIT a significant increase in FOXO3α activity was observed in cells with deleted FKBP5.

4.2.5 Inhibition of autophagic flux by HDAC inhibitors

The striking effects in responsiveness to treatment with psychopharmaca were observed with the class of mood stabilisers (chapter 4.2.3). In particular, VPA treatment regulated autophagy markers like BECN1 and VPA. Controversial effects of VPA treatment on autophagy have been published. Therefore, VPA induced upstream autophagy induction in contrast to downstream blockade of autophagosome processing were analysed next.

Those two effects can be discriminated in a cellular setup with inhibited maturation of autophagic vehicles. Autophagosome fusion with lysosomes in the late phase of autophagy is dependent on the activity of vacuolar H^+ ATPase and can be pharmacologically blocked by treatment with Bafilomycin A1 (Yamamoto et al., 1998).

In order to determine a Bafilomycin A1 concentration suitable for the induction of an autophagic block in the MEF cells, accumulation of LC3-II was analysed by western detection in response to increasing concentrations of Bafilomycin A1 (Figure 29). Treatment with 3 nM to 30 nM Bafilomycin A1 dose-dependently increased LC3 conversion. No further increase in LC3 conversion was observed in response to higher Bafilomycin A1 concentration. Therefore, the concentration 50 nM Bafilomycin A1, which was in the low range of concentrations inducing a plateau of accumulating LC3 lipidation, was chosen for the pharmacological induction of autophagic blockade in MEF cells in the subsequent experiments as additional markers of autophagy.

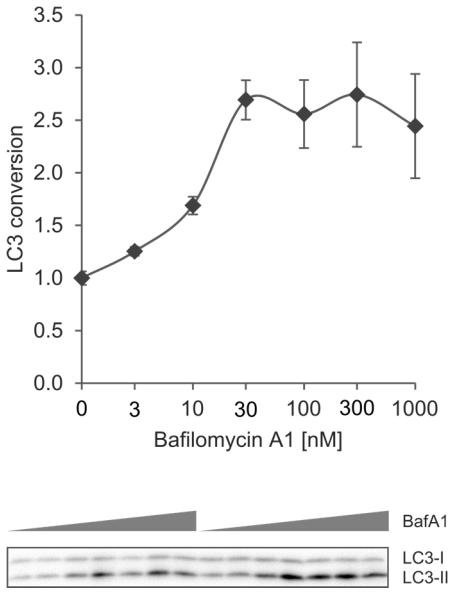

Figure 29: **Induction of autophagic block by Bafilomycin A1.** MEF cells were treated with increasing concentrations of Bafilomycin A1 for 2 hours. After cell lysis, conversion of LC3 was analysed by western detection. Level of LC3-II was quantified and normalised to the level of LC3-I from two biological replicates. Conversion in response to Bafilomycin A1 treatment was calculated compared to conversion in control treated cells. Dots show the mean value and error bars represent the standard error of the mean.

VPA has been reported to exert at least part of its effects by inhibiting HDACs. In order to unravel the role of VPA in modulating autophagy, potential epigenetic effects via HDACs were pharmacologically analysed. Therefore, co-treatment with two further HDAC inhibitors, butyrate (BUT) and TSA, in cells with pharmacologically blocked autophagy was tested for effects on LC3 conversion as well as P62, VPS34 and BECN1 accumulation.

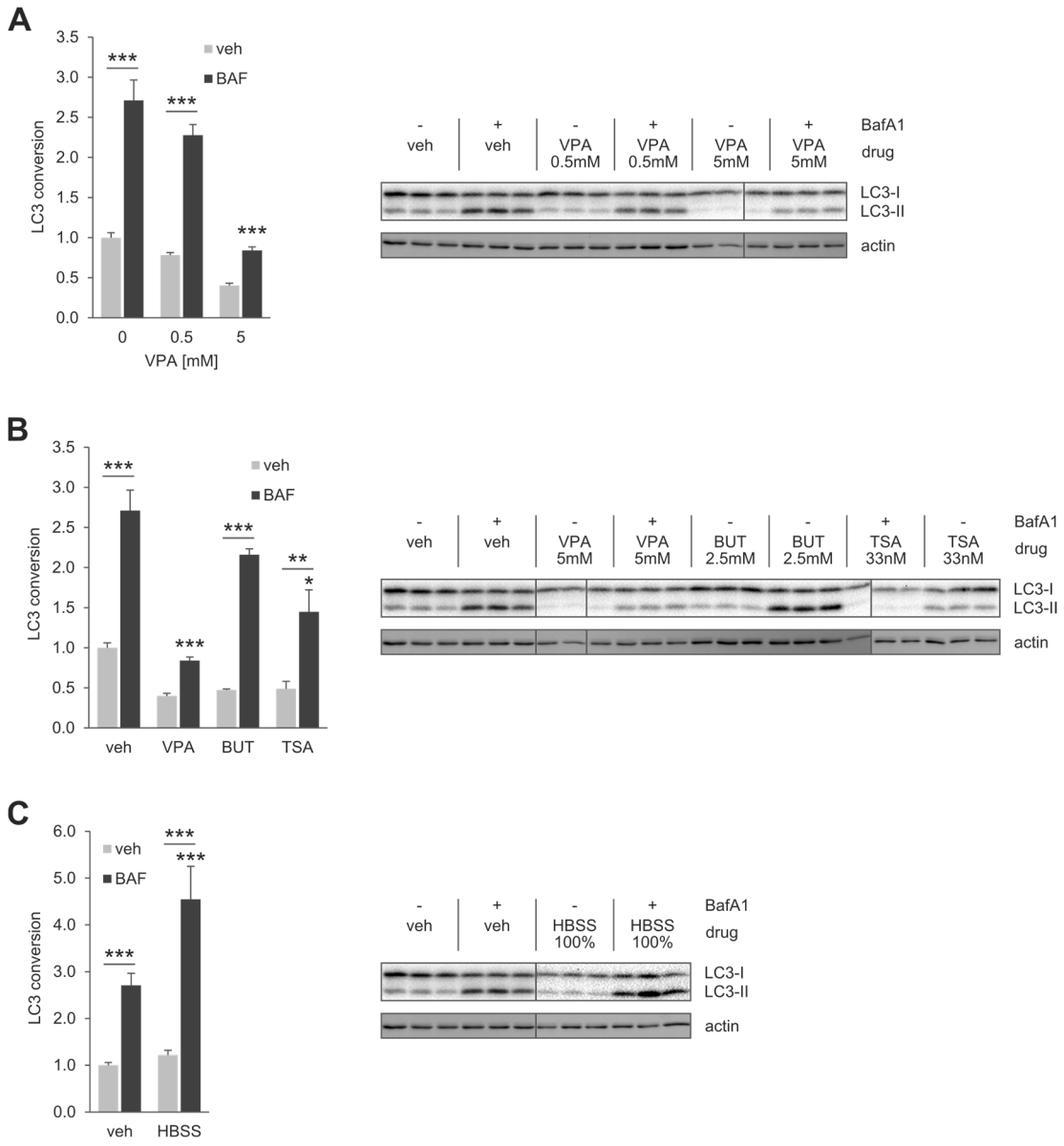

Figure 30: **Characterizing the effect of VPA and HDAC inhibitors on the autophagic marker LC3.** LC3 conversion in MEF was analysed by western detection with correspondent western blots shown next to the graphs. Level of LC3-II was quantified and normalised to the level of LC3-I from three biological replicates. Autophagy was pharmacologically blocked by co-treatment with 50 nM Bafilomycin A1 for 2 hours. Responsiveness to treatment with HDAC inhibitors or growth medium starvation in cells with and without autophagic blockade was calculated as ratio of values upon treatment divided by the value upon control treatment without autophagy blockade. Responsiveness of LC3 conversion to autophagy blockade in combination with treatment with 0.5 mM and 5 mM VPA for 48 hours (**A**), treatment with 5 mM VPA, 2.5 mM BUT and 33 nM TSA for 48 hours (**B**) or exchange of growth medium to HBSS for 4 hours (**C**) was assessed. Bars show the mean value and error bars represent the standard error of the mean. Statistical significances were calculated by a two-way analysis of variance combined with a Bonferroni post-hoc test and are depicted as follows: * for $p \leq 0.05$, ** for $p \leq 0.01$ and *** for $p \leq 0.001$.

First, LC3 conversion in combined treatment with increasing concentrations of VPA and Bafilomycin A1 was analysed (Figure 30A). Treatment with VPA dose-dependently inhibited LC3 conversion in the absence of autophagic blockade. This effect, however, was not significant for either 0.5 mM or 5 mM VPA. Treatment with Bafilomycin A1 significantly increased LC3 conversion due to inhibition of autophagosome maturation. This effect was dose-dependently attenuated by treatment with VPA.

Indeed, treatment with either VPA, BUT or TSA decreased LC3 conversion in a, however, non-significant magnitude (Figure 30B). When autophagy was pharmacologically blocked, co-treatment with at least TSA significantly attenuated the Bafilomycin A1 induced increase in LC3 conversion comparably to co-treatment with VPA, hinting to an inhibition of autophagy at an early stage in response to VPA and TSA treatment. As an internal control, cells were nutrient-starved by the exchange of growth medium to HBSS, which is well known to induce autophagy (Figure 30C). Under nutrient starvation, slightly less LC3 conversion was observed. When autophagy was pharmacological blocked, HBSS induced starvation, indeed, significantly increased the accumulation of lipidated LC3 above the level measured in cells with a pharmacological block of autophagy grown in full medium.

Originally, autophagy was regarded as a non-selective process. Accumulating evidence, however, indicates that certain proteins guarantee for selective degradation of many types of cargo. Hence, P62 has been identified to target specific cargoes for autophagy (Lamark et al., 2009). Lack of autophagy, however, has been shown to result in the accumulation of P62 and increased P62 accumulation could therefore serve as a marker for inhibited autophagy (Rusten and Stenmark, 2010). In line with an inhibition of autophagy at an early stage by VPA, accumulation of P62 was detected when cells were treated with 5 mM, but not 0.5 mM VPA (Figure 31A).

An increase in P62 accumulation as a combined effect of treatment with both Bafilomycin A1 and VPA, however, was not observed. Increased P62 accumulation in response to VPA treatment was mimicked by treatment with TSA but not with BUT (Figure 31B). Combined treatment with Bafilomycin 1 and TSA increased accumulation of P62, too. No effect on P62 accumulation was observed in response to nutrient-starvation induction of autophagy alone or combined with pharmacological blockade of autophagy by Bafilomycin A1 (Figure 31C).

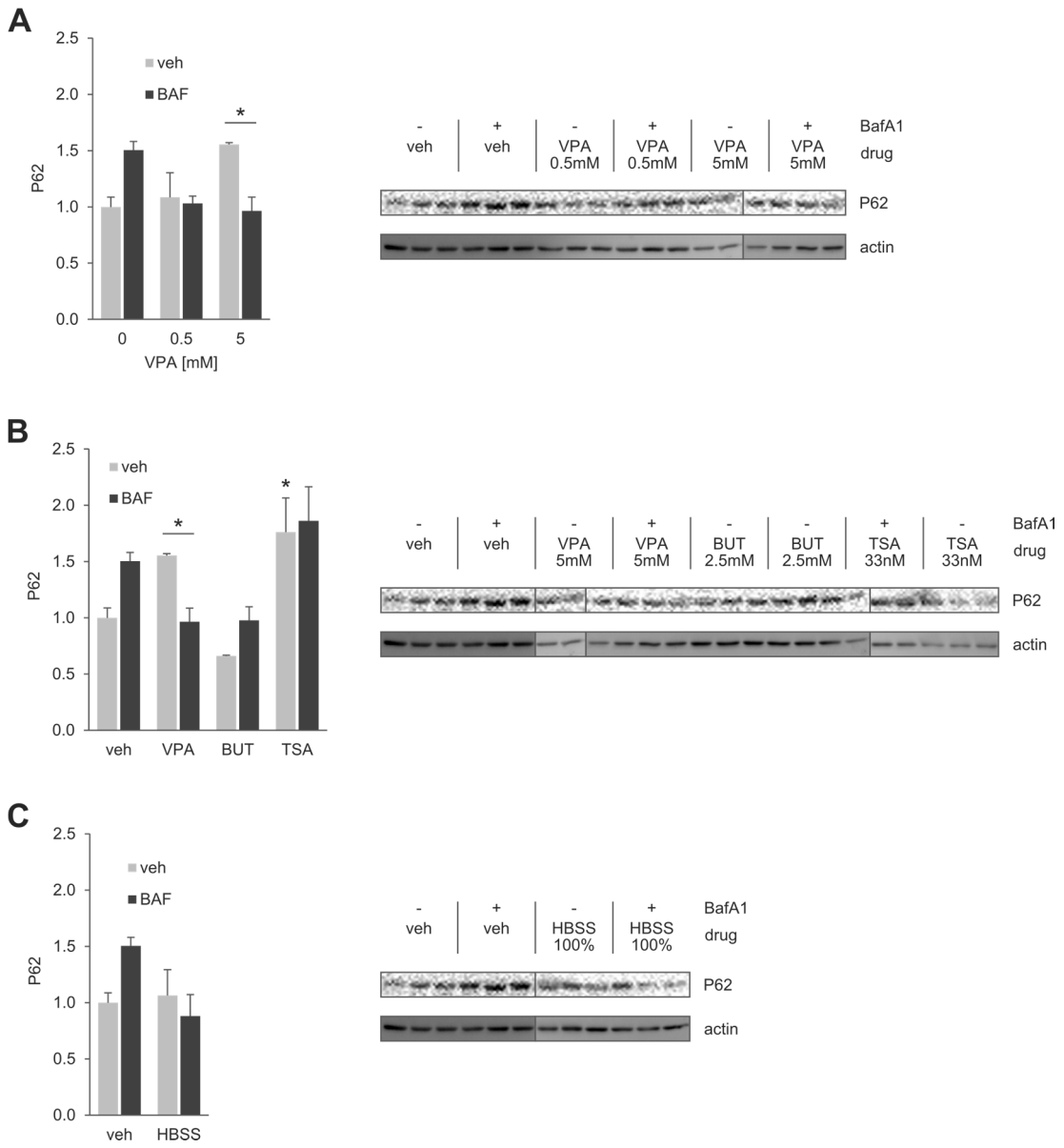

Figure 31: **Characterizing the effect of VPA and HDAC inhibitors on the autophagic marker P62.** P62 expression levels in MEF cells were analysed by western detection with correspondent western blots shown next to the graphs. Level of P62 was quantified and normalised to the level of actin from three biological replicates. Autophagy was pharmacologically blocked by co-treatment with 50 nM Bafilomycin A1 for 2 hours. Responsiveness to treatment with HDAC inhibitors or growth medium starvation in cells with and without autophagic blockade was calculated as ratio of values upon treatment divided by the value upon control treatment without autophagy blockade. Responsiveness of P62 expression to autophagy blockade in combination with treatment with 0.5 mM and 5 mM VPA for 48 hours (**A**), treatment with 5 mM VPA, 2.5 mM BUT and 33 nM TSA for 48 hours (**B**) or exchange of growth medium to HBSS for 4 hours (**C**) was assessed. Bars show the mean value and error bars represent the standard error of the mean. Statistical significances were calculated by a two-way analysis of variance combined with a Bonferroni post-hoc test and are depicted as follows: * for $p \leq 0.05$, ** for $p \leq 0.01$ and *** for $p \leq 0.001$.

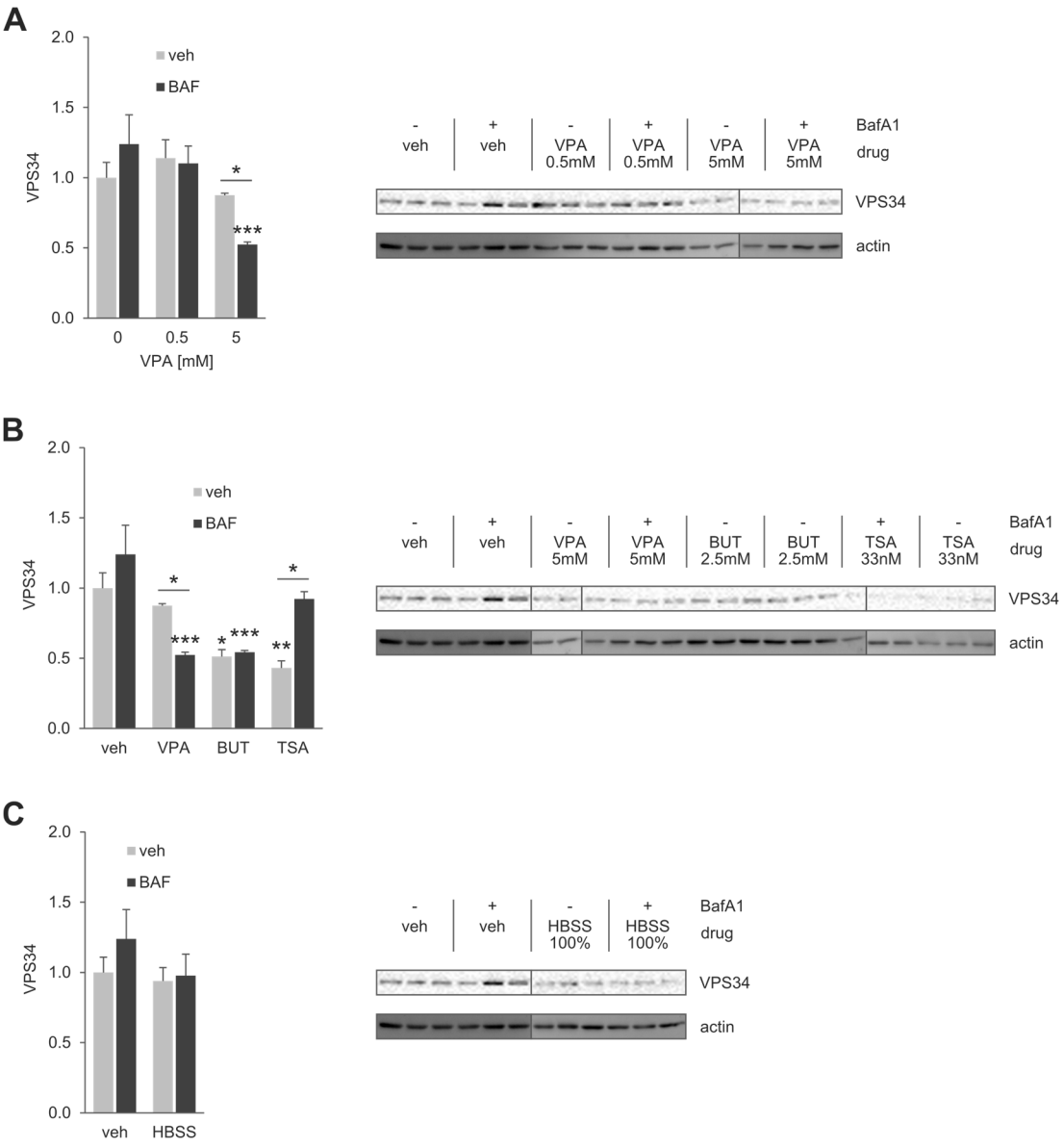

Figure 32: **Characterizing the effect of VPA and HDAC inhibitors on the autophagic marker VPS34.** VPS34 expression levels in MEF cells were analysed by western detection with correspondent western blots shown next to the graphs. Level of VPS34 was quantified and normalised to the level of actin from three biological replicates. Autophagy was pharmacologically blocked by co-treatment with 50 nM Bafilomycin A1 for 2 hours. Responsiveness to treatment with HDAC inhibitors or growth medium starvation in cells with and without autophagic blockade was calculated as ratio of values upon treatment divided by the value upon control treatment without autophagy blockade. Responsiveness of VPS34 expression to autophagy blockade in combination with treatment with 0.5 mM and 5 mM VPA for 48 hours (**A**), treatment with 5 mM VPA, 2.5 mM BUT and 33 nM TSA for 48 hours (**B**) or exchange of growth medium to HBSS for 4 hours (**C**) was assessed. Bars show the mean value and error bars represent the standard error of the mean. Statistical significances were calculated by a two-way analysis of variance combined with a Bonferroni post-hoc test and are depicted as follows: * for $p \leq 0.05$, ** for $p \leq 0.01$ and *** for $p \leq 0.001$.

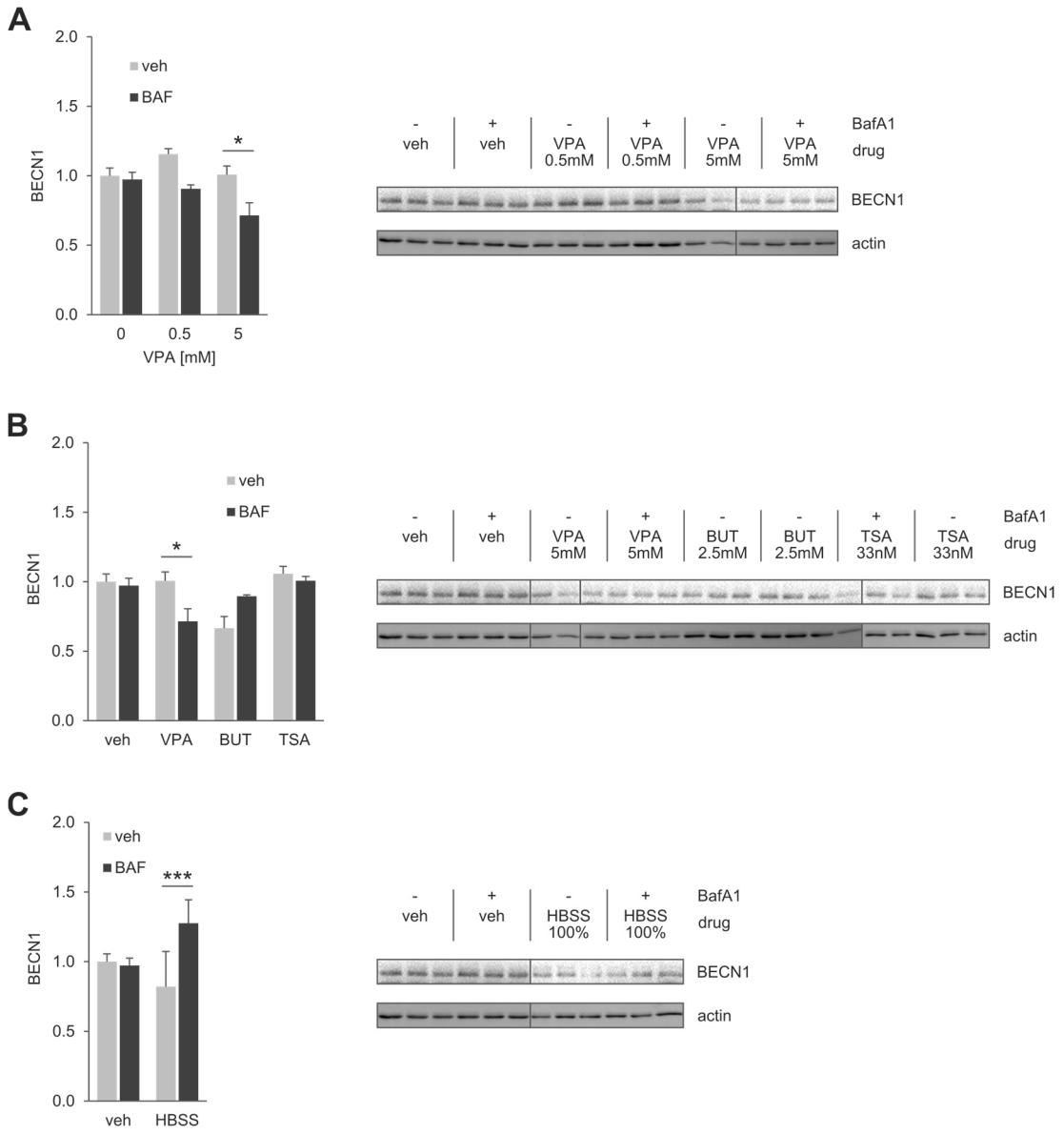

Figure 33: **Characterizing the effect of VPA and HDAC inhibitors on the autophagic marker BECN1.** BECN1 expression levels in MEF cells were analysed by western detection with correspondent western blots shown next to the graphs. Level of BECN1 was quantified and normalised to the level of actin from three biological replicates. Autophagy was pharmacologically blocked by co-treatment with 50 nM Bafilomycin A1 for 2 hours. Responsiveness to treatment with HDAC inhibitors or growth medium starvation in cells with and without autophagic blockade was calculated as ratio of values upon treatment divided by the value upon control treatment without autophagy blockade. Responsiveness of BECN1 expression to autophagy blockade in combination with treatment with 0.5 mM and 5 mM VPA for 48 hours (**A**), treatment with 5 mM VPA, 2.5 mM BUT and 33 nM TSA for 48 hours (**B**) or exchange of growth medium to HBSS for 4 hours (**C**) was assessed. Bars show the mean value and error bars represent the standard error of the mean. Statistical significances were calculated by a two-way analysis of variance combined with a Bonferroni post-hoc test and are depicted as follows: * for $p \leq 0.05$, ** for $p \leq 0.01$ and *** for $p \leq 0.001$.

VPS34 is the only class III phosphoinositide 3-kinase in mammals, phosphorylating phosphatidylinositol to produce phosphatidylinositol 3-phosphate (Volinia et al., 1995). Phosphatidylinositol 3-phosphate production has been implicated in promoting autophagy (Backer, 2008). In line with the assumption of a VPA induced inhibition of autophagy at an early stage, decreased levels of VPS34 were detected in cells with pharmacologically blocked autophagy in response to co-treatment with 5 mM but not 0.5 mM VPA (Figure 32A). A similar effect was detected in response to co-treatment with BUT (Figure 32B). Decreased levels of VPS34 were also observed in response to treatment with BUT or TSA. No effect on VPS34 expression level was observed in response to nutrient-starvation induction of autophagy alone or combined with pharmacological blockade of autophagy by Bafilomycin A1 (Figure 32C).

Next, the expression of BECN1 in response to pharmacologic blockade of autophagy and treatment with HDAC inhibitors was analysed. Bafilomycin A1 induced blockade of autophagy itself had not effect on the expression level of BECN1 (Figure 33A). When co-treated with 5 mM VPA, however, Bafilomycin A1 decreased expression levels of BECN1. Upregulation of BECN1 in response to treatment with VPA as reported in section 4.2.3 was not recapitulated in this experiment. BECN1 levels were also not responsive to treatment with either BUT or TSA. Induction of autophagy by nutrient-starvation increased expression levels of BECN1 when autophagy was blocked pharmacologically.

4.2.6 Induction of transcriptionally controlled autophagy by VPA

As shown in chapter 4.2.4, transcriptional activity upstream of a FOXO3α responsive promoter was markedly increased in response to treatment with VPA. Interestingly, FOXO3α activity has been shown to correlate with increased transcription of several genes involved in autophagy (Feng et al., 2015; Mammucari et al., 2007).

Pharmacological regulation of FOXO3α activity could therefore provide a potential mechanistic link how VPA modulates autophagy on the transcriptional level. In order to test this hypothesis, the expression levels of five genes, which are controlled by FOXO transcription factor signalling and exert key roles in regulation of autophagy, were checked. The five selected genes have been shown to regulated autophagy at different stages with initiation of autophagy being affected by ULK1, BECN1, and VPS34, autophagosome formation being regulated by ATG5 and autophagosome maturation being controlled by LC3. Transcription of the genes was analysed in response to

treatment with VPA in comparison to treatment with the two additional HDAC inhibitors BUT and TSA (Figure 34).

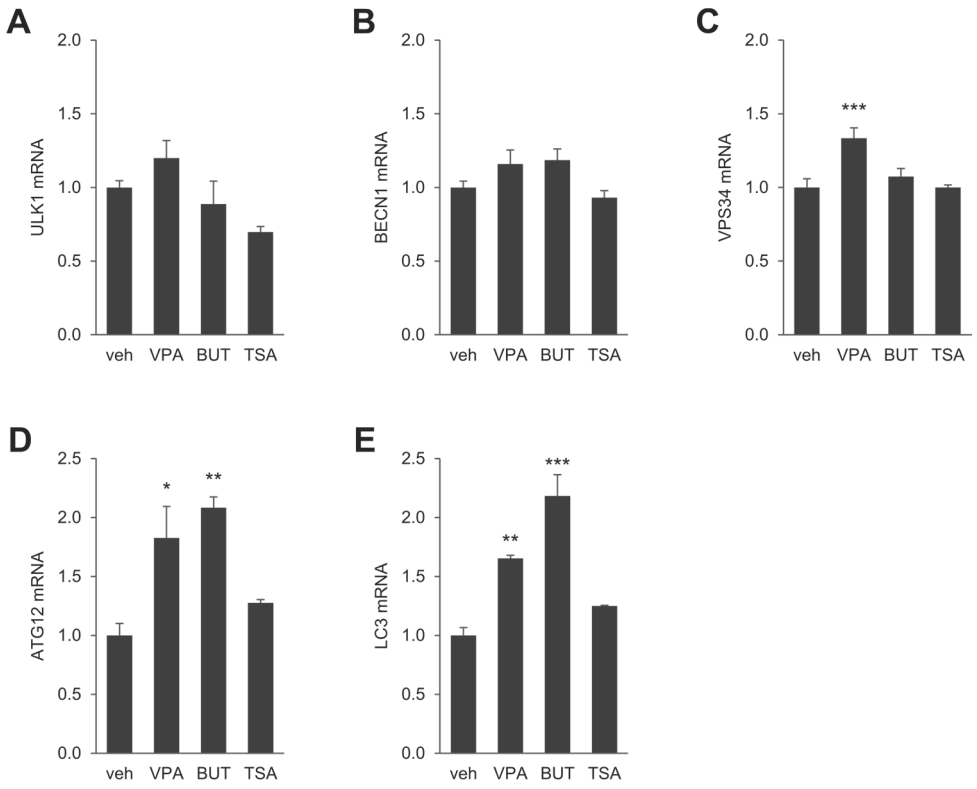

Figure 34: **Transcriptional regulation of FoxO3α responsive autophagy related genes by VPA and HDAC inhibitors.** mRNA levels of selected autophagy related genes (as indicated in **A** – **E**) in MEF cells was analysed by qRT-PCR. Level of target gene mRNA was quantified and normalised to the mRNA level of HPRT from three biological replicates in technical duplicates. Responsiveness to treatment with 5 mM VPA, 2.5 mM BUT and 33 nM TSA was calculated as ratio of values upon drug treatment divided by the value upon control treatment. Bars show the mean value and error bars represent the standard error of the mean. Statistical significances were calculated by a one-way analysis of variance combined with a Bonferroni post-hoc test and are depicted as follows: * for $p \leq 0.05$, ** for $p \leq 0.01$ and *** for $p \leq 0.001$.

Treatment with VPA significantly increased the transcription of VPS34, ATG12 and LC3, while the increase in transcription of ULK1 and BECN1 was not significant. A similar profile of transcriptional enhancement was also observed in in response to treatment with BUT, with significantly enhanced levels of ATG12 and LC3. In contrast, no significant changes in mRNA levels of the five autophagy genes was detected in response to treatment with TSA.

5 Discussion

It has become widely recognised that dysregulation of the stress hormone system as a consequence of excessive exposure to stress is a major factor for developing stress-related psychiatric diseases. A regulatory component of this system, FKBP5, was detected as a genetic risk factor. Indeed, FKBP5 has been shown to be part of an intracellular ultra-short negative feedback loop that regulates GR receptor activity. Besides regulation of GR receptor activity, recent studies reported additional effects of FKBP5. On this basis, effects of FKBP5 on gene transcription as well as on activity of selected kinases were analysed in this thesis.

5.1 GLO1 gene duplication in FKBP5-KO mice

FKBP5 dependent effects on global gene transcription were analysed in an unbiased approach using RNA microarrays. Besides downregulation of FKBP5 transcription, which is presumably due to altered chromatin architecture as a result of the truncated FKBP5 gene or to nonsense-mediated decay of the mutated FKBP5 mRNA (Baker and Parker, 2004), the transcription of the three genes FGD2, GLO1 and RBM12 was found to be upregulated in FKBP5-KO animals. Upregulation could not be verified by RT-PCR for RBM12. It could finally be shown that increased GLO1 mRNA and protein levels are caused by a genetic copy number variance of GLO1 co-segregated with the FKBP5 alleles. The FGD2 gene is located in close proximity to the FKBP5 and GLO1 loci and increased FGD2 mRNA is very likely due to *cis* genetic alterations in mice carrying the FKBP5 deletion and the GLO1 duplication.

In the process of generating a knock out mouse line with the conventional technique of homologous recombination, i.e. the replacement of an endogenous gene by a truncated or mutated homologue in a donor stem cell, mice with different genetic background are used. Embryonal stem cells are usually isolated from blastocysts of mice from the 129 strain and subsequently genetically modified, selected for the modification and inserted into the blastocyst of a foster mouse. Resulting new-born chimeric mice with gonads originating from the modified stem cell are crossbred with mice of the desired genetic background for breeding and phenotyping. As the two inbred mouse lines used as stem

cell donor and genetic background donor differ in their genetic endowment, at least ten rounds of back crossing are required as good laboratory praxis and generally considered sufficient to generate a homogeneous genetic background (Silva et al., 1997). In each breeding round, mice are segregated according to their deleted or non-deleted version of the gene of interest with the deleted version originating from the stem cell donor and the wild type version originating from the back crossing mice. Genetic variances in close genetic proximity to the gene of interest, however, co-segregate with the gene of interest as the rate of crossing over is a function of how close the genes are to each other on a given chromosome. The phenomenon which is caused by the genetic linkage of genetic variances with the gene of interest is called flanking gene problem (Crusio, 2004).

In the last two decades, research based on genetically engineered mice has become indispensable for studying gene function in a mammalian animal model. After the establishment of the conventional knockout strategy, it took several years until it was noticed that there was a systematic bias inherent to this strategy: genes flanking the induced null mutation would also be homozygous for alleles derived from the ES cell donor in homozygous knockout mutants (Gerlai, 1996). This is inevitable, because it is due to the different genetic background of the mutant and the wild type version of the targeted gene. The flanking gene problem in a newly designed knockout mouse model can be circumvented using a gene knockout strategy based on the Cre/loxP system, if the Cre recombinase constitutively expressing mice are controlled for the flanking gene problem or if the Cre recombinase is activated pharmacologically, e.g. in a tetracycline- or tamoxifen-controlled setting of the Cre recombinase transcriptional activation. Furthermore, the possibility to directly target an embryo of any available genetic background by microinjection of RNAs using the CRISPR/Cas9 system redundantises the detour of crossbreeding subsequent to targeting of ES cells from the 129 strain (Singh et al., 2015).

Here, due to the flanking gene problem, the FKBP5 knockout mouse model is affected by a copy number variance in the GLO1 gene resulting in higher GLO1 expression in FKBP5-KO mice. The GLO1 gene is located approximately 2 Mb upstream of the FKBP5 gene on chromosome 17 in mice. Although recombination rates vary between genomic loci, the assumption is made that 1 centimorgan corresponds to approximately 2 Mb on average in mice (Jensen-Seaman et al., 2004). This would mean that there is a 1 % chance that a marker at one genetic locus on a chromosome will be separated from a marker at a second locus by crossing over in a single generation, if the two markers are 2 Mb apart from each other. Therefore, a 1 % chance of homologous recombination event during meiosis is expected, which results in a chromosomal arrangement of a deleted FKBP5 allele next to a single copy of GLO1. Thus there would approximately be

one in a hundred FKBP5-HET offspring without the GLO1 duplication. Experimental FKBP5-KO mice are bred from two parental FKBP5-HET mice, each of them being liberated from the GLO1 duplication by a chance of 1 %. Thus, there is an approximately 0.01 % total chance of an FKBP5-KO offspring mouse without the GLO1 gene duplication. In other words, even after several rounds of breeding, there is little chance that the GLO1 duplication in FKBP5-KO mice is lost due to homologous recombination events. The FKBP5 mouse model therefore provides an example where a genetic variance in close proximity to the knock out allele, i.e. the GLO1 duplication, might potentially influence the phenotype.

Interestingly, one of the FKBP5-KO mice showed only one copy of the GLO1 duplication in our genotyping assay. This mouse very likely has one chromatid with the GLO1 duplication and the sister chromatid without the duplication (Figure 4A).

The Glo1 gene has been described to influence anxiety-related behaviour (Distler and Palmer, 2012). No overt anxiety related behaviour, however, was observed in the FKBP5 knockout mouse model (Hartmann et al., 2012; Touma et al., 2011). In a study using BAC transgenic mice, GLO1 overexpression caused increased anxiety-related behaviour (Distler et al., 2012). This effect, however, was only observed in mouse lines with the highest copy numbers. It seems therefore plausible that the increased GLO1 protein level, which is very likely due to the duplication of GLO1 in FKBP5-KO animals, might not be high enough to induce an overt anxiety phenotype. The GLO1 status should nevertheless be taken into consideration when interpreting data from FKBP5 knockout mice and descending cells.

Noteworthy, FGD2, the gene showing the most significant upregulation of gene expression in the microarray (Figure 1), is located in between the loci coding for FKBP5 and GLO1 on mouse chromosome 17. Although the analysed copy number variance for the GLO1 spanning region does not contain the FGD2 gene, a *cis* genetic effect underlying the upregulation of the FGD2 gene cannot be excluded. For example, the deletion of FKBP5 as well as the duplication of the GLO1 spanning locus could change the chromatin structure and hereby modulate the transcription of FGD2. The deletion in FKBP5 is 0.8 Mb and the duplication border of the GLO1 spanning region 1.3 Mb apart from the FGD2 gene. It is possible that those alterations are sufficient to modify DNA looping responsible for FGD2 transcriptional initiation, elongation and termination (Mercer and Mattick, 2013). Alternatively, the chromosomal region around GLO1 might provide a potential hub for duplication events. In analogy to the postulated origin of the GLO1 copy number variance by a non-allelic homologous recombination event, a second independent non-allelic homologous recombination event might have generated a

duplication of the FGD2 spanning region in the stem cell donor mice 129SvJ mouse line (Hastings et al., 2009). Given the possibility that genomic rearrangements are responsible for the differences of FGD2 mRNA in the FKBP5 knockout mouse model, a functional link between FKBP5 and FGD2 was not further explored.

5.2 The role of FKBP5 in modulating cellular pathways used by psychopharmaca

It remains elusive why more than half of the patients with major depressive disorder do not fully respond to the treatment with a first antidepressant (Trivedi et al., 2006). While switching antidepressants is a common strategy for treatment of non-responder patients, clinicians could benefit from further knowledge about the actions of different antidepressants. Understanding the molecular mechanisms how different antidepressants exert beneficial effects over a variety of drug targets might improve targeting and efficacy in the use of existing antidepressants. In addition, identification of molecular key players in pathways, which are convergently targeted by a majority of existing antidepressants, could serve as entry to the development of novel target-specific drugs for the treatment of stress-related psychiatric diseases.

First evidence for a role of FKBP5 in antidepressant response came from genetic studies (Binder et al., 2004). A recent study in our group further discovered that FKBP5 enhanced autophagy to synergise with antidepressant action of a TCA and two SSRIs (Gassen et al., 2014). A further study in our group showed that FKBP51 inhibited GSK3β and augmented the effects of psychotropic medications with a mood stabiliser and an SSRI (Gassen et al., 2015).

The findings of these studies drew the interest to analyse a broad list of psychopharmaca for their effects evoked on those pathways. Therefore, expression and phosphorylation levels of proteins presumably targeted by antidepressant treatment were analysed in this thesis. In response to treatment with 13 psychopharmaca from different drug classes and two experimental substances, general effects evoked by antidepressant treatment as well as synergistic effects of FKBP5 in response to antidepressant treatment were analysed on cellular pathways that previously had been shown to be affected by treatment with certain antidepressants. Therefore the expression, the phosphorylation and the activity of those proteins were compared in MEFs with functional and deleted FKBP5.

These pathways were heterogeneously affected by different psychopharmaca, with members of the same psychopharmaca class not stringently evoking similar effects. The most pronounced effects were observed in response to treatment with the mood stabilisers LIT and, in particular, VPA. FKBP5 generally determined ERK phosphorylation in response to psychopharmaca action. Responsiveness of GSK3β and AKT phosphorylation as well as regulation of downstream targets was partially affected by FKBP5.

5.2.1 Choice of cellular system

Genetically manipulated knockout mouse lines have become an invaluable tool for defining the function of genes in a physiological context. Ex-vivo culturing of cells, however, enables simple and fast experimental manipulation by extensive drug treatment and overexpression of proteins. Hence, isolated and cultured mutant cells from genetically manipulated knockout mouse lines are valuable tools for studying the mechanistic function of genes. The major drawback of primary tissue, which have to be isolated from embryonic donor animals, can be circumvented by the immortalisation of primary cells. Transforming or passaging primary fibroblasts from embryonal mice into MEFs with permanent growth features is well established.

In this work, MEFs from mice with or without deleted FKBP5 were utilised as cell system to study the function of FKBP5 in psychopharmacologically targeted pathways. FKBP51 is strongly expressed in MEF cells with functional FKBP5 providing a great difference in FKBP5 levels in comparison to cells with deleted FKBP5. The pathway analysis in FKBP5-expression-rescued MEFs, facilitated by the ectopic expression of FKBP5 in cells with deleted FKBP5 and comparison with their parent mutant cells, was experimentally not accessible due to low transfection efficiency in those MEFs. Moreover, pathway analysis in MEFs might not fully reflect the regulation of pathways by psychopharmaca treatment in a physiological context. Differential proteomic profiles of cell types might account for the absence of psychopharmaca evoked effects in MEFs.

5.2.2 Cell viability in response to treatment

It is plausible that antidepressants exert their actions in a dose dependent matter, either applied in clinics or in cell culture. Nevertheless, drug dosage cannot easily be converted from clinics to cell culture in particular due to different pharmacokinetics. Without the prior knowledge of molecular markers of drug effectiveness, a two-sided appraisal has to be made for the selection of appropriate drug concentrations in cell culture. On the one hand, relevant drug effects are likely to be overseen when drug concentrations are too low. On the other hand, disproportionately high drug concentrations might activate, amongst others, pathways of toxicity, which may confound changes induced in pathways relevant for treatment.

It appears to be current practice in cell culture, however, to apply antidepressants of the classes of TCAs, SSRIs, SSNRIs and atypical antidepressants at a standard concentration of 10 μM. In order to at least exclude toxic effects in the analysis of posttranslational

protein modification analysed in response to treatment, two orthogonal methods were assessed to measure cell viability in response to treatment. In a first step, the toxicity of 13 antidepressants as well as two additional experimental drugs was therefore analysed with the two viability assays, the MTT assay and the LDH assay at three time points of the exposure.

Data from MTT and LDH assays concordantly indicated slight effects on viability at drug concentrations of 10 µM, when cells were treated with either the two SSRIs FLX and PRX or the SSNRI VTX for 48 hours. Differing from the standard concentration of 10 µM, FLX, PRX and VTX were therefore applied at a slightly lower concentration of 3 µM as standard concentration. In response to treatment with DXP, however, viability started to be decreased at slightly higher concentrations compared to other antidepressants. Differing again from the standard concentration of 10 µM, DXP was used at a concentration of 30 µM. Correspondently established standard concentrations for the application of mood stabilisers, the anaesthetic KTM, and the two experimental drugs in cell culture were not found in the literature. Therefore subtoxic concentrations were chosen derived from the two viability assays.

Interestingly, a concentration dependent increase in MTT signal was detected as a characteristic feature of eight of the 13 antidepressants and one of the two experimental drugs. The characteristic increase in MTT signal, however, which could be misinterpreted as increase in cell viability, was not accompanied by an increase in LDH signal. Concordantly for most drugs, the concentration dependent increase in MTT signal was arising after 12 hours, most pronounced after 24 hours and diminished after 48 hours treatment. Certainly, the MTT assay is an indirect measure of cell viability. The exact cellular mechanism of MTT reduction into formazan is not completely understood, but likely involves reaction with NADH or similar reducing molecules that transfer electrons to MTT (Marshall et al., 1995). Speculation in the early literature involving specific mitochondrial enzymes has led to the assumption that MTT is measuring mitochondrial activity (Berridge and Tan, 1993). Antidepressants have been shown to influence mitochondrial function and particularly mitochondrial respiratory chain complex activity (Abdel-Razaq et al., 2011; Hroudova and Fisar, 2010; Scaini et al., 2011). Therefore, care has to be taken when interpreting MTT data in response to treatment with drugs that might interfere with mitochondrial activity. Increased signals in MTT but not in LDH test observed for subtoxic concentrations of CTP, PRX, VTX, AMT, DXP, CLP, LMT and LIT hint to augmented metabolism or mitochondrial activity in response to treatment at certain concentration of these drugs. Interestingly, augmented metabolism was also observed in response to treatment with subtoxic concentrations of CHI. This is in line with a recent report that described the involvement of mitochondrial GSK3β in

production of redox equivalents via regulation of NADH:ubiquinone oxidoreductase (complex I) (King et al., 2008). Of note, mitochondrial dysfunction has been linked to the pathophysiology of depression (Karabatsiakis et al., 2014). Treatment with subtoxic concentrations of CTP, PRX, VTX, AMT, DXP, CLP, LMT and LIT appears to interfere with mitochondrial activity. With eight of 13 drugs increasing mitochondrial activity as represented by the MTT signal, a causative contribution of the observed effect in clinical effectiveness might be possible.

5.2.3 Partial FKBP5 dependence of psychopharmaca action on pathways

In two recent publications, we could show that the FKBP5 status determined the responsiveness of certain drugs on both cellular pathway and stress related coping behaviour (Gassen et al., 2014, 2015). In contrast, pure genotype effects on behaviour have not been observed in mice with deleted FKBP5 (Touma et al., 2011). In the analysis of cellular pathways in MEF cells with deleted FKBP5 compared to MEF cells with functional FKBP5, however, a differential protein status was detected in suspected targets of FKBP51. Phosphorylation of ERK and AKT was enhanced in cells with deleted FKBP5. A mechanism for FKBP51 mediated dephosphorylation was recently provided with the characterisation of the recruitment of PHLPP phosphatase to AKT by FKBP51 (Pei et al., 2009). A similar scenario could underlie the enhanced phosphorylation of ERK in cells with deleted FKBP5. Increased phosphorylation of AKT, however, did not impact on FOXO3a phosphorylation at Ser-318 and Ser-321 or FOXO3α activity. Autophagy appeared slightly enhanced in cells with deleted FKBP5 as indicated by increased levels of the autophagy initiator BECN1 and augmented conversion of LC3-II/I. Distinct regulation of the GSK3β pathway was not detected in cells with deleted FKBP5, which is in line with the unchanged phosphorylation of GSK3β detected in the hippocampus from mice with deleted FKBP5 (Gassen et al., 2015).

Responsiveness of the pathways analysed in this work did not generally depend on the presence of FKBP5. Responsiveness of certain targets, however, was dependent on FKBP5. Most markedly, responsiveness of ERK phosphorylation to psychopharmaca treatment in cells with functional FKBP5 was abolished in cells with deleted FKBP5. In cells with functional FKBP5, treatment with psychopharmaca increased phosphorylation up to five fold. This is in the range of the increase of ERK phosphorylation detected in untreated cells devoid of FKBP5 in comparison to WT cells. This hints to a two partied

mechanism of FKBP51 adjusted ERK phosphorylation, where on the one hand, the presence of FKBP51 decreased the phosphorylation of ERK and on the other hand, psychopharmaca evoked increases in ERK phosphorylation depended on the presence of FKBP51. However, it is also possible that ERK was extensively phosphorylated in cells with deleted FKBP5, thus precluding a further increase in ERK phosphorylation by the treatment with psychopharmaca. Differential effects with regard to FKBP5 were also evoked for VPA dependent TCF/LEF and FOXO3α activity, with enhanced effects in cells with deleted FKBP5. Similarly, enhancement of TCF/LEF activity was detected in response to HDAC inhibitor TSA and enhancement of FOXO3α activity in response to the AKT inhibitor TCB. Effect sizes in cells with deleted FKBP5, however, could hardly be attenuated by the rescue of the FKBP5 expression status via transient transfection. This hints to a cell line dependent effect in responsiveness of FOXO3α to HDAC inhibitors, which was not directly caused by the FKBP5 deletion. Presumably, differential transfection efficiencies in cells with deleted and functional FKBP5 contributed to heterogeneous expression of reporter gene constructs and therefore differential TCF/LEF activity.

5.2.4 Common effects of psychopharmaca treatment

SSRIs and TCAs

A more homogeneous pattern was observed for the regulation of cellular pathways by the three SSRIs (CTP, FLX, and PRX) and the three TCAs (AMT, DXP, and CLP) in the MEF model.

Treatment with neither SSRIs nor TCAs did generally affect GSK3β phosphorylation and regulation of its reported downstream targets BCAT and CRMP2. Slight inhibition of TCF/LEF activity was detected in response to treatment with PRX and CLP. In both brain tissue from mice and cortical astrocytes from rat, treatment with the SSRI PRX increased the phosphorylation of GSK3β (Gassen et al., 2015). Increased phosphorylation of GSK3β in response to treatment with PRX was reflected by an increase in TCF/LEF activity in cortical astrocytes. The concentration of PRX used for treatment of astrocytes, however, was higher than the concentration used in this work.

Modulation of ERK phosphorylation in response to treatment was not detected in response to 48 hour treatment with neither SSRIs nor TCAs in MEF cells with the exception that CTP induced ERK phosphorylation in cells with functional FKBP5. In

contrast, a cell-specific decrease of ERK phosphorylation was observed in response to acute treatment with a SSRI and a TCA in mice (Di Benedetto et al., 2013). As the ERK pathway is well known to transduce fast answers in response to environmental stimuli, usually acute effects on ERK phosphorylation are analysed. A study analysing chronic treatment effects in response to a SSRI and a TCA found both increased and decreased ERK phosphorylation depending on the localisation of ERK in different intracellular compartments (Fumagalli et al., 2005).

AKT phosphorylation was increased in response to treatment with SSRIs and partially TCA. Increased AKT activity, however, was not reflected by regulation of FOXO3α phosphorylation and activity as well as modulation of levels of the autophagy initiator BECN1. Regulation of autophagy in response to treatment with SSRIs and TCAs was indicated by an increased ratio of LC3-II/I. In principle, increased ratio of LC3-II/I can be caused by either enhanced production of LC3-II or by blockade of degradation of autophagic cargo, thereby inhibiting the removal of LC3-II (Gassen et al., 2014; Rossi et al., 2009; Zschocke et al., 2011). In brains from animals with functional, but not deleted, FKBP5, acute treatment with the SSRI PRX or the TCA AMT had led to dephosphorylation of AKT, accumulation of BECN1 and enhanced conversion of LC3-II/I (Gassen et al., 2014). In mice, acute treatment increased autophagy presumably via inhibition of AKT and FKBP51 mediated action of AKT on BECN1 (Gassen et al., 2014; Wang et al., 2012). In MEFs, in contrast, data from this work hint to a regulation of LC3-II/I conversion in response to treatment with SSRIs and TCAs, which is independent of AKT phosphorylation and BECN1 levels.

SSNRIs and the atypical antidepressant TNP

The pattern of the regulation of cellular pathways in the MEF model was very similar for the two SSNRIs (VTX and VNF) and the atypical antidepressants (TNP).

In general, treatment with neither SSNRIs nor the atypical antidepressant affected GSK3β phosphorylation and regulation of its downstream target BCAT. Out of the three drugs, only TNP increased CRMP2 phosphorylation in cells with deleted FKBP5. In cells with functional FKBP5, TCF/LEF activity was inhibited in response to treatment with VTX. Regulation of CRMP2 phosphorylation as well as TCF/LEF activity by psychopharmaca may not uniquely be regulated by GSK3β, explaining modulation of downstream targets in the absence of effects on GSK3β activity.

Treatment with SSNRIs and the atypical antidepressant increased the phosphorylation of ERK in cells with functional FKBP5. As mentioned above, ERK phosphorylation did not respond to treatment with the drugs in cells with deleted FKBP5.

AKT phosphorylation was not affected by treatment with SSNRIs or the atypical antidepressant. Moreover, the drugs did not modulate the phosphorylation and activity of FOXO3α. Likewise, BECN1 levels did not change in response to treatment with the drugs. VTX increased the conversion of LC3-II/I irrespectively of FKBP5, whereas VNF and TNP did not modulate LC3-II/I conversion. As observed with SSRIs and TCAs, regulation of LC3-II/I conversion by SSNRIs and TNP seems to be uncoupled from FKBP5 dependent regulation of BECN1 by AKT.

Mood stabiliser

In respect of structure, the group of mood stabiliser (VPA, LMT, and LIT) was comprised by highly diverse psychopharmaca. All the more surprising, a more or less common pattern was observed in the regulation of cellular pathways in response to treatment with the mood stabiliser in the MEF model. This pattern, in turn, diverged from the patterns evoked by other classes of psychopharmaca analysed in this work.

GSK3β is discussed as a central modulator in mood regulation and a well-known target of psychopharmacological treatment with LIT (Li and Jope, 2010). In line, increased phosphorylation as indicator of inhibited GSK3β activity was detected in response to treatment with LIT and LMT and also CHI, but not VPA, solely in cells with functional FKBP5. This is in line with the observation that treatment with LIT only increased phosphorylation of GSK3β in tissue from mice with functional FKBP5 (Gassen et al., 2015). Inhibition of GSK3β activity in response to treatment with the mood stabilisers or CHI resulted in reduced phosphorylation of its target CRMP2. Furthermore, inhibited GSK3β activity in response to treatment with the mood stabiliser LIT and VPA or CHI was reflected by, however non-significantly, increased TCF/LEF activity but not by increased BCAT levels, hinting to an activation of Wnt signalling, which was not detectable on the level of BCAT. Recently, we also had shown that treatment with either VPA or LIT increased TCF/LEF activity with different significance in neurons and cortical astrocytes from rats (Gassen et al., 2015). VPA is a well-known activator of Wnt signalling (Blaheta and Cinatl, 2002). In contrast to activation of Wnt signalling by LIT, activation of Wnt signalling by VPA is proposed to be independent of GSK3β and rather be based on activation of Wnt dependent gene expression through inhibition of HDACs (Phiel et al., 2001). This is reflected by a non-significant decrease in GSK3β

phosphorylation and BCAT stability countered by increased TCF/LEF activity in response to treatment with VPA observed in this work.

Treatment with the three mood stabiliser markedly increased the phosphorylation of ERK in cells with functional FKBP5. This effect was abolished in cells with deleted FKBP5. The ERK pathway has recently been reported to be under control of LIT, with dependency of LIT effects on both GSK3β and ERK (Zassadowski et al., 2015). In line, ERK2 phosphorylation was highly sensitive to GSK3β inhibition by CHI in this work. Increased ERK phosphorylation in response to treatment with VPA observed in this work is in line with numerous reports underlining its role in activation of the ERK pathway (Blaheta and Cinatl, 2002).

Mood stabilisers did largely not affect AKT phosphorylation, its downstream targets and autophagy. Only LMT increased AKT phosphorylation, and solely in cells with functional FKBP5, which was again not reflected on the level of BECN1. GSK3β has been reported to be inactivated by AKT (Woodgett, 2005). This hints to an indirect effect in inhibition of GSK3β via activation of AKT in response to treatment with LMT, as described earlier. Phosphorylation of FOXO3α at the suspected AKT target site was also not affected by treatment with mood stabilisers.

Both AKT and ERK regulate FOXO3 activity via specific phosphorylation and subsequent ubiquitination and degradation (Yamaguchi et al., 2012). Ubiquitination by SKP2 has been shown to be dependent on AKT induced phosphorylation and ubiquitination by MDM2 on ERK induced phosphorylation. Interestingly, increased activity of FOXO3α was detected in response to treatment with VPA and LIT. Hence, the induction of FOXO3α transcriptional activity in response to treatment with VPA or LIT is not caused by either AKT or ERK dependent phosphorylation of FOXO3α, which is reported to inhibit FOXO3α transcriptional activity.

NMDA receptor antagonists

KTM and other NMDA receptor antagonists have been reported to inhibit GSK3β whereas phosphorylation of AKT at Ser-473 remained unchanged (Iadarola et al., 2015; Miller et al., 2014). Within this work, however, treatment with KTM or LNC did not regulate the phosphorylation of GSK3β and AKT. Missing expression of NMDA receptor in fibroblast could prevent the action of KTM and LNC on targets downstream of NMDA receptor signalling (Miller et al., 2014). Expression, phosphorylation and activity of GSK3β and AKT downstream targets BCAT, TCF/LEF, CRMP2, FOXO3α, BECN1 and LC3-II/I was also not affected by treatment with the two NDMA receptor

antagonists, with the exception that LNC decreased phosphorylation of CRMP2 in cells with deleted FKBP5.

The phosphorylation of ERK, however, was enhanced in response to treatment with KTM in cells with functional FKBP5. As observed in treatment with other psychopharmaca, this effect was abolished in cells with deleted FKBP5. The action of KTM on ERK phosphorylation appears not to depend on NMDA receptor signalling. Both KTM and LNC are considered to exert non-selective NMDA channel blocking activities (Zarate et al., 2013). Interestingly, LNC did not enhance ERK activation hinting to a mechanism beyond NMDA receptor signalling unique for KTM.

5.2.5 Regulation of autophagy by VPA

Recent research has illustrated a link from autophagy to neurotransmission, which likely modulates neuronal network dynamics and, ultimately, behaviour (Hernandez et al., 2012; Kim et al., 2012). Interestingly, HDACs have recently been shown to suppress autophagy (Cao et al., 2011). Strikingly, the effects in regulation and activity of autophagy markers LC3 and FOXO3α with VPA were opposite to the ones observed with other psychopharmaca, here. Treatment with VPA did not increase but decrease the ratio of the autophagic marker LC3-II/I and attenuated the accumulation of LC3-II upon blockade of autophagy processing. Together, this hints to a slowed down autophagy with VPA treatment with decreased conversion of LC3-II/I.

Treatment with VPA increased the transcriptional activity of FOXO3α. A two-partied function in regulation of autophagy has been discussed for FOXO transcription factors. On the one hand, activity of FOXO3α has been reported to be controlled by the rapamycin independent mTOR complex, mTORC2, which itself is under the control of upstream autophagy signalling (Feng et al., 2015). On the other hand, the regulation of autophagy by FOXO proteins on a transcriptional level has been described in various cell types with transcription of several key players of autophagy being controlled by FOXO transcription factors (Feng et al., 2015).

ATG12, BECN1, LC3, ULK1, and VPS34 are amongst the genes that are controlled by FOXO signalling (Feng et al., 2015). Transcription of autophagy genes being involved in regulation of late-early (VPS34), late-intermediate (ATG12) and delayed (LC3) autophagy but not in early (ULK1, BECN1) autophagy was induced in response to treatment with VPA as observed in this work. A similar profile of transcription regulation of suspected FOXO target genes was observed in response to treatment with BUT, with

transcription induction of late-intermediate (ATG12) and delayed (LC3) autophagy genes. In contrast to the HDAC inhibitors VPA and BUT, no effect on the transcription on the suspected FOXO target genes was detected in response to treatment with the HDAC inhibitor TSA.

Studies have shown that early life stress can influence the expression of HDAC enzymes in the murine brain (Levine et al., 2012; Tesone-Coelho et al., 2015). HDAC enzymes lead to more condensed chromatin structure and a less transcriptionally active chromatin structure. In addition, an age dependent inversive expression of histone modifying enzymes in response to early life stress was found. Animals that were exposed to early life stress showed a decreased expression of HDACs in youth and an increased expression of HDACs in adultness (Suri et al., 2014).

HDAC inhibitors are classified in respect to their chemical structure as well as their HDAC target selectivity. VPA and BUT are short-chain fatty acids that show in vitro potency against classes I and classes II HDACs in the millimolar range (Grayson et al., 2010). TSA is composed of a hydroxamate structure and shows in vitro potency against classes I and classes II HDACs in the nanomolar range (Grayson et al., 2010). VPA is an established psychopharmacon that has been used as an anti-convulsant, mood stabiliser, and adjuvant treatment for schizophrenia. Treatment with BUT has been reported to exert antidepressant-like properties in the mouse (Schroeder et al., 2007). Experimental or clinical evidence for the effectiveness of TSA in stress related diseases, however, is lacking.

This work showed that autophagy is not a general feature of HDAC inhibitors. Of note, only HDAC inhibitors that were shown to regulate autophagy in this work, are known to be active in stress related diseases. It cannot be excluded that the underlying mechanism involves HDACs, but HDAC inhibition alone appears not to be sufficient.

5.2.6 Regulation of treatment outcome by antidepressants

Overall, the provided data hint to non-linear pathway connections of proteins affected by antidepressant treatment. Considering the only rudimentally understood molecular mechanism by which antidepressants act, at least the pathways analysed in this work appear to be uniquely regulated by different psychopharmaca treatments and FKBP5 status (Figure 35). It remains, however, unclear to what extent single pathways contribute to overall treatment outcome. In line with this, additional pathways are very likely to be targeted by psychopharmaca treatment and be involved in conveying treatment outcome.

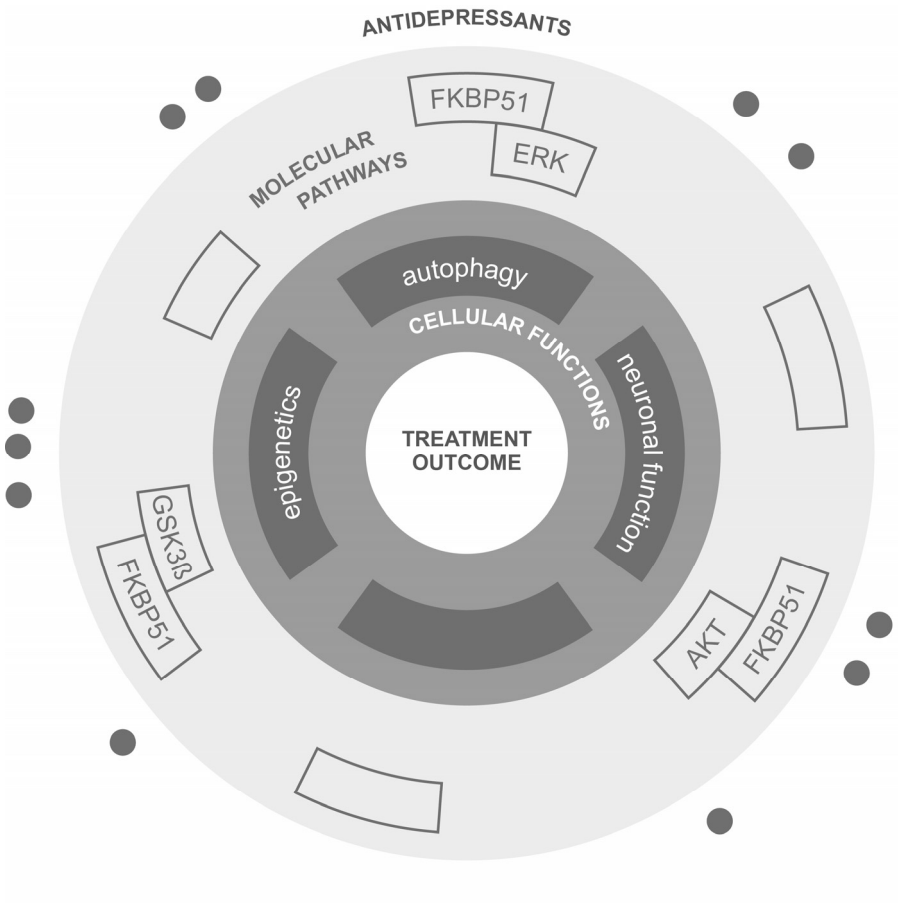

Figure 35: **Simplified sketch of molecular pathways underlying psychopharmaca induced treatment outcome.** Antidepressant treatment modulates the protein status of certain pathways leading to re-adaption of cellular function and hence treatment outcome. Unique patterns of protein modulation in response to treatment with a certain antidepressant appear to underlie the effectiveness of treatment outcome in regard to the environment shaped framework of gene activity. Antidepressants are represented by black circles. Pathway proteins and cellular functions are represented by black boxes. Unlabeled boxes represent to be discovered pathways and cellular functions.

Non-linearity of pathway connections can be exemplified by the regulation of BCAT, which was not significantly regulated by antidepressant treatment. BCAT is phosphorylated by GSK3β, which itself is inhibited by ERK and AKT. Phosphorylation of BCAT by GSK3β facilitates β-TrCP dependent ubiquitination and proteasomal degradation of BCAT. Moreover, BCAT is at a further site also directly phosphorylated by AKT, thus exerting a stabilising effect on BCAT (Yamaguchi et al., 2012). As observed in this work, treatment with psychopharmaca exerted differential effects on the activity of the three kinases GSK3β, ERK, and AKT in a more or less psychopharmaca class-dependent manner. With the three kinases being regulated by psychopharmaca

treatment, BCAT could serve as a hub for the integration of upstream pathway signals elicited by psychopharmaca treatment.

Likewise, the activity of a certain pathway is likely to excel other pathways in response to external stimuli or as maladaptive process in response to prolonged stressors, leading to imbalances in the molecular network and symptoms of stress related diseases. The regulation of FKBP51 by glucocorticoids likely links all the molecular actions of FKBP51 to stress (Hubler and Scammell, 2004; Klengel et al., 2013). With pathways being differentially affected by FKBP51, the FKBP5 status appears to at least partially influence the re-balancing of those pathways in response to treatment, leading to context dependent effectiveness of certain psychopharmaca.

5.3 Outlook

While this work sheds light on the role of FKBP5 in transcription regulation and in shaping cellular pathways of psychopharmaca action, it also underlines the incompleteness of our current understanding of FKBP5´s action in the therapy of stress related diseases.

With GSK3β, AKT, and ERK, three important kinases with multiple pathway connections were observed to be regulated by psychopharmaca. The effects were not homogeneous across all psychopharmaca and only loosely followed drug classes. Moreover, regulation of these kinases as well as their downstream targets was non-uniformly influenced by FKBP51. This raises the question of a cell type specificity of certain psychopharmaca effects, as different cell types provide differential pathway activities. As psychopharmaca presumably take effect in the brain, the analysis of pathway regulation by psychopharmaca and the role of FKBP5 in shaping this regulation would best be addressed in a mixed culture of the respective neuronal and glial cells. Analysis of pathway regulation in a human brain-like context should be approachable by the use of induced pluripotent stem-cells (iPSCs). Recently, hippocampal dentate gyrus-like neurons derived from iPSCs of patients with bipolar disorder were described as a human model for stress related diseases (Mertens et al., 2015). With this model, cells obtained from patients responding or not responding to a specific psychopharmaca treatment could be utilised to characterise pathways relevant for treatment outcome.

As observed in the FKBP5 knockout cell model, drug regulation of the kinases GSK3β, AKT, and ERK as well as their downstream targets was non-uniformly influenced by FKBP51. Pharmacologically targeting FKBP51 has recently come into focus, also because decreased depression-like behaviour was observed in older mice with deleted FKBP5. The original concept was to enhance GR function by inhibiting FKBP51. The data presented here underline a role of FKBP51 beyond inhibition of glucocorticoid signalling and raise the question of the specificity of FKBP5 targeting drugs. Even an FKBP51 ligand specifically disrupting the inhibitory effect of FKBP51 on the glucocorticoid receptor would not only affect HPA axis signalling but thereby also lead to enhanced transcription of FKBP5 and thus likely enhance functions of FKBP51 beyond glucocorticoid signalling. Importantly, at least part of these functions have already been linked to successful treatment outcome (Gassen et al., 2014, 2015). Indeed, it has recently been reported that targeting FKBP51 with a ligand exerted antidepressant-like effects in mice (Gaali et al., 2015). Hence, it will be interesting to understand how this ligand affects pathways beyond glucocorticoid signalling and how this might contribute to antidepressant-like effects.

Appendix

References

Abdel-Razaq, W., Kendall, D.A., and Bates, T.E. (2011). The effects of antidepressants on mitochondrial function in a model cell system and isolated mitochondria. Neurochem. Res. *36*, 327–338.

Alers, S., Löffler, A.S., Wesselborg, S., and Stork, B. (2012). Role of AMPK-mTOR-Ulk1/2 in the regulation of autophagy: cross talk, shortcuts, and feedbacks. Mol. Cell. Biol. *32*, 2–11.

Alfonso, J., Frasch, A.C., and Flugge, G. (2005). Chronic stress, depression and antidepressants: effects on gene transcription in the hippocampus. Rev. Neurosci. *16*, 43–56.

Baastrup, P.C., and Schou, M. (1967). Lithium as a prophylactic agents. Its effect against recurrent depressions and manic-depressive psychosis. Arch. Gen. Psychiatry *16*, 162–172.

Backer, J.M. (2008). The regulation and function of Class III PI3Ks: novel roles for Vps34. Biochem. J. *410*, 1–17.

Baker, K.E., and Parker, R. (2004). Nonsense-mediated mRNA decay: terminating erroneous gene expression. Curr. Opin. Cell Biol. *16*, 293–299.

Beaulieu, J.-M., Gainetdinov, R.R., and Caron, M.G. (2009). Akt/GSK3 signaling in the action of psychotropic drugs. Annu. Rev. Pharmacol. Toxicol. *49*, 327–347.

Berridge, M.V., and Tan, A.S. (1993). Characterization of the cellular reduction of 3-(4,5-dimethylthiazol-2-yl)-2,5-diphenyltetrazolium bromide (MTT): subcellular localization, substrate dependence, and involvement of mitochondrial electron transport in MTT reduction. Arch. Biochem. Biophys. *303*, 474–482.

Binder, E.B., and Holsboer, F. (2006). Pharmacogenomics and antidepressant drugs. Ann. Med. *38*, 82–94.

Binder, E.B., Salyakina, D., Lichtner, P., Wochnik, G.M., Ising, M., Pütz, B., Papiol, S., Seaman, S., Lucae, S., Kohli, M.A., et al. (2004). Polymorphisms in FKBP5 are associated with increased recurrence of depressive episodes and rapid response to antidepressant treatment. Nat. Genet. *36*, 1319–1325.

Binder, E.B., Bradley, R.G., Liu, W., Epstein, M.P., Deveau, T.C., Mercer, K.B., Tang, Y., Gillespie, C.F., Heim, C.M., Nemeroff, C.B., et al. (2008). Association of FKBP5 polymorphisms and childhood abuse with risk of posttraumatic stress disorder symptoms in adults. JAMA *299*, 1291–1305.

Blaheta, R.A., and Cinatl, J. (2002). Anti-tumor mechanisms of valproate: a novel role for an old drug. Med. Res. Rev. *22*, 492–511.

Buchsbaum, R.J. (2007). Rho activation at a glance. J. Cell Sci. *120*, 1149–1152.

Cade, J.F.J. (1949). Lithium salts in the treatment of psychotic excitement. Med. J. Aust. *2*, 349–352.

Cao, D.J., Wang, Z.V., Battiprolu, P.K., Jiang, N., Morales, C.R., Kong, Y., Rothermel, B.A., Gillette, T.G., and Hill, J.A. (2011). Histone deacetylase (HDAC) inhibitors attenuate cardiac hypertrophy by suppressing autophagy. Proc. Natl. Acad. Sci. U. S. A. *108*, 4123–4128.

Carlsson, A., Fuxe, K., and Ungerstedt, U. (1968). The effect of imipramine on central 5-hydroxytryptamine neurons. J. Pharm. Pharmacol. *20*, 150–151.

Chrousos, G.P., and Gold, P.W. (1992). The concepts of stress and stress system disorders. Overview of physical and behavioral homeostasis. JAMA *267*, 1244–1252.

Cohen, P., and Frame, S. (2001). The renaissance of GSK3. Nat. Rev. Mol. Cell Biol. *2*, 769–776.

Covington, H.E., Maze, I., LaPlant, Q.C., Vialou, V.F., Ohnishi, Y.N., Berton, O., Fass, D.M., Renthal, W., Rush, A.J., Wu, E.Y., et al. (2009). Antidepressant actions of histone deacetylase inhibitors. J. Neurosci. Off. J. Soc. Neurosci. *29*, 11451–11460.

Crusio, W.E. (2004). Flanking gene and genetic background problems in genetically manipulated mice. Biol. Psychiatry *56*, 381–385.

Datson, N.A., Speksnijder, N., Mayer, J.L., Steenbergen, P.J., Korobko, O., Goeman, J., de Kloet, E.R., Joëls, M., and Lucassen, P.J. (2012). The transcriptional response to chronic stress and glucocorticoid receptor blockade in the hippocampal dentate gyrus. Hippocampus *22*, 359–371.

Davies, T.H., Ning, Y.-M., and Sánchez, E.R. (2005). Differential control of glucocorticoid receptor hormone-binding function by tetratricopeptide repeat (TPR) proteins and the immunosuppressive ligand FK506. Biochemistry (Mosc.) *44*, 2030–2038.

De Ferrari, G.V., Chacón, M.A., Barría, M.I., Garrido, J.L., Godoy, J.A., Olivares, G., Reyes, A.E., Alvarez, A., Bronfman, M., and Inestrosa, N.C. (2003). Activation of Wnt signaling rescues neurodegeneration and behavioral impairments induced by beta-amyloid fibrils. Mol. Psychiatry *8*, 195–208.

Di Benedetto, B., Radecke, J., Schmidt, M.V., and Rupprecht, R. (2013). Acute antidepressant treatment differently modulates ERK/MAPK activation in neurons and astrocytes of the adult mouse prefrontal cortex. Neuroscience *232*, 161–168.

Distler, M.G., and Palmer, A.A. (2012). Role of Glyoxalase 1 (Glo1) and methylglyoxal (MG) in behavior: recent advances and mechanistic insights. Front. Genet. *3*, 250.

Distler, M.G., Plant, L.D., Sokoloff, G., Hawk, A.J., Aneas, I., Wuenschell, G.E., Termini, J., Meredith, S.C., Nobrega, M.A., and Palmer, A.A. (2012). Glyoxalase 1 increases anxiety by reducing GABAA receptor agonist methylglyoxal. J. Clin. Invest. *122*, 2306–2315.

Dou, F., Yuan, L.-D., and Zhu, J.-J. (2005). Heat shock protein 90 indirectly regulates ERK activity by affecting Raf protein metabolism. Acta Biochim. Biophys. Sin. *37*, 501–505.

Duman, R.S., Li, N., Liu, R.-J., Duric, V., and Aghajanian, G. (2012). Signaling pathways underlying the rapid antidepressant actions of ketamine. Neuropharmacology *62*, 35–41.

Dunlop, B.W., and Nemeroff, C.B. (2007). The role of dopamine in the pathophysiology of depression. Arch. Gen. Psychiatry *64*, 327–337.

Duric, V., Banasr, M., Licznerski, P., Schmidt, H.D., Stockmeier, C.A., Simen, A.A., Newton, S.S., and Duman, R.S. (2010). A negative regulator of MAP kinase causes depressive behavior. Nat. Med. *16*, 1328–1332.

Dwivedi, Y., Rizavi, H.S., Roberts, R.C., Conley, R.C., Tamminga, C.A., and Pandey, G.N. (2001). Reduced activation and expression of ERK1/2 MAP kinase in the post-mortem brain of depressed suicide subjects. J. Neurochem. *77*, 916–928.

Egan, C.M., Sridhar, S., Wigler, M., and Hall, I.M. (2007). Recurrent DNA copy number variation in the laboratory mouse. Nat. Genet. *39*, 1384–1389.

Einat, H., Yuan, P., Gould, T.D., Li, J., Du, J., Zhang, L., Manji, H.K., and Chen, G. (2003). The role of the extracellular signal-regulated kinase signaling pathway in mood modulation. J. Neurosci. Off. J. Soc. Neurosci. *23*, 7311–7316.

Emamian, E.S. (2012). AKT/GSK3 signaling pathway and schizophrenia. Front. Mol. Neurosci. *5*, 33.

Evangelisti, C., Ricci, F., Tazzari, P., Chiarini, F., Battistelli, M., Falcieri, E., Ognibene, A., Pagliaro, P., Cocco, L., McCubrey, J.A., et al. (2011). Preclinical testing of the Akt inhibitor triciribine in T-cell acute lymphoblastic leukemia. J. Cell. Physiol. *226*, 822–831.

Everett, and Tolman (1959). Mode of action of rauwolfia alkaloids and motor activity. Biol. Psychiatry 75–81.

Fallin, M.D., Lasseter, V.K., Avramopoulos, D., Nicodemus, K.K., Wolyniec, P.S., McGrath, J.A., Steel, G., Nestadt, G., Liang, K.-Y., Huganir, R.L., et al. (2005). Bipolar I disorder and schizophrenia: a 440-single-nucleotide polymorphism screen of 64 candidate genes among Ashkenazi Jewish case-parent trios. Am. J. Hum. Genet. *77*, 918–936.

Feng, Y., Yao, Z., and Klionsky, D.J. (2015). How to control self-digestion: transcriptional, post-transcriptional, and post-translational regulation of autophagy. Trends Cell Biol. *25*, 354–363.

Ferrari, A.J., Charlson, F.J., Norman, R.E., Patten, S.B., Freedman, G., Murray, C.J.L., Vos, T., and Whiteford, H.A. (2013). Burden of depressive disorders by country, sex, age, and year: findings from the global burden of disease study 2010. PLoS Med. *10*, e1001547.

Fumagalli, F., Molteni, R., Calabrese, F., Frasca, A., Racagni, G., and Riva, M.A. (2005). Chronic fluoxetine administration inhibits extracellular signal-regulated kinase 1/2 phosphorylation in rat brain. J. Neurochem. *93*, 1551–1560.

Gaali, S., Kirschner, A., Cuboni, S., Hartmann, J., Kozany, C., Balsevich, G., Namendorf, C., Fernandez-Vizarra, P., Sippel, C., Zannas, A.S., et al. (2015). Selective inhibitors of the FK506-binding protein 51 by induced fit. Nat. Chem. Biol. *11*, 33–37.

Gardner, A., and Boles, R.G. (2010). Beyond the serotonin hypothesis: Mitochondria, inflammation and neurodegeneration in major depression and affective spectrum disorders. Prog. Neuropsychopharmacol. Biol. Psychiatry.

Gassen, N.C., Hartmann, J., Zschocke, J., Stepan, J., Hafner, K., Zellner, A., Kirmeier, T., Kollmannsberger, L., Wagner, K.V., Dedic, N., et al. (2014). Association of FKBP51 with priming of autophagy pathways and mediation of antidepressant treatment response: evidence in cells, mice, and humans. PLoS Med. *11*, e1001755.

Gassen, N.C., Hartmann, J., Zannas, A.S., Kretzschmar, A., Zschocke, J., Maccarrone, G., Hafner, K., Zellner, A., Kollmannsberger, L.K., Wagner, K.V., et al. (2015). FKBP51 inhibits GSK3β and augments the effects of distinct psychotropic medications. Mol. Psychiatry.

Gawlik, M., Moller-Ehrlich, K., Mende, M., Jovnerovski, M., Jung, S., Jabs, B., Knapp, M., and Stoeber, G. (2006). Is FKBP5 a genetic marker of affective psychosis? A case control study and analysis of disease related traits. BMC Psychiatry *6*, 52.

Gerlai, R. (1996). Gene-targeting studies of mammalian behavior: is it the mutation or the background genotype? Trends Neurosci. *19*, 177–181.

Glowinski, J., and Axelrod, J. (1964). Inhibition of Uptake of Tritiated-noradrenaline in the Intact Rat Brain by Imipramine and Structurally Related Compounds. Nature *204*, 1318–1319.

Goldsmith, D.R., Wagstaff, A.J., Ibbotson, T., and Perry, C.M. (2003). Lamotrigine: a review of its use in bipolar disorder. Drugs *63*, 2029–2050.

Göttlicher, M., Minucci, S., Zhu, P., Krämer, O.H., Schimpf, A., Giavara, S., Sleeman, J.P., Lo Coco, F., Nervi, C., Pelicci, P.G., et al. (2001). Valproic acid defines a novel class of HDAC inhibitors inducing differentiation of transformed cells. EMBO J. *20*, 6969–6978.

Grad, I., and Picard, D. (2007). The glucocorticoid responses are shaped by molecular chaperones. Mol. Cell. Endocrinol. *275*, 2–12.

Grayson, D.R., Kundakovic, M., and Sharma, R.P. (2010). Is there a future for histone deacetylase inhibitors in the pharmacotherapy of psychiatric disorders? Mol. Pharmacol. *77*, 126–135.

Gutierrez, M.A., Stimmel, G.L., and Aiso, J.Y. (2003). Venlafaxine: a 2003 update. Clin. Ther. *25*, 2138–2154.

Hartmann, J., Wagner, K.V., Liebl, C., Scharf, S.H., Wang, X.-D., Wolf, M., Hausch, F., Rein, T., Schmidt, U., Touma, C., et al. (2012). The involvement of FK506-binding protein 51 (FKBP5) in the behavioral and neuroendocrine effects of chronic social defeat stress. Neuropharmacology *62*, 332–339.

Harwood, A.J. (2001). Regulation of GSK-3: a cellular multiprocessor. Cell *105*, 821–824.

Harwood, A.J., and Agam, G. (2003). Search for a common mechanism of mood stabilizers. Biochem. Pharmacol. *66*, 179–189.

Hastings, P.J., Lupski, J.R., Rosenberg, S.M., and Ira, G. (2009). Mechanisms of change in gene copy number. Nat. Rev. Genet. *10*, 551–564.

Hernandez, D., Torres, C.A., Setlik, W., Cebrián, C., Mosharov, E.V., Tang, G., Cheng, H.-C., Kholodilov, N., Yarygina, O., Burke, R.E., et al. (2012). Regulation of presynaptic neurotransmission by macroautophagy. Neuron *74*, 277–284.

Holsboer, F. (2000). The corticosteroid receptor hypothesis of depression. Neuropsychopharmacology *23*, 477–501.

Holsboer, F., von Bardeleben, U., Wiedemann, K., Müller, O.A., and Stalla, G.K. (1987). Serial assessment of corticotropin-releasing hormone response after dexamethasone in depression. Implications for pathophysiology of DST nonsuppression. Biol. Psychiatry *22*, 228–234.

Hroudova, J., and Fisar, Z. (2010). Activities of respiratory chain complexes and citrate synthase influenced by pharmacologically different antidepressants and mood stabilizers. Neuro Endocrinol. Lett. *31*, 336–342.

Huber, C., Mårtensson, A., Bokoch, G.M., Nemazee, D., and Gavin, A.L. (2008). FGD2, a CDC42-specific exchange factor expressed by antigen-presenting cells, localizes to early endosomes and active membrane ruffles. J. Biol. Chem. *283*, 34002–34012.

Hubler, T.R., and Scammell, J.G. (2004). Intronic hormone response elements mediate regulation of FKBP5 by progestins and glucocorticoids. Cell Stress Chaperones *9*, 243–252.

Hur, E.-M., and Zhou, F.-Q. (2010). GSK3 signalling in neural development. Nat. Rev. Neurosci. *11*, 539–551.

Iadarola, N.D., Niciu, M.J., Richards, E.M., Vande Voort, J.L., Ballard, E.D., Lundin, N.B., Nugent, A.C., Machado-Vieira, R., and Zarate, C.A. (2015). Ketamine and other N-methyl-D-aspartate receptor antagonists in the treatment of depression: a perspective review. Ther. Adv. Chronic Dis. *6*, 97–114.

Ip, J.P.K., Fu, A.K.Y., and Ip, N.Y. (2014). CRMP2: functional roles in neural development and therapeutic potential in neurological diseases. Neurosci. Rev. J. Bringing Neurobiol. Neurol. Psychiatry *20*, 589–598.

Ising, M., Depping, A.-M., Siebertz, A., Lucae, S., Unschuld, P.G., Kloiber, S., Horstmann, S., Uhr, M., Müller-Myhsok, B., and Holsboer, F. (2008). Polymorphisms in the FKBP5 gene region modulate recovery from psychosocial stress in healthy controls. Eur. J. Neurosci. *28*, 389–398.

Jensen-Seaman, M.I., Furey, T.S., Payseur, B.A., Lu, Y., Roskin, K.M., Chen, C.-F., Thomas, M.A., Haussler, D., and Jacob, H.J. (2004). Comparative recombination rates in the rat, mouse, and human genomes. Genome Res. *14*, 528–538.

Joëls, M., Krugers, H., and Karst, H. (2008). Stress-induced changes in hippocampal function. Prog. Brain Res. *167*, 3–15.

Jope, R.S., and Roh, M.-S. (2006). Glycogen synthase kinase-3 (GSK3) in psychiatric diseases and therapeutic interventions. Curr. Drug Targets *7*, 1421–1434.

Kabeya, Y., Mizushima, N., Ueno, T., Yamamoto, A., Kirisako, T., Noda, T., Kominami, E., Ohsumi, Y., and Yoshimori, T. (2000). LC3, a mammalian homologue of yeast Apg8p, is localized in autophagosome membranes after processing. EMBO J. *19*, 5720–5728.

Karabatsiakis, A., Böck, C., Salinas-Manrique, J., Kolassa, S., Calzia, E., Dietrich, D.E., and Kolassa, I.-T. (2014). Mitochondrial respiration in peripheral blood mononuclear cells correlates with depressive subsymptoms and severity of major depression. Transl. Psychiatry *4*, e397.

Karege, F., Perroud, N., Burkhardt, S., Schwald, M., Ballmann, E., La Harpe, R., and Malafosse, A. (2007). Alteration in kinase activity but not in protein levels of protein kinase B and glycogen synthase kinase-3beta in ventral prefrontal cortex of depressed suicide victims. Biol. Psychiatry *61*, 240–245.

Kessler, R.C. (2012). The Costs of Depression. Psychiatr. Clin. North Am. *35*, 1–14.

Kessler, R.C., and Bromet, E.J. (2013). The epidemiology of depression across cultures. Annu. Rev. Public Health *34*, 119–138.

Kim, C.S., Chang, P.Y., and Johnston, D. (2012). Enhancement of dorsal hippocampal activity by knockdown of HCN1 channels leads to anxiolytic- and antidepressant-like behaviors. Neuron *75*, 503–516.

King, T.D., Clodfelder-Miller, B., Barksdale, K.A., and Bijur, G.N. (2008). Unregulated mitochondrial GSK3beta activity results in NADH: ubiquinone oxidoreductase deficiency. Neurotox. Res. *14*, 367–382.

Klengel, T., Mehta, D., Anacker, C., Rex-Haffner, M., Pruessner, J.C., Pariante, C.M., Pace, T.W.W., Mercer, K.B., Mayberg, H.S., Bradley, B., et al. (2013). Allele-specific FKBP5 DNA demethylation mediates gene-childhood trauma interactions. Nat. Neurosci. *16*, 33–41.

de Kloet, E.R., Joëls, M., and Holsboer, F. (2005). Stress and the brain: from adaptation to disease. Nat. Rev. Neurosci. *6*, 463–475.

Knol, M.J., Twisk, J.W.R., Beekman, A.T.F., Heine, R.J., Snoek, F.J., and Pouwer, F. (2006). Depression as a risk factor for the onset of type 2 diabetes mellitus. A meta-analysis. Diabetologia *49*, 837–845.

Koenen, K.C., Saxe, G., Purcell, S., Smoller, J.W., Bartholomew, D., Miller, A., Hall, E., Kaplow, J., Bosquet, M., Moulton, S., et al. (2005). Polymorphisms in FKBP5 are associated with peritraumatic dissociation in medically injured children. Mol. Psychiatry *10*, 1058–1059.

Kollmannsberger, L.K., Gassen, N.C., Bultmann, A., Hartmann, J., Weber, P., Schmidt, M.V., and Rein, T. (2013). Increased glyoxalase-1 levels in Fkbp5 knockout mice caused by glyoxalase-1 gene duplication. G3 Bethesda Md *3*, 1311–1313.

Lamark, T., Kirkin, V., Dikic, I., and Johansen, T. (2009). NBR1 and p62 as cargo receptors for selective autophagy of ubiquitinated targets. Cell Cycle Georget. Tex *8*, 1986–1990.

Lee, T.-Y., Lai, T.-Y., Lin, S.-C., Wu, C.-W., Ni, I.-F., Yang, Y.-S., Hung, L.-Y., Law, B.K., and Chiang, C.-W. (2010). The B56γ3 Regulatory Subunit of Protein Phosphatase 2A (PP2A) Regulates S Phase-specific Nuclear Accumulation of PP2A and the G1 to S Transition. J. Biol. Chem. *285*, 21567–21580.

Lefloch, R., Pouysségur, J., and Lenormand, P. (2009). Total ERK1/2 activity regulates cell proliferation. Cell Cycle Georget. Tex *8*, 705–711.

Lekman, M., Laje, G., Charney, D., Rush, A.J., Wilson, A.F., Sorant, A.J.M., Lipsky, R., Wisniewski, S.R., Manji, H., McMahon, F.J., et al. (2008). The FKBP5-gene in depression and treatment response--an association study in the Sequenced Treatment Alternatives to Relieve Depression (STAR*D) Cohort. Biol. Psychiatry *63*, 1103–1110.

Levine, A., Worrell, T.R., Zimnisky, R., and Schmauss, C. (2012). Early life stress triggers sustained changes in histone deacetylase expression and histone H4 modifications that alter responsiveness to adolescent antidepressant treatment. Neurobiol. Dis. *45*, 488–498.

Li, X., and Jope, R.S. (2010). Is glycogen synthase kinase-3 a central modulator in mood regulation? Neuropsychopharmacol. Off. Publ. Am. Coll. Neuropsychopharmacol. *35*, 2143–2154.

Lôo, H., Saiz-Ruiz, J., Costa E Silva, J.A., Ansseau, M., Herrington, R., Vaz-Serra, A., Dilling, H., and De Risio, S. (2001). Efficacy and safety of tianeptine in the treatment of depressive disorders in comparison with fluoxetine*. Hum. Psychopharmacol. *16*, S31–S38.

Mahableshwarkar, A.R., Jacobsen, P.L., and Chen, Y. (2013). A randomized, double-blind trial of 2.5 mg and 5 mg vortioxetine (Lu AA21004) versus placebo for 8 weeks in adults with major depressive disorder. Curr. Med. Res. Opin. *29*, 217–226.

Mammucari, C., Milan, G., Romanello, V., Masiero, E., Rudolf, R., Del Piccolo, P., Burden, S.J., Di Lisi, R., Sandri, C., Zhao, J., et al. (2007). FoxO3 controls autophagy in skeletal muscle in vivo. Cell Metab. *6*, 458–471.

Marmol, F. (2008). Lithium: bipolar disorder and neurodegenerative diseases Possible cellular mechanisms of the therapeutic effects of lithium. Prog. Neuropsychopharmacol. Biol. Psychiatry *32*, 1761–1771.

Marshall, N.J., Goodwin, C.J., and Holt, S.J. (1995). A critical assessment of the use of microculture tetrazolium assays to measure cell growth and function. Growth Regul. *5*, 69–84.

Martinez-Lopez, N., Athonvarangkul, D., Mishall, P., Sahu, S., and Singh, R. (2013). Autophagy proteins regulate ERK phosphorylation. Nat. Commun. *4*, 2799.

Mathew, S.J., Manji, H.K., and Charney, D.S. (2008). Novel drugs and therapeutic targets for severe mood disorders. Neuropsychopharmacol. Off. Publ. Am. Coll. Neuropsychopharmacol. *33*, 2080–2092.

McEwen, B.S. (2000). Allostasis and allostatic load: implications for neuropsychopharmacology. Neuropsychopharmacol. Off. Publ. Am. Coll. Neuropsychopharmacol. *22*, 108–124.

Mercer, T.R., and Mattick, J.S. (2013). Understanding the regulatory and transcriptional complexity of the genome through structure. Genome Res. *23*, 1081–1088.

Mertens, J., Wang, Q.-W., Kim, Y., Yu, D.X., Pham, S., Yang, B., Zheng, Y., Diffenderfer, K.E., Zhang, J., Soltani, S., et al. (2015). Differential responses to lithium in hyperexcitable neurons from patients with bipolar disorder. Nature *527*, 95–99.

Miller, J.S., Barr, J.L., Harper, L.J., Poole, R.L., Gould, T.J., and Unterwald, E.M. (2014). The GSK3 signaling pathway is activated by cocaine and is critical for cocaine conditioned reward in mice. PloS One *9*, e88026.

Mizushima, N., and Komatsu, M. (2011). Autophagy: renovation of cells and tissues. Cell *147*, 728–741.

Montgomery, S.A. (1989). The efficacy of fluoxetine as an antidepressant in the short and long term. Int. Clin. Psychopharmacol. *4 Suppl 1*, 113–119.

Murgatroyd, C., Patchev, A.V., Wu, Y., Micale, V., Bockmühl, Y., Fischer, D., Holsboer, F., Wotjak, C.T., Almeida, O.F.X., and Spengler, D. (2009). Dynamic DNA methylation programs persistent adverse effects of early-life stress. Nat. Neurosci. *12*, 1559–1566.

Nicholson, A., Kuper, H., and Hemingway, H. (2006). Depression as an aetiologic and prognostic factor in coronary heart disease: a meta-analysis of 6362 events among 146 538 participants in 54 observational studies. Eur. Heart J. *27*, 2763–2774.

Nishimura, M., Yu, G., Levesque, G., Zhang, D.M., Ruel, L., Chen, F., Milman, P., Holmes, E., Liang, Y., Kawarai, T., et al. (1999). Presenilin mutations associated with Alzheimer disease cause defective intracellular trafficking of beta-catenin, a component of the presenilin protein complex. Nat. Med. *5*, 164–169.

Noda, N.N., Kumeta, H., Nakatogawa, H., Satoo, K., Adachi, W., Ishii, J., Fujioka, Y., Ohsumi, Y., and Inagaki, F. (2008). Structural basis of target recognition by Atg8/LC3 during selective autophagy. Genes Cells Devoted Mol. Cell. Mech. *13*, 1211–1218.

Ozer, E.J., Best, S.R., Lipsey, T.L., and Weiss, D.S. (2003). Predictors of posttraumatic stress disorder and symptoms in adults: a meta-analysis. Psychol. Bull. *129*, 52–73.

Papiol, S., Arias, B., Gastó, C., Gutiérrez, B., Catalán, R., and Fañanás, L. (2007). Genetic variability at HPA axis in major depression and clinical response to antidepressant treatment. J. Affect. Disord. *104*, 83–90.

Pariante, C.M., and Miller, A.H. (2001). Glucocorticoid receptors in major depression: relevance to pathophysiology and treatment. Biol. Psychiatry *49*, 391–404.

Pei, H., Li, L., Fridley, B.L., Jenkins, G.D., Kalari, K.R., Lingle, W., Petersen, G., Lou, Z., and Wang, L. (2009). FKBP51 affects cancer cell response to chemotherapy by negatively regulating Akt. Cancer Cell *16*, 259–266.

Phiel, C.J., Zhang, F., Huang, E.Y., Guenther, M.G., Lazar, M.A., and Klein, P.S. (2001). Histone deacetylase is a direct target of valproic acid, a potent anticonvulsant, mood stabilizer, and teratogen. J. Biol. Chem. *276*, 36734–36741.

Pratt, W.B., and Toft, D.O. (1997). Steroid receptor interactions with heat shock protein and immunophilin chaperones. Endocr. Rev. *18*, 306–360.

Preskorn, S., Ross, R., and Stanga, C.Y. (2004). Selective Serotonin Reuptake Inhibitors. In Antidepressants: Past, Present, and Future, (Berlin ; New York: Springer),.

Puri, C., Renna, M., Bento, C.F., Moreau, K., and Rubinsztein, D.C. (2013). Diverse autophagosome membrane sources coalesce in recycling endosomes. Cell *154*, 1285–1299.

Qi, H., Mailliet, F., Spedding, M., Rocher, C., Zhang, X., Delagrange, P., McEwen, B., Jay, T.M., and Svenningsson, P. (2009). Antidepressants reverse the attenuation of the neurotrophic MEK/MAPK cascade in frontal cortex by elevated platform stress; reversal of effects on LTP is associated with GluA1 phosphorylation. Neuropharmacology *56*, 37–46.

Rena, G., Woods, Y.L., Prescott, A.R., Peggie, M., Unterman, T.G., Williams, M.R., and Cohen, P. (2002). Two novel phosphorylation sites on FKHR that are critical for its nuclear exclusion. EMBO J. *21*, 2263–2271.

Rossi, M., Munarriz, E.R., Bartesaghi, S., Milanese, M., Dinsdale, D., Guerra-Martin, M.A., Bampton, E.T.W., Glynn, P., Bonanno, G., Knight, R.A., et al. (2009). Desmethylclomipramine induces the accumulation of autophagy markers by blocking autophagic flux. J. Cell Sci. *122*, 3330–3339.

Rossman, K.L., Der, C.J., and Sondek, J. (2005). GEF means go: turning on RHO GTPases with guanine nucleotide-exchange factors. Nat. Rev. Mol. Cell Biol. *6*, 167–180.

aan het Rot, M., Mathew, S.J., and Charney, D.S. (2009). Neurobiological mechanisms in major depressive disorder. CMAJ Can. Med. Assoc. J. J. Assoc. Medicale Can. *180*, 305–313.

Rubinfeld, H., and Seger, R. (2005). The ERK cascade: a prototype of MAPK signaling. Mol. Biotechnol. *31*, 151–174.

Ruelas, E.G., Diaz-Martinez, A., and Ruiz, R.M. (1997). An open assessment of the acceptability, efficacy, and tolerance of venlafaxine in usual care settings. Curr. Ther. Res. *58*, 609–630.

Russell, R.C., Tian, Y., Yuan, H., Park, H.W., Chang, Y.-Y., Kim, J., Kim, H., Neufeld, T.P., Dillin, A., and Guan, K.-L. (2013). ULK1 induces autophagy by phosphorylating Beclin-1 and activating VPS34 lipid kinase. Nat. Cell Biol. *15*, 741–750.

Rusten, T.E., and Stenmark, H. (2010). p62, an autophagy hero or culprit? Nat. Cell Biol. *12*, 207–209.

Scaini, G., Maggi, D.D., De-Nês, B.T., Gonçalves, C.L., Ferreira, G.K., Teodorak, B.P., Bez, G.D., Ferreira, G.C., Schuck, P.F., Quevedo, J., et al. (2011). Activity of mitochondrial respiratory chain is increased by chronic administration of antidepressants. Acta Neuropsychiatr. *23*, 112–118.

Scammell, J.G., Denny, W.B., Valentine, D.L., and Smith, D.F. (2001). Overexpression of the FK506-binding immunophilin FKBP51 is the common cause of glucocorticoid resistance in three New World primates. Gen. Comp. Endocrinol. *124*, 152–165.

Schildkraut, J.J. (1965). The catecholamine hypothesis of affective disorders: a review of supporting evidence. Am. J. Psychiatry *122*, 509–522.

Schroeder, F.A., Lin, C.L., Crusio, W.E., and Akbarian, S. (2007). Antidepressant-like effects of the histone deacetylase inhibitor, sodium butyrate, in the mouse. Biol. Psychiatry *62*, 55–64.

Sengupta, A., Molkentin, J.D., and Yutzey, K.E. (2009). FoxO transcription factors promote autophagy in cardiomyocytes. J. Biol. Chem. *284*, 28319–28331.

Shafie, A., Xue, M., Thornalley, P.J., and Rabbani, N. (2014). Copy number variation of glyoxalase I. Biochem. Soc. Trans. *42*, 500–503.

Silva, A.J., Simpson, E.M., Takahashi, J.S., Lipp, H.-P., Nakanishi, S., Wehner, J.M., Giese, K.P., Tully, T., Abel, T., Chapman, P.F., et al. (1997). Mutant Mice and Neuroscience: Recommendations Concerning Genetic Background. Neuron *19*, 755–759.

Sinars, C.R., Cheung-Flynn, J., Rimerman, R.A., Scammell, J.G., Smith, D.F., and Clardy, J. (2003). Structure of the large FK506-binding protein FKBP51, an Hsp90-binding protein and a component of steroid receptor complexes. Proc. Natl. Acad. Sci. U. S. A. *100*, 868–873.

Singh, P., Schimenti, J.C., and Bolcun-Filas, E. (2015). A mouse geneticist's practical guide to CRISPR applications. Genetics *199*, 1–15.

Slatkin, M. (2009). Epigenetic inheritance and the missing heritability problem. Genetics *182*, 845–850.

Snyder, J.T., Worthylake, D.K., Rossman, K.L., Betts, L., Pruitt, W.M., Siderovski, D.P., Der, C.J., and Sondek, J. (2002). Structural basis for the selective activation of Rho GTPases by Dbl exchange factors. Nat. Struct. Biol. *9*, 468–475.

Spina, E., Santoro, V., and D'Arrigo, C. (2008). Clinically relevant pharmacokinetic drug interactions with second-generation antidepressants: an update. Clin. Ther. *30*, 1206–1227.

Stover, C., Gradl, G., Jentsch, I., Speicher, M.R., Wieser, R., and Schwaeble, W. (2001). cDNA cloning, chromosome assignment, and genomic structure of a human gene encoding a novel member of the RBM family. Cytogenet. Cell Genet. *92*, 225–230.

Sun, Y., Liu, W.-Z., Liu, T., Feng, X., Yang, N., and Zhou, H.-F. (2015). Signaling pathway of MAPK/ERK in cell proliferation, differentiation, migration, senescence and apoptosis. J. Recept. Signal Transduct. Res. *35*, 600–604.

Suri, D., Bhattacharya, A., and Vaidya, V.A. (2014). Early stress evokes temporally distinct consequences on the hippocampal transcriptome, anxiety and cognitive behaviour. Int. J. Neuropsychopharmacol. Off. Sci. J. Coll. Int. Neuropsychopharmacol. CINP *17*, 289–301.

Taipale, M., Jarosz, D.F., and Lindquist, S. (2010). HSP90 at the hub of protein homeostasis: emerging mechanistic insights. Nat. Rev. Mol. Cell Biol. *11*, 515–528.

Tesone-Coelho, C., Morel, L.J., Bhatt, J., Estevez, L., Naudon, L., Giros, B., Zwiller, J., and Daugé, V. (2015). Vulnerability to opiate intake in maternally deprived rats: implication of MeCP2 and of histone acetylation. Addict. Biol. *20*, 120–131.

Thornalley, P.J. (2008). Protein and nucleotide damage by glyoxal and methylglyoxal in physiological systems--role in ageing and disease. Drug Metabol. Drug Interact. *23*, 125–150.

Touma, C., Gassen, N.C., Herrmann, L., Cheung-Flynn, J., Büll, D.R., Ionescu, I.A., Heinzmann, J.-M., Knapman, A., Siebertz, A., Depping, A.-M., et al. (2011). FK506 binding protein 5 shapes stress responsiveness: modulation of neuroendocrine reactivity and coping behavior. Biol. Psychiatry *70*, 928–936.

Trivedi, M.H., Rush, A.J., Wisniewski, S.R., Nierenberg, A.A., Warden, D., Ritz, L., Norquist, G., Howland, R.H., Lebowitz, B., McGrath, P.J., et al. (2006). Evaluation of outcomes with citalopram for depression using measurement-based care in STAR*D: implications for clinical practice. Am. J. Psychiatry *163*, 28–40.

Tsankova, N.M., Berton, O., Renthal, W., Kumar, A., Neve, R.L., and Nestler, E.J. (2006). Sustained hippocampal chromatin regulation in a mouse model of depression and antidepressant action. Nat. Neurosci. *9*, 519–525.

U, M., Shen, L., Oshida, T., Miyauchi, J., Yamada, M., and Miyashita, T. (2004). Identification of novel direct transcriptional targets of glucocorticoid receptor. Leukemia *18*, 1850–1856.

Ustün, T.B., Ayuso-Mateos, J.L., Chatterji, S., Mathers, C., and Murray, C.J.L. (2004). Global burden of depressive disorders in the year 2000. Br. J. Psychiatry J. Ment. Sci. *184*, 386–392.

Vale, W., Spiess, J., Rivier, C., and Rivier, J. (1981). Characterization of a 41-residue ovine hypothalamic peptide that stimulates secretion of corticotropin and beta-endorphin. Science *213*, 1394–1397.

Valentino, R.J., Foote, S.L., and Aston-Jones, G. (1983). Corticotropin-releasing factor activates noradrenergic neurons of the locus coeruleus. Brain Res. *270*, 363–367.

Vermeer, H., Hendriks-Stegeman, B.I., van der Burg, B., van Buul-Offers, S.C., and Jansen, M. (2003). Glucocorticoid-induced increase in lymphocytic FKBP51 messenger ribonucleic acid expression: a potential marker for glucocorticoid sensitivity, potency, and bioavailability. J. Clin. Endocrinol. Metab. *88*, 277–284.

Volinia, S., Dhand, R., Vanhaesebroeck, B., MacDougall, L.K., Stein, R., Zvelebil, M.J., Domin, J., Panaretou, C., and Waterfield, M.D. (1995). A human phosphatidylinositol 3-kinase complex related to the yeast Vps34p-Vps15p protein sorting system. EMBO J. *14*, 3339–3348.

Wang, J., Whiteman, M.W., Lian, H., Wang, G., Singh, A., Huang, D., and Denmark, T. (2009). A non-canonical MEK/ERK signaling pathway regulates autophagy via regulating Beclin 1. J. Biol. Chem. *284*, 21412–21424.

Wang, R.C., Wei, Y., An, Z., Zou, Z., Xiao, G., Bhagat, G., White, M., Reichelt, J., and Levine, B. (2012). Akt-mediated regulation of autophagy and tumorigenesis through Beclin 1 phosphorylation. Science *338*, 956–959.

Warner-Schmidt, J.L., and Duman, R.S. (2006). Hippocampal neurogenesis: opposing effects of stress and antidepressant treatment. Hippocampus *16*, 239–249.

Williams, R., Lim, J.E., Harr, B., Wing, C., Walters, R., Distler, M.G., Teschke, M., Wu, C., Wiltshire, T., Su, A.I., et al. (2009). A common and unstable copy number variant is associated with differences in Glo1 expression and anxiety-like behavior. PloS One *4*, e4649.

Willour, V.L., Chen, H., Toolan, J., Belmonte, P., Cutler, D.J., Goes, F.S., Zandi, P.P., Lee, R.S., MacKinnon, D.F., Mondimore, F.M., et al. (2009). Family-based association of FKBP5 in bipolar disorder. Mol. Psychiatry *14*, 261–268.

Wochnik, G.M., Rüegg, J., Abel, G.A., Schmidt, U., Holsboer, F., and Rein, T. (2005). FK506-binding proteins 51 and 52 differentially regulate dynein interaction and nuclear translocation of the glucocorticoid receptor in mammalian cells. J. Biol. Chem. *280*, 4609–4616.

Woodgett, J.R. (2005). Recent advances in the protein kinase B signaling pathway. Curr. Opin. Cell Biol. *17*, 150–157.

Xing, Y., Clements, W.K., Kimelman, D., and Xu, W. (2003). Crystal structure of a beta-catenin/axin complex suggests a mechanism for the beta-catenin destruction complex. Genes Dev. *17*, 2753–2764.

Yamaguchi, H., Hsu, J.L., and Hung, M.-C. (2012). Regulation of ubiquitination-mediated protein degradation by survival kinases in cancer. Front. Oncol. *2*, 15.

Yamamoto, A., Tagawa, Y., Yoshimori, T., Moriyama, Y., Masaki, R., and Tashiro, Y. (1998). Bafilomycin A1 prevents maturation of autophagic vacuoles by inhibiting fusion between autophagosomes and lysosomes in rat hepatoma cell line, H-4-II-E cells. Cell Struct. Funct. *23*, 33–42.

Yang, J.-Y., Zong, C.S., Xia, W., Yamaguchi, H., Ding, Q., Xie, X., Lang, J.-Y., Lai, C.-C., Chang, C.-J., Huang, W.-C., et al. (2008). ERK promotes tumorigenesis by inhibiting FOXO3a via MDM2-mediated degradation. Nat. Cell Biol. *10*, 138–148.

Yehuda, R., Golier, J.A., Yang, R.-K., and Tischler, L. (2004). Enhanced sensitivity to glucocorticoids in peripheral mononuclear leukocytes in posttraumatic stress disorder. Biol. Psychiatry *55*, 1110–1116.

Yehuda, R., Cai, G., Golier, J.A., Sarapas, C., Galea, S., Ising, M., Rein, T., Schmeidler, J., Müller-Myhsok, B., Holsboer, F., et al. (2009). Gene expression patterns associated with posttraumatic stress disorder following exposure to the World Trade Center attacks. Biol. Psychiatry *66*, 708–711.

Yoshimura, T., Kawano, Y., Arimura, N., Kawabata, S., Kikuchi, A., and Kaibuchi, K. (2005). GSK-3beta regulates phosphorylation of CRMP-2 and neuronal polarity. Cell *120*, 137–149.

Yuan, P.X., Huang, L.D., Jiang, Y.M., Gutkind, J.S., Manji, H.K., and Chen, G. (2001). The mood stabilizer valproic acid activates mitogen-activated protein kinases and promotes neurite growth. J. Biol. Chem. *276*, 31674–31683.

Zarate, C.A., Singh, J.B., Carlson, P.J., Brutsche, N.E., Ameli, R., Luckenbaugh, D.A., Charney, D.S., and Manji, H.K. (2006). A randomized trial of an N-methyl-D-aspartate antagonist in treatment-resistant major depression. Arch. Gen. Psychiatry *63*, 856–864.

Zarate, C.A., Mathews, D., Ibrahim, L., Chaves, J.F., Marquardt, C., Ukoh, I., Jolkovsky, L., Brutsche, N.E., Smith, M.A., and Luckenbaugh, D.A. (2013). A randomized trial of a low-trapping nonselective N-methyl-D-aspartate channel blocker in major depression. Biol. Psychiatry *74*, 257–264.

Zassadowski, F., Pokorna, K., Ferre, N., Guidez, F., Llopis, L., Chourbagi, O., Chopin, M., Poupon, J., Fenaux, P., Ann Padua, R., et al. (2015). Lithium chloride antileukemic activity in acute promyelocytic leukemia is GSK-3 and MEK/ERK dependent. Leukemia.

Zeller, E.A., Barsky, J., Fouts, J.R., Kirchheimer, W.F., and Orden, L.S.V. (1952). Influence of isonicotinic acid hydrazide (INH) and 1-isonicotinyl-2-isopropyl hydrazide (IIH) on bacterial and mammalian enzymes. Experientia *8*, 349–350.

Zimmermann, N., Zschocke, J., Perisic, T., Yu, S., Holsboer, F., and Rein, T. (2012). Antidepressants inhibit DNA methyltransferase 1 through reducing G9a levels. Biochem. J. *448*, 93–102.

Zou, Y.-F., Wang, F., Feng, X.-L., Li, W.-F., Tao, J.-H., Pan, F.-M., Huang, F., and Su, H. (2010). Meta-analysis of FKBP5 gene polymorphisms association with treatment response in patients with mood disorders. Neurosci. Lett. *484*, 56–61.

Zschocke, J., Zimmermann, N., Berning, B., Ganal, V., Holsboer, F., and Rein, T. (2011). Antidepressant drugs diversely affect autophagy pathways in astrocytes and neurons--dissociation from cholesterol homeostasis. Neuropsychopharmacol. Off. Publ. Am. Coll. Neuropsychopharmacol. *36*, 1754–1768.

List of abbreviations

ACTH	adrenocorticotropic hormone
AMT	Amitriptyline
BCAT	β-catenin
BECN1	Beclin-1
BUT	butyric acid
CHI	CHIR-99021
CLP	Clomipramine
CRH	corticotropin-releasing hormone
CRMP2	Collapsing response mediator protein 2
CTP	Citalopram
DXP	Doxepin
DNMT	DNA methyltransferase
ERK	extracellular signal-regulated kinase
FKBP51	FK506 binding protein 51
FGD2	faciogenital dysplasia 2
FLX	fluoxetine
FOXO	forkhead box O
GLO1	glyoxalase 1
GR	glucocorticoid receptor
GRE	glucocorticoid response element
GSK3β	glycogen synthase kinase 3 β
HDAC	Histone deacetylase
HPA	hypothalamic-pituitary-adrenal
HSP70	heatshock protein 70
HSP90	heatshock protein 90
iPSC	Induced pluripotent stem-cell
KO	knockout
KTM	Ketamine
LC3	microtubule-associated protein 1 light chain 3
LDH	lactate dehydrogenase
LIT	lithium
LMT	Lamotrigine
LNC	Lanicemine
Mb	mega bases
MEF	mouse embryonal fibroblast
MR	mineralcorticoid receptor
MTT	3-(4,5-dimethylthiazol-2-yl)-2,5-diphenyltetrazolium

nt	nucleotides
PTSD	post-traumatic stress disorder
PRX	Paroxetine
RBM12	RNA binding motif protein 12
SNP	single nucleotide polymorphism
SSNRI	serotonin and norepinephrine reuptake inhibitor
SSRI	selective serotonin reuptake inhibitor
TCA	tricyclic antidepressant
TCB	triciribine
TCF/LEF	T-cell factor/lymphoid enhancing factor
TNP	Tianeptine
TPR	tetratricopeptide repeat
TSA	trichostatin A
VNF	Venlafaxine
VPA	valproic acid
VTX	Vortioxetine
WT	wildtype

List of figures

List of tables

Publication record

Gassen NC, Hartmann J, Zannas AS, Kretzschmar A, Zschocke J, Maccarrone G, Hafner K, Zellner A, **Kollmannsberger LK**, Wagner KV, Mehta D, Kloiber S, Turck CW, Lucae S, Chrousos GP, Holsboer F, Binder EB, Ising M, Schmidt MV, Rein T. (2015). FKBP51 inhibits GSK3β and augments the effects of distinct psychotropic medications. Mol Psychiatry.

Gassen NC, Hartmann J, Zschocke J, Stepan J, Hafner K, Zellner A, Kirmeier T, **Kollmannsberger LK**, Wagner KV, Dedic N, Balsevich G, Deussing JM, Kloiber S, Lucae S, Holsboer F, Eder M, Uhr M, Ising M, Schmidt MV, Rein T. (2014). Association of FKBP51 with priming of autophagy pathways and mediation of antidepressant treatment response: evidence in cells, mice, and humans. PLoS Med. 11(11):e1001755.

Knapp RT, Wong MJ, **Kollmannsberger LK**, Gassen NC, Kretzschmar A, Zschocke J, Hafner K, Young JC, Rein T. (2014). Hsp70 cochaperones HspBP1 and BAG-1M differentially regulate steroid hormone receptor function. PLoS One 9(1): e85415.

Kollmannsberger LK, Gassen NC, Bultmann A, Hartmann J, Weber P, Schmidt MV, Rein T. (2013). Increased glyoxalase-1 levels in Fkbp5 knockout mice caused by glyoxalase-1 gene duplication. G3 Bethesda Md 3(8):1311-3.

Acknowledgements

Zu aller erst möchte ich mich bei Theo für die interessanten Forschungsprojekte bedanken. Vielen Dank, Theo, dass du immer eine offene Tür und zwei offene Ohren für wissenschaftliche Fragen und Anliegen hattest! Danke, dass du dir immer sehr viel Zeit genommen hast und mich so gut unterstützt hast.

Besonders bedanken möchte ich mich auch bei Nils. Danke für richtungsweisende Projektbesprechungen, wissenschaftliche Diskussionen, kleine Bürospielereien, epische Tischtennisschlachten, zehrende Mountainbike Touren und, nicht zu vergessen, die legendäre Konferenz in Shanghai!

Vielen Dank, Kirmi, für zahlreiche Diskussionen und Ideen. Danke Chris und danke Klaus für die Teilnahme an meinem Thesis Advisory Committee.

Des Weiteren danke ich Prof. Florian Holsboer und Dr. Elisabeth Binder für die Möglichkeit, im Rahmen meiner Doktorarbeit am Max Planck Institut für Psychiatrie zu forschen. Auch Prof. Haralabos Zorbas möchte ich für die Fachvertretung meiner Doktorarbeit an der Fakultät für Chemie und Pharmazie der LMU danken. Neben Prof. Haralabos Zorbas danke ich auch den weiteren Mitgliedern meiner Prüfungskommission Prof. Chris Turck, Dr. Theo Rein, Prof. Prof. Florian Holsboer, Prof. Klaus Förstemann und Prof. Karl-Peter Hopfner.

Der gesamten Arbeitsgruppe AG Rein und allen weiteren MPIlern, mit denen ich zusammen arbeiten durfte, will ich für die angenehme und anregende Arbeitsatmosphäre danken: Andreas, Anja, Anna, Bärbel, Bozo, Christine, Claudia, Gabriel, Jürgen, Kathi, Nicki, Svenja und Tatjana.

Zu guter Letzt danke ich von ganzem Herzen meinen Eltern Claudia und Hans, meinem Bruder Sebastian und meiner Freundin Babsi. Ihr habt mich immer unterstützt und mir den nötigen Rückhalt gegeben um diese Arbeit fertigzustellen.